THE PROTECTIVE EFFECTS OF PURPLE CORN SILK CRUDE EXTRACT ON UVB-IRRADIATED KERATINOCYTE CELL LINE (HACAT)

WATCHARAPORN POORAHONG

Graduate School Srinakharinwirot University

2021

ผลของสารสกัดหยาบจากใยข้าวโพดสีม่วงในการป้องกันเซลล์เพาะเลี้ยงคีราติโนไซต์ที่ถูกอาบด้วยรังสีอัลตราไวโอเลตบี

วัชราภรณ์ ภู่ระหงษ์

ปริญญานิพนธ์นี้เป็นส่วนหนึ่งของการศึกษาตามหลักสูตร
ปรัชญาดุษฎีบัณฑิต สาขาวิชาชีวภาพการแพทย์
คณะแพทยศาสตร์ มหาวิทยาลัยศรีนครินทรวิโรฒ
ปีการศึกษา 2564

THE PROTECTIVE EFFECTS OF PURPLE CORN SILK CRUDE EXTRACT ON UVB-IRRADIATED KERATINOCYTE CELL LINE (HACAT)

WATCHARAPORN POORAHONG

A Dissertation Submitted in Partial Fulfillment of the Requirements

for the Degree of DOCTOR OF PHILOSOPHY

(Biomedical Sciences)

Faculty of Medicine, Srinakharinwirot University

2021

THE DISSERTATION TITLED

THE PROTECTIVE EFFECTS OF PURPLE CORN SILK CRUDE EXTRACT
ON UVB-IRRADIATED KERATINOCYTE CELL LINE (HACAT)

BY

WATCHARAPORN POORAHONG

HAS BEEN APPROVED BY THE GRADUATE SCHOOL IN PARTIAL FULFILLMENT
OF THE REQUIREMENTS FOR THE DOCTOR OF PHILOSOPHY
IN BIOMEDICAL SCIENCES AT SRINAKHARINWIROT UNIVERSITY

(Assoc. Prof. Dr. Chatchai Ekpanyaskul, MD.)
Dean of Graduate School

ORAL DEFENSE COMMITTEE

..... Major-advisor
(Prof. Dr.Ramida Watanapokasin)

..... Chair
(Asst. Prof. Dr.Aungkana Krajarng)

..... Committee
(Asst. Prof. Dr.Orapin Gerdprasert)

..... Committee
(Asst. Prof. Dr.Yamaratee Jaisin)

Title	THE PROTECTIVE EFFECTS OF PURPLE CORN SILK CRUDE EXTRACT ON UVB-IRRADIATED KERATINOCYTE CELL LINE (HACAT)
Author	WATCHARAPORN POORAHONG
Degree	DOCTOR OF PHILOSOPHY
Academic Year	2021
Thesis Advisor	Professor Dr. Ramida Watanapokasin

The exposure of skin to UVB could lead to inflammation and apoptosis. Purple corn silk (PCS), which is agricultural waste, has multiple pharmacological properties. This study aims to determine the protective effects of PCS extract on UVB-induced cell damage on human keratinocyte HaCaT cells. The results showed that the PCS extract strongly absorbed UVB spectrum and showed antioxidant activity. The cells were pre-treated with PCS extract, followed by UVB exposure showed the increase in cell viability and a decrease in ROS, DNA damage via reduced γ-H2AX as well as the DNA in the comet tail. Moreover, the PCS extract decreased inflammatory response in cells via the reduction of NF-κB, iNOS, and COX-2, as well as attenuated UVB-mediated apoptosis through the decrease in apoptotic bodies, sub-G1 DNA content, cleaved-caspases 8, -9, and -7, and cleaved-PARP. The PCS extract also stabilized the potential of the mitochondrial membrane via enhanced anti-apoptotic protein and inhibited pro-apoptotic proteins, including suppressed p-c-Jun when compared with the UVB control group. These findings suggested that the PCS extract reduces the deleterious effects from UVB exposure through decreased DNA damage, inflammatory response, and apoptosis induction in human keratinocyte HaCaT cells. Therefore, to enhance the value of agricultural waste, PCS extract could be a new candidate for development as an UVB preventive agent in skincare products

Keyword : purple corn silk, apoptosis, inflammation, UVB protection, Keratinocyte cells

ACKNOWLEDGEMENTS

I deeply appreciate my supervisor, Prof. Dr. Ramida Watanapokasin for guidance and help throughout this research. The provided opportunity and advice from her encourage me to develop myself, learn to be self-responsibility and others, and enhance my knowledge. My thesis would not succeed without her valuable supports.

I am deeply grateful for the financial and materials support provided by Research and Researcher for Industries (RRi) Grant no. PHD57I0075, the Thailand Research Fund (TRF) corroboration with Prof. Dr. Malyn Ungsurungsie, S & J International Enterprises Public Company Limited, Bangkok, Thailand.

Furthermore, I appreciate the graduate school of Srinakharinwirot University and Faculty of Medicine, especially the Department of Biochemistry, Srinakharinwirot University, Bangkok, Thailand for materials, instruments, and laboratory rooms. Additionally, I would like to thank all my laboratory members for the fun and encouragement, and I deeply special thanks to Dr. Sukanda Innajak for her support and advice on molecular techniques.

Finally, I sincerely appreciate my family for their love, especially, my mother, father, brother, and sisters who are extremely supportive and understanding only troubles in Ph. D. student life. Without their encouragement, I would not succeed in my research and graduation.

WATCHARAPORN POORAHONG

TABLE OF CONTENTS

Page

LIST OF TABLES

Page

LIST OF FIGURES

Page

CHAPTER 1
INTRODUCTION

1.1 Background

Ultraviolet (UV) radiation could induce skin carcinogenesis, 10%decreased ozone layer leading to an additional skin cancer cases. Besides, the risk of skin cancer is increasing with UV exposure time, especially in people who work outdoors and those prefer to sunbathe [1].

Three components of solar UV radiation, UVC can be blocked by the ozone layer, with only 90-95 % of UVA and 5-10% of UVB showed impact on the human skin [2, 3]. Exposure of the skin to UVB causes intracellular ROS overproduction and induces DNA single- and double-strand break leads to increased γ-H2AX and DNA photoproducts such as 8-hydroxyguanine (8-OHdG) and cyclobutane pyrimidine dimers (CPDs) [4]. Moreover, UVB and intracellular ROS also oxidizing various molecules such as lipid and proteins, resulting in lipid and protein peroxidation, impaired mitochondrial membrane function as well as inflammatory response stimulation via increasing inflammatory cytokines such as COX-2 and iNOS. However, the damaged cells can be fixed by the repair mechanism. Nevertheless, unrepairable cells were eliminated by apoptosis induction via the decreased expression of anti-apoptotic proteins and an increased pro-apoptotic proteins which promote cytochrome c release leading to activate caspase cascade resulting in apoptosis cell death induction [5, 6]. Furthermore, UVB can activate MAPK and Akt signaling pathways, which are a key mediator of cell inflammation, survival and apoptosis, through the change of various protein expression such as IL-1β, iNOS, NF-ƙB, p53, FasL, and Bcl-2 [7, 8].

Recently, many plants have been used as ingredients, supplements, or medicine. Corn silk (female flower part), is an agricultural waste [9]. Corn silk was processed into cosmetic ingredients, tea, and corn powder in many countries such as China, Korea, and France. In traditional medicine, corn silk has been used for the treatment of many diseases such as edema, urinary infection, and obesity [6, 9-14]. These

reports suggest that corn silk is abundant with phenolic content exhibited antioxidant activity. Additionally, corn silk extract also showed antibacterial activities, immune enhancement, and neuroprotective effect against oxidative stress [10, 11, 15, 16]. Previous studies reported that purple corn silk rich in phenolic, flavonoid, and anthocyanins contents had antioxidant activities by free radical scavenging, antioxidant enzyme enhancing, lipid peroxidation inhibition, hypertension, and against diabetes and cancer [9, 11-13, 17]. However, purple corn silk is a waste material from cultivation without value and, is not popular for the development of commercial skincare products. Furthermore, the study of hydroglycolic purple corn silk extract on UVB-induced cell damage in human keratinocytes has not yet been reported. Therefore, in this study, we investigated the effects of hydroglycolic purple corn silk (PCS) extract on UVB-induced cell damage in human keratinocytes by using the HaCaT cell line as a model. In addition, we investigated the effect of PCS extract on the stress-sensitive MAPK and Akt signaling pathways, which are essential in regulating cell inflammation, cellular stress, cell survival and death. This finding is basic knowledge for developing hydroglycolic purple corn silk extract to be cosmetic ingredients such as cream and sunscreen resulting in increased waste-material value.

1.2 Objective

1.2.1 To investigate the protective effects of purple corn silk crude extract on UVB-induced cell damage in human keratinocyte (HaCaT) cell line.

1.2.2 To investigate the protective effects of purple corn silk crude extract on signaling pathway associate cell survival, inflammation, and cell death induction on UVB-induced cell damage in HaCaT cell line.

CHAPTER 2
REVIEW LITTERATURE

2.1 The skin structure

Skin is the largest organ of the body. The skins act as a barrier between intracellular and extracellular environments. It has various functions such as protecting the body against pathogens, waterproof, thermoregulation, recognize sensation (pain, heat, and cold), and Vitamin D production [18]. The skin is composed of three layers including epidermis, dermis, and subcutaneous layer. The epidermis is the outermost layers of the skin mainly composed of keratinocytes. Whereas the dermis is the thick layer below the epidermis composed of collagen and elastin. This layer allows skin tough, flexible, and is locating of appendages derived such as hair follicles and sweat glands. The lowest layer of skin is subcutaneous tissue containing fat cells (lipocytes) and large blood vessels. This layer protects the body from cold and pressure, and also attaches the skin to the muscles and connective tissue lying below it [19, 20].

2.1.1 Epidermis layer

The epidermis consists of keratinocyte and dendritic cells. The average thickness of this layer is 0.1 mm [20]. This layer is a continuous renewing layer. Cells in this layer are characterized into two type consisting of keratinocyte and non-keratinocyte [18]. The keratinocyte is divided into four layers stratum basale, stratum spinosum, stratum granulosum, and stratum corneum. The stratum spinosum together with stratum corneum referred to Malpighian layer. In addition, in the thick epidermis, also appears the stratum lucidum as a thin layer presents a transform of stratum granulosum to stratum corneum which unfound in the thin epidermis (Fig. 1) [21].

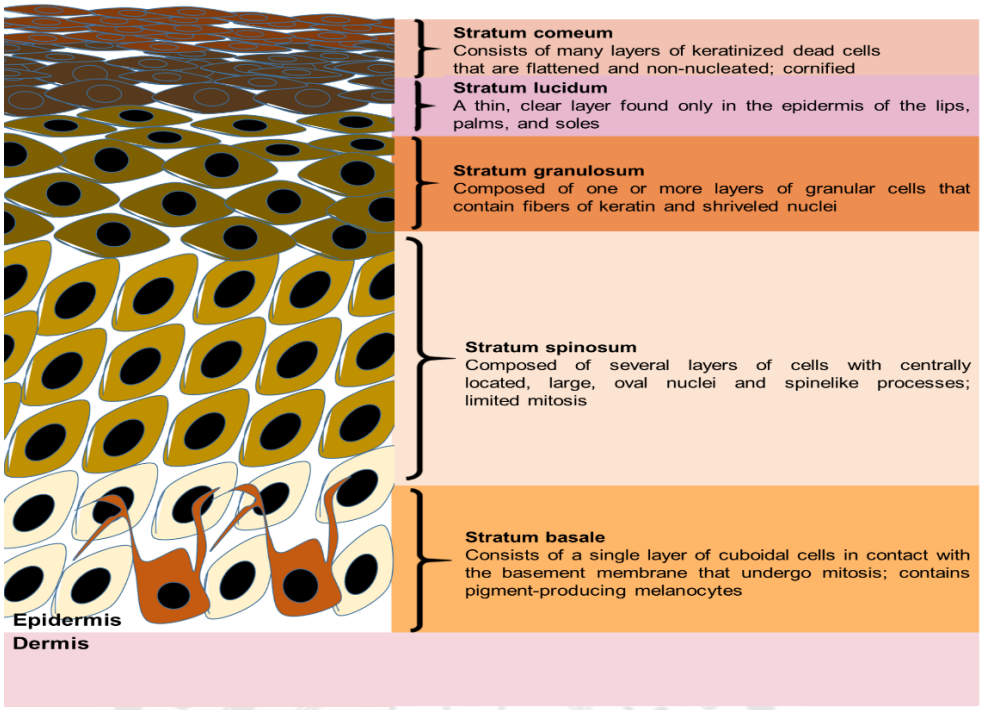

Figure 1 The layer of epidermis.

Source: Ramadon D, McCrudden MTC, Courtenay AJ, and Donnelly RF. (2021). Enhancement strategies for transdermal drug delivery systems: current trends and applications. Drug Delivery and Translational Research. p. 3.

2.1.1.1 Keratinocyte

The keratinocytes are the composition of at least 80% of cells in the epidermis [18], bridged together by desmosomes protein. The renewing of epidermis associated with the process is called keratinization or maturation of the skin cells. The keratinization consists of the synthesis and degradation [19]. The differentiation of keratinocyte leads to cell migration from the basal layer to the surface of the skin. In the synthesis phase, the keratinocyte cells produce keratin proteins in alpha-helical fibrous intermediate filament, which acts as a waterproof structure and cell cytoskeleton. While the degradation phase, keratinocytes are pushed away and activated program cell death. The cellular organelles and the nuclei is degraded. Finally, cells death and remain resemble flat dead, called corneocytes in a horny layer [19, 20, 22].

The basal cell layer (stratum germinativum) is a column shaped keratinocyte interact with basement membrane by hemidesmosomes lies adjacent to the dermis layer. This layer contains stem cells, important to the epidermis renewing. The stem cells act as precursors of the keratinocytes and activate cell division. In normal condition, epidermal stem cell has a long lifespan because of the slowly of cell cycle but hyperplasiogenic conditions can be stimulated the division of stem cells such as wounding.

The squamous cell layer (stratum spinosum) consists of cells developed from stratum germinativum. Cells in this layer are high variation in shapes, structures, and subcellular properties, which depend on the localization of cells. For example, polyhedral keratinocytes function to produce the fibrillar proteins (cytokeratin) lead to tonofibrils and desmosomes forming, which enhance strong connections between adjacent keratinocytes. Moreover, in this layer found Langerhans cells, the dendritic cell which function as a macrophage on against the pathogens entering such as bacteria.

The granular cell layer (stratum granulosum) consists of living keratinocytes migrating from stratum spinosum containing all organelles. The cells are abundant with keratohyalin granules in the cytoplasm which are responsible for further synthesis and modification of proteins in keratinization through adding the histidine- and cysteine-rich resulting in holding the keratin filaments together. Furthermore, cells secrete lamellar bodies consist of lipids and proteins to the extracellular space at the transition zone between the granular and the stratum corneum leads to hydrophobic lipid envelope formation, which acts as skin's barrier properties. After that, these cells develop into flattened cells and transit to stratum corneum [18-20, 22].

The cornified or horny cell layer (stratum corneum) consist of death cells (horny cells or corneocytes). This layer is the outermost of the epidermis, a barrier between the body and the external environment. This layer plays an important role to protect infection, dehydration, chemicals, and mechanical stress in skin. The thickness of this layer is due to involucrin protein production from both of stratum granulosum and stratum corneum, which forming on the inner side of the plasma membrane. Cells in this

layer is transition from the granular cell layer, become mature keratinized and begin to flatten out. Then, cells fused with lipids secreted from the stratum granulosum and push away to outermost of the skin. The desquamation (die and break apart) of skin cells associated with lysosomal enzymes activities to break down complex molecules resulting in cell death and break apart to skin.

2.1.1.2 Non-keratinocyte

Non-keratinocyte cells consist of melanocytes, Langerhans cells, and Markel cells. Melanocyte is a dendritic that synthesize the melanin pigments. In white skin, the melanosomes are small and the melanin can be removed rapidly. Whereas in dark skin, the melanosomes are larger and containing more melanin. Langerhans cells are other cells found in epidermis about 2-8% of the total epidermis. It is a variety of T-cell which migrated from the bone marrow to dominantly in stratum spinosum serve as recognize the antigens found in skin tissue. While, Markel cell is a dendritic cell found in basal layer which functions as a receptor to response for stimulating sensory nerves by secreting a chemical signal such as catecholamine and generates an action potential to transduce signal to the brain [20, 22].

2.1.2 Dermis layer

The dermis is the thickest layer of skin cells (1.5-4 mm thick) presented under the epidermis, locate of blood vessel function to support nutrients and oxygen and regulate the temperature. Moreover, this layer is a connective tissue abundance with collagen, elastin produced from fibroblasts, and other molecules necessary for support the elasticity of the skin. Dermis layer can be divided into 2 types consisting of papillary layer and reticular layer. Papillary layer, the superficial layer of the dermis which built up from loose connective tissue contains fibroblast and connected with epidermis layer at basal layer. This layer also consists of phagocytes, lymphatic capillaries, nerve fibers, and abundance of small blood vessels. Whereas in reticular layer, underlying the papillary layer and thicker than papillary layer. It composes of dense together with irregular connective tissue and a rich sensory and sympathetic nerve. The reticular layer contains the tight network of fibers including elastin fibers. In addition, this layer consists of collagen fibers provide tensile strength. Moreover, in

dermis found the specialized neurons consist of Pacinian corpuscles and mechanoreceptor nerves, are localized deep in the skin response to heavy pressure. Meissner's corpuscles are localized close to the skin surface response to light touch. Krause end bulbs and Ruffian end organs detect cold temperature, warm temperature changes, touch, and pressure. And the nerve endings are lying close to the dermal surface for response to pain [19].

2.1.3 Subcutaneous layer

The lowest of the skin is the subcutaneous layer (hypodermis layer) serves to connect the skin to the bones and muscles. This slayer is loosely attached to connective tissue leading to the skin can move relatively freely. This layer abundance of fat cells provides to store fat and energy, and provides insulation and cushioning for the integument. In addition, the subcutaneous layer is localized of root hair follicles and blood vessels [19, 20, 22].

2.2 The radiation and sunlight

The electromagnetic radiation (EMR) spectrum is divided into two part based on the wavelength range; first is non-ionizing radiation consists of with three mains spectrum regions include ultraviolet (UV); region covers the wavelength range 100-400 nm, visible; region wavelengths range from approximately 400-700 nm, and infrared radiation; region wavelengths range higher than 700 nm [4]. Another EMR spectrum is ionizing radiation including gamma-ray and X-ray (Fig. 2) [23].

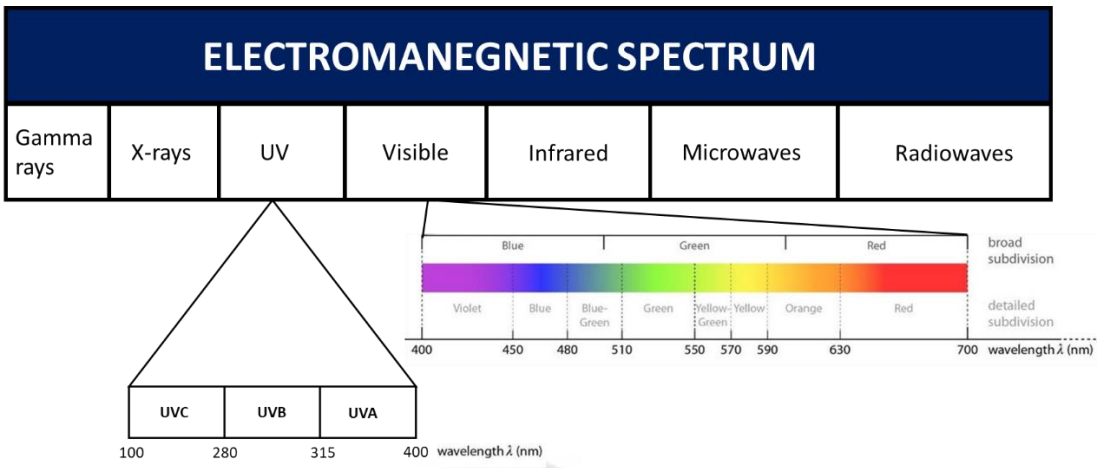

Figure 2 The electromagnetic spectrum (EMR).

Source: Ultraviolet Radiation. Available from: https://www.ccohs.ca/oshanswers/phys_agents/ultravioletradiation.html.

The sunlight consists of various types of UV radiation as shown in table1. The intensity of each radiation is different between Earth's surface and outside of atmosphere. Because the ozone layer of earth can block some radiation before through into the Earth's surface as shown in table1 [24].

Table 1 The component of radiation in sunlight

Wavelength (nm)	Irradiance (W/cm^2)	Outside of atmosphere (%)	Inside of atmosphere (%)
UVC	6.4	0.5	0
UVB	21.1	1.5	0.5
UVA	85.7	6.3	6.3
Visible	352	38.9	38.9
Solar constant	1.37 kW/m^2	100	100

2.2.1 UV radiation (UVR)

The UVR radiation is divided into three sections include UVA, UVB, and UVC [25].

Ultraviolet A: is region covers the wavelength range 400-320 nm, referring as a longest wavelength of UV radiation which present the deepest permeability properties, but lowest energy. In the solar UV radiation, it consists of 90-95% of UV radiation which can be penetrated through water, fog, clouds, and deeper into the dermis layer of the skin (Fig. 3). The UVA is the main cause of skin sagging and wrinkling. Hence, UVA is considered as the aging ray.

Ultraviolet B: region covers the wavelength range 320-290 nm. UVB is a middle wavelength between UVA and UVC. Although UVB has lower permeability properties than UVA and some can be blocked by the ozone layer, but amount 5% of the total solar UV radiation is UVB reaching the Earth's surface. The UVB is mainly cause of variety of skin diseases, especially skin carcinogenesis (Fig. 3).

Ultraviolet C: is the shortest wavelength was found between 200-280 nm of UV radiation, which has lowest permeability properties. It is absolutely blocked by the atmospheric ozone layer. Thus, UVC does not appear in surface's Earth but also found in artificial lamp that uses for wastewater treatment, laboratories, medical, and hospital for satirizing instruments, work surfaces and the air [26]. The UVC is causing damage to the cornea, painful burns, and erythema, (Fig. 3) [27, 28].

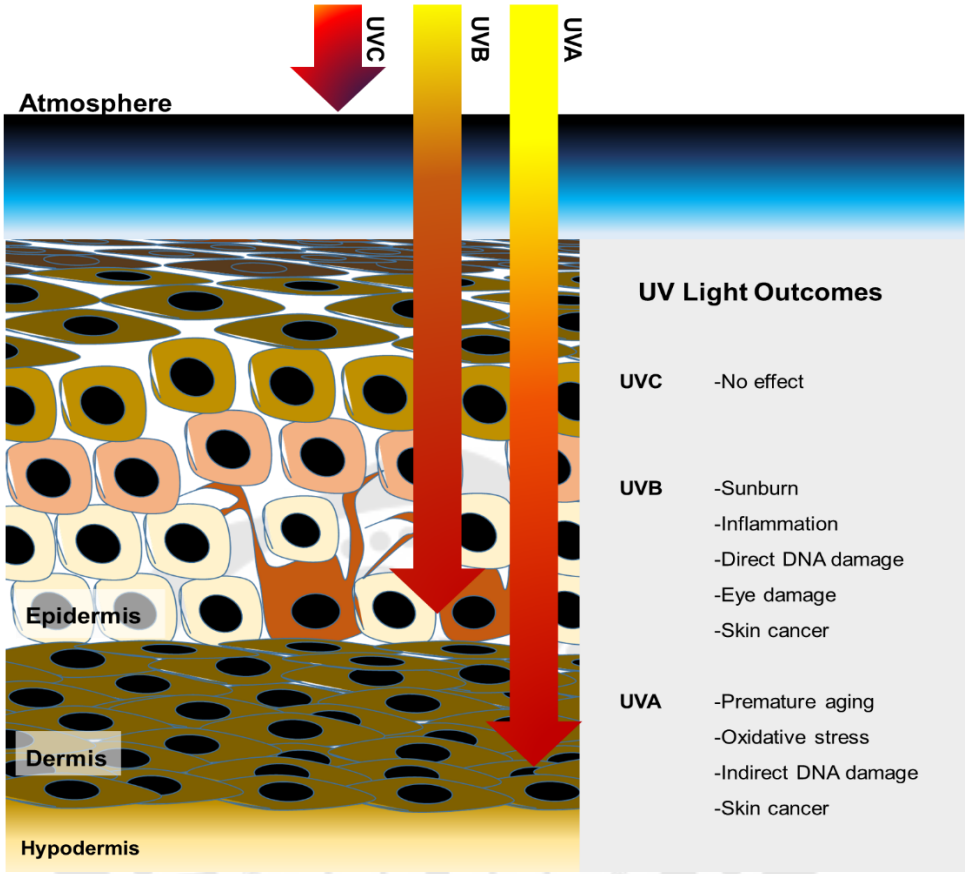

Figure 3 The permeability properties of solar UV radiation and their effects on human skin. UVC is completely absorbed by the ozone layer. Therefore, it is not affected human skin; UVB can reach the epidermis and directly induces DNA breaks, skin cell death and inflammation; UVA penetrates the dermis and indirectly induces DNA damage and aging on the skin.

Source: Amaro-Ortiz A, Yan B, and D'Orazio JA. (2014). Ultraviolet radiation, aging and the skin: prevention of damage by topical cAMP manipulation. Molecules. p. 6203.

2.3 The effects of UV radiation on the skin cells

Usually, the UV radiation is spread out which humans has been exposed to and cannot be avoided. The atmosphere consists of the ozone layer is serves as the radiation barrier and plays a key role in blocking some part of harmful radiation from the sun reaching into the Earth. Unfortunately, the industry and daily consumer products

such as air-conditioning, hair spray, and body spray are contained chlorofluorocarbons (CFCs) as a component lead to the leaking of the ozone layer. The depleting of the ozone layer enhances the UV radiation intensity on the Earth's surface and affects skin health [30]. The excessive UV exposure on skin causes inflammation, epidermal hyperplasia, immune suppression, photoaging, and carcinogenesis of the skin. In contrast, UV radiation is also necessary for vitamin D synthesis, killing skin pathogens, treating skin disorder such as psoriasis and vitiligo. World Health Organization reported that at low levels of UV exposure induce dysfunction of the musculoskeletal system and may increase risk of various autoimmune [31]. Thus, the appropriate UV intensity on the skin is important with human health.

2.3.1 Advantage of the UV exposure

2.3.1.1 Vitamin D synthesis

The UV sunlight is an initiator for vitamin D synthesis in the skin. Over 90% of vitamin D is stimulated by UVB act as a precursors [32] During UV exposure, UVB in sunlight changes photolyzes 7-dehydrocholesterol (7-DHC) in the epidermis layer into pre-vitamin D3. The body heat isomerizes pre-vitamin D to generate vitamin D3 and transport it through the blood to the liver and converted to 25-hydroxyvitamin D (25(OH)D) before transport to the kidney. At the kidney, it is modified to the active form of vitamin D; 1, 25(OH) 2D, which is controlled by the parathyroid hormone (PTH) and transported to other tissues, respectively [33]. The important vitamin D is maintaining the serum calcium and phosphorous level to support most of the metabolism. Moreover, vitamin D is an important enhancer in neuromuscular transmission, bone mineralization, and immune system functioning against bacterial and viral, and fungal infections [31]. The effectiveness of vitamin D3 synthesis depends on the solar angle (season and latitude), time of day, and individual skin tone [34]. The low levels of UV exposure of skin lead to lacking vitamin D and reduction of bone mass [35]. Besides, vitamin D deficiency leading to rickets and lack of calcium in bone in children, and leading to osteomalacia in elderly [31]. Moreover, many reports showed that vitamin D level is involving many diseases such as tuberculosis and cancer. For example, *in vivo* study, have shown that vitamin D showed a direct relationship with tuberculosis. Briefly, a high level of vitamin D

enhanced the monocyte activities against intracellular TB growth. Additionally, the results suggested that greater sunlight exposure or supplement diet contain vitamin D leading to a decreasing in breast and prostate cancer mortality, and against colorectal cancer growth via increases calcium levels on cancer cell [30].

2.3.1.2 Phototherapy

Some UV radiation at low energy such as UVB broadband, UVA broadband, UVA-1, and UVA in combination with a light-sensitive drug known as psoralen [36] present potency for treating various diseases such as psoriasis, vitiligo, large-plaque parapsoriasis, and cutaneous T-cell lymphoma (CTCL) (Table 2) [36]. For example, psoriasis is an autoimmune disease due to the dysfunction of helper T cells resulting in stimulatinghost immune to induce the overexpression of cytokines. Three main T helper subsets in Th1-, Th2- and Th17-helper associated with psoriasis disease. The overexpression of Th1 and Th17 lead to cytokines secretion such as IL-12, IL-17, and IL-23, interferon (INFα), and Tumor necrosis factor (TNFγ) resulting in hyperproliferation, inflammation, painful, scaly, and inflamed patches of skin (plaques) [37, 38]. Psoriasis can be treated by using a combination psoralen drug with the UVA, called this PUVA treatment. Indeed, psoralen is a novel treatment agent, is act as a TNF inhibitor and interfere T cell activation. The combination between psoralen drug and UVA resulting in shifting the immune response towards the counter-regulatory Th2. This event leads to the increasing of IL-10 and IL-4 and suppressed Th1 and Th2 levels, resulting in attenuated keratinocyte proliferation and skin inflammation. Moreover, PUVA also activates apoptosis of T lymphocytes in psoriatic lesions and keratinocyte cells through the increased p53 protein level [36].

Table 2 Clinical phototherapy modalities

Type of phototherapy	Wavelength used (nm)	Photosensitizer	Most common responsive diseases
UVB broadband	290-320	None	Psoriasis, atopic eczema, polymorphic light eruption, pruritus
UVB 311 nm	311-313	None	Psoriasis, atopic eczema, vitiligo, polymorphic light eruption, cutaneous T cell lymphoma (CTCL)
UVA broadband	320-400	None	Atopic eczema
UVA-1	340-400	None	Atopic eczema, localized scleroderma, urticaria pigmentosa (mastocytosis)
Psoralen + UVA photochemotherapy (PUVA)	340-400	5- or 8-Methoxypsoralen, trioxsalen	Psoriasis, atopic eczema, vitiligo, polymorphic light eruption, urticaria pigmentosa, graft-versus-host disease (GVHD), CTCL
Extracorporeal photochemotherapy (photopheresis)	340-400	8-Methoxypsoralen	Sezary syndrome, CTCL, GVHD, systemic scleroderma
Photodynamic therapy (PDT)	400-700	porphyrin derivatives and precursors (aminolevulinic acid or methyl aminolevulinate)	Basal cell carcinoma, actinic keratosis, Morbus Bowen (in situ squamous cell carcinoma)

2.3.2 Disadvantage of the UV exposure

2.3.2.1 Short-term effects of UV on human skin

Acute UV radiation causes DNA damage such as CPDs and pyrimidine 6-4PPs, and oxidative stress induction. Moreover, UV radiation can cause damage of the number of macromolecules and organelles in cells including proteins and lipid which lead to inflammation and cell death [(4)].

2.3.2.1.1 UV-induced genotoxicity

The DNA molecules can be absorbed in a range wavelength of the UV spectrum, especially UVB and UVC. This absorbing results in DNA breakage and gene mutations. While UVA is poorly absorbed by DNA molecules. Thus, UVA is less harmful than UVB and UVC [39]. However, UVA can induce singlet oxygen and hydroxyl free radical–overproduction causing oxidative stress. The evidence demonstrated that UVA significantly increases oxidative stress and causing photoaging such as skin sagging and wrinkling in human skin [27]. While UVB and UVC produce single molecular oxygen, one-electron, and hydroxyl radical to interfere guanine and pyrimidine base in DNA chain led to the formation of 8-OHdG and 6-4PPs. In addition, UVB and UVC can directly induce CPDs in DNA molecules in both hetero and euchromatin regions. Importantly, it induces single and double-strand breaks of DNA. This lesion can cause skin carcinogenesis [40].

Furthermore, the RNA base can absorb UVB, causing breakage in the mRNA structure and translated to dysfunctional proteins. While the aromatic amino acid in epidermal proteins such as tryptophan (Trp), tyrosine (Tyr), and cysteine (Cys) is oxidized after absorbing UVB, called photooxidation. This event generates photoproducts such as carbonyl proteins. The photooxidation of protein is divided into two sub-types. Type I photooxidation is a directly interacting of one-electron with disulphide bonds of Trp and Tyr resulting in disulphide redical anion ($RSSR^{-\bullet}$) formation [41]. $RSSR^{-\bullet}$ react with oxygen molecule producing $^{\bullet}O_2^-$ and RSSR. Type II photooxidation is UV-induced protein modification by reaction with single oxygen. The modification of proteins due to UV exposure leads to lose function of proteins including enzymes and cell components [42].

Tropically, the undamaged DNA is wrapped with a core histone and form nucleosome complex. Histone cores consist of H2A, H2B, H3, and H4. The H2A family proteins have many variants; H2A1, H2A2, H2AX, and H2AZ. H2AX is a key mediator protein which promotes DNA repair through phosphorylation at the serine 139 (Ser139) residue, called γ-H2AX, and then recruited to damage sites. In mammalian cells, ATM

and ATR are responsible for the DNA repair by transforming the signaling via γ-H2AX activation [43]. The γ-H2AX are colocalizing with DNA repair proteins and maintenance of these factors at damaged sites to activate downstream factors (Fig. 4) [44, 45].

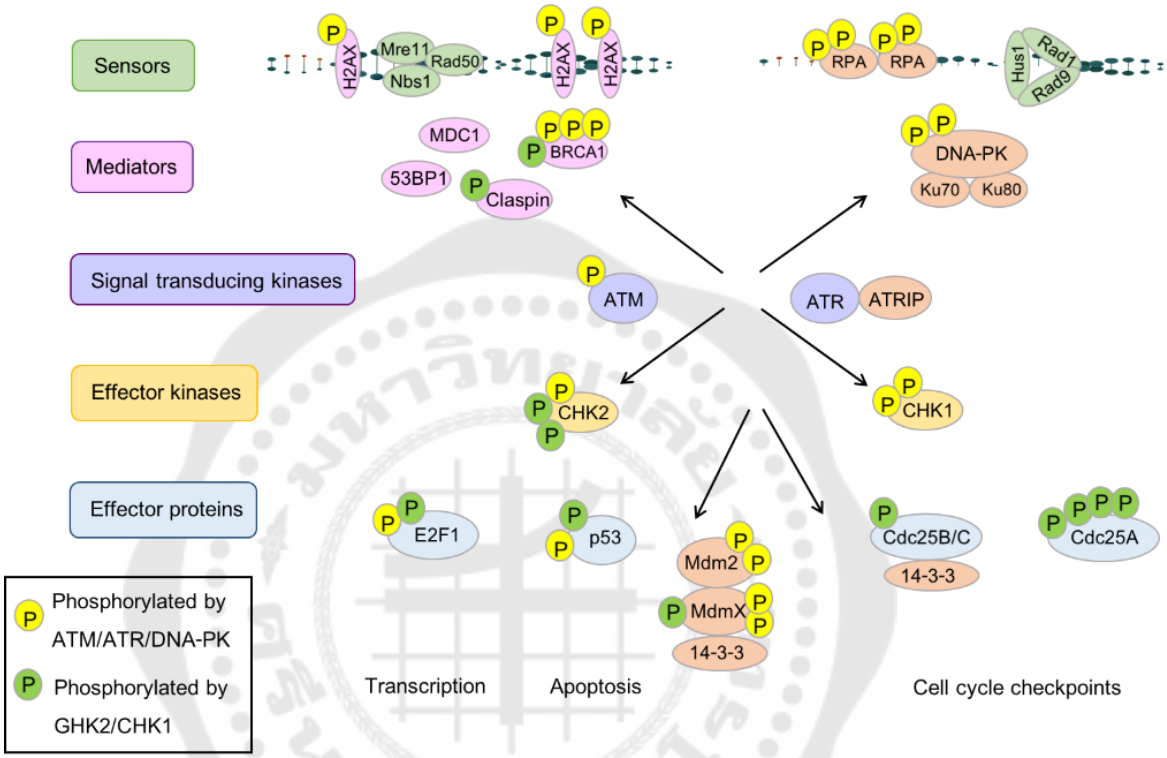

Figure 4 Mechanism of cellular response to DNA damage. Upon sensing DNA damage, cells are activating the sensors (green), mediators (pink), signal transducing kinases (purple), effector kinases (pink), and effector proteins (blue) proteins.

Source: Freeman AK and Monteiro AN. (2010). Phosphatases in the cellular response to DNA damage. Cell Communication and Signaling. p. 2.

Moreover, ATM/ATR also directly inhibits Mdm2 by phosphorylated on Ser395 and Ser407 of Mdm2 leads to activation and accumulation of tumor protein 53 (p53) [45, 46]. p53 serves as DNA damage checkpoint in G1 phase. The accumulation of p53 triggers the transcription of cyclin-dependent kinase inhibitors (CKIs). The

increasing of p21 resulting in suppression of cyclin E and cyclin A complex with cyclin-dependent kinase 2 (CDK2) activities lead to prevent G1/S phase progression [47]. Whereas p27 bind to Cyclin E-CDK2 to inhibit their activities to block the G1/S transition. Moreover, ATM/ATR activates Chk1 and Chk2, which lead to the phosphorylation of p53 and cell division cycle 25 (Cdc25). Cdc25A is phosphorylated at Ser123 residue and rapidly degraded and inhibits activating cyclin A-CDK2, cyclin E-CDK2, and cyclin B-CDK1 resulting in G1 and G2 arrest [46, 48, 49]. In addition, Chk1 and Chk2 phosphorylated Cdc25c at Ser216 lead to Cdc25c facilitated from nucleus to cytosol and bind to 14-3-3σ proteins resulting in attenuated activity. Furthermore, the UV also induce p38 activities. The active p38 inhibit cyclin B-CDK1 activity via the phosphorylation of Cdc25B at the position Ser309 in G2 arrest (Fig. 5) [48, 50, 51].

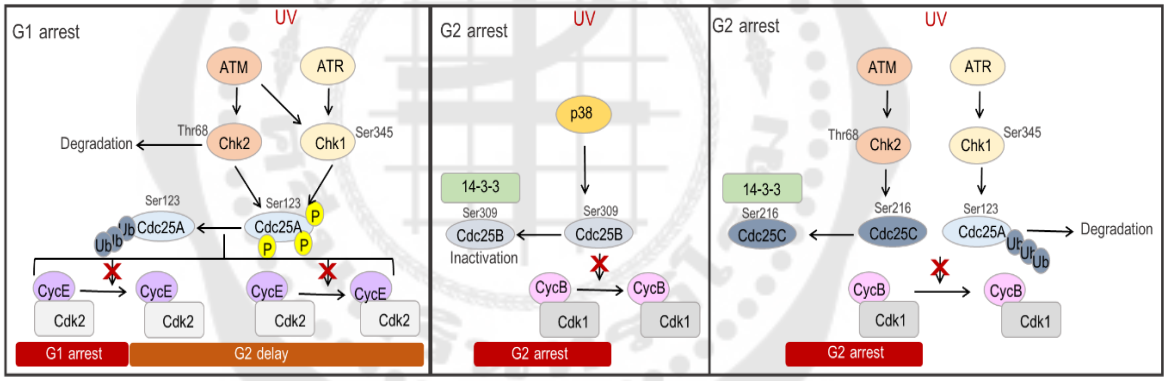

Figure 5 The regulation of Cdc25 proteins in response to UV radiation. After UV irradiation, the checkpoint kinases (Chk2 and Chk1) and Cdc25 proteins (Cdc25A and Cdc25C) are activated by ATM/ATR proteins. Phosphorylated Cdc25A and Cdc25C are degraded through the ubiquitin (Ub)-proteasome pathway or binds to 14-3-3 proteins, which prevent Cdk1/cyclin B (CycB) forming resulting in G1 and G2 arrest. In addition, p38 MAPKs protein phosphorylates Cdc25B, resulting in G2 arrest.

Source: Donzelli M and Draetta GF. (2003). Regulating mammalian checkpoints through Cdc25 inactivation. European Molecular Biology Organization reports. p.674-75.

2.3.2.1.2 UV-induced apoptosis

DNA damage due to UV exposure activates p53 mediated apoptosis. Briefly, DNA damage promotes an increase of p53 protein level and activate their activities through the phosphorylation at Ser15 and Ser20 of p53 protein [27]. Moreover, p53 induces $p21^{WAF1/CIP1}$ accumulation. p21 is an inhibitor of CDK via competitively react with CDK leads to blocking cyclin-CDK complex in the G1 arrest. Active p53 inhibits the cell cycle to repair DNA damage before continuing to the S phase. However, in unrepairable cases, p53 plays a role in inducing apoptotic pathways through upregulation of proapoptotic proteins and downregulating antiapoptotic [2, 27]. Furthermore, UV activates p53-independent apoptosis through stimulating death receptors on skin cells. p53-independent apoptosis corresponds with death receptor activities and mitochondrial dysfunction [4]. Generally, the epidermis is the area exposed to the chemical, mechanical stress, wind, radiation, and wounding. Thus, this layer is abundance with the expression of Bcl-xL to prevent skin cell death. After UV exposure to skin, cells enhance several antioxidant enzymes such as SOD, GPx, and CAT. These enzymes is activated to remove free-radical from UV exposure and block apoptosis [27, 52]. The depletion of endogenous antioxidants resulting in insufficient protection [53]. The UVB exposure in high intensity and long periods induces apoptosis in keratinocytes via depleting antioxidant enzymes, suppress antiapoptotic proteins, and enhance caspases activities which subsequently inactivate Poly (ADP-ribose) polymerase (PARP) [2, 27, 52]. Furthermore, UV induces multimerization of CD95 to activating the recruitment of Fas associated death domain (FADD). This event induces caspase8 and -7 activities resulting in apoptosis [54]. Recent reports showed that UVB and UVC induce various initiator apoptotic signals including DNA damage, intracellular ROS, and cytokine deprivation lead to mitochondrial dysfunction and apoptosis induction (Fig. 6) [2, 27, 52].

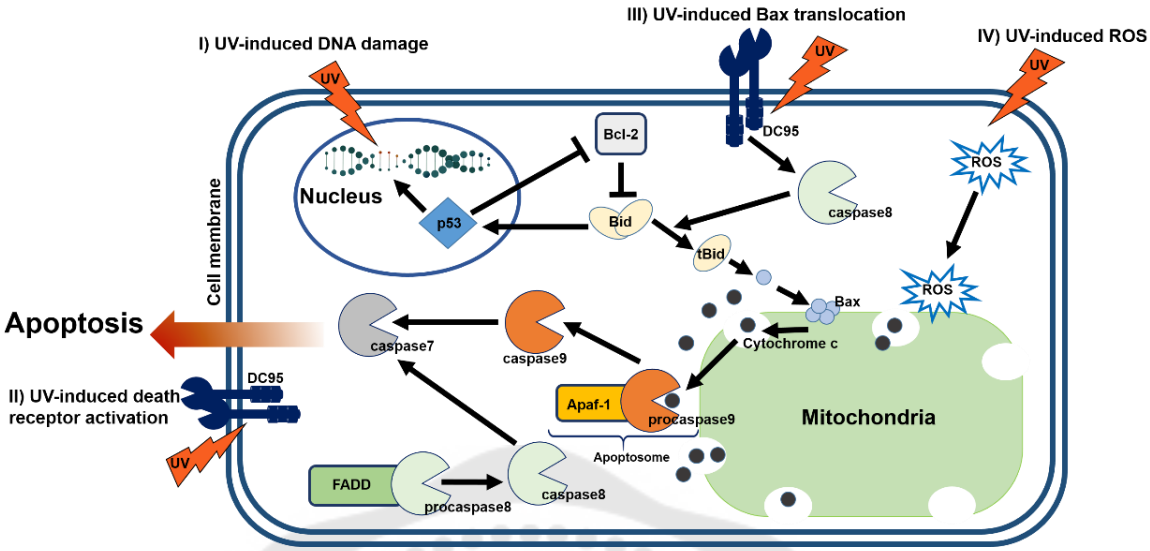

Figure 6 Diagram of cellular response to UV radiation through the apoptosis induction. (I) UV induces DNA damages; (II) UV activating death receptors (extrinsic pathway); (III) UV promote the Bax activity; (IV) UV induces overproduction of intracellular ROS, leads to apoptosis induction.

Source: Lee CH, Wu SB, Hong CH, Yu HS, and Wei YH. (2013). Molecular mechanisms of UV-Induced apoptosis and its effects on skin residential cells: the implication in UV-based phototherapy. International Journal of Molecular Sciences. p. 6418.

2.3.2.1.3 UV-induced sunburn inflammation

The major acute clinical effects of UV radiation on human skin are sunburn and inflammation. UV causes histological changes such as edema and perivascular infiltration [4]. Excessive exposure to UVB induces intracellular ROS leads to oxidative stress and play a critical role in the inflammatory response. This event leads to activating the nuclear factor kappa B (NF-ƙB) pathway [55]. NF-ƙB is a member of the Rel family proteins composed of heterodimer p50 and p65 subunits [56]. In a latent form, NF-ƙB is bound to the NF-ƙB inhibitor (IƙBα). The stimulation of ROS and cytokines consequence activating NF-ƙB and degradation of the IƙBα [56, 57]. The overproduction of intracellular

ROS promotes the p65 phosphorylation and active p65 translocation into the nucleus and enhance the expression of inflammatory cytokines such as COX-2, iNOS, IL-1, IL-6, and TNFα as shown in figure 7 [55]. The COX-2 is a rate-limiting factor, is convert arachidonic acid (AA) into prostaglandins (PGs) and prostaglandins E2 (PGE2). This change leading to an increase vascular permeability and promote inflammation and edema [58]. Normally, COX-2 highly inducible by infection and UVB exposure, serves as a marker of acute skin inflammation. UVB exposed HaCat cell line with high intrcellular ROS leads to an increase of the COX-2 levels [59]. Meanwhile, the production of TNFα, IL-1, and IL-6 enhance proliferation of keratinocytes mainly in stratum basale, which related to hyperplasia in the skin [60]. While UVB exposure enhances iNOS converts L-arginine and oxygen into citrulline and nitric oxide (NO). Moreover, the increased NO subsequently stimulates peroxynitrite ($ONOO^-$), which can react with superoxide radicals (O_2^-), to be more stable free radical and directly damage DNA molecules. This event has been linked to cell necrosis, cell injury and chronic inflammation [53, 55, 56, 61].

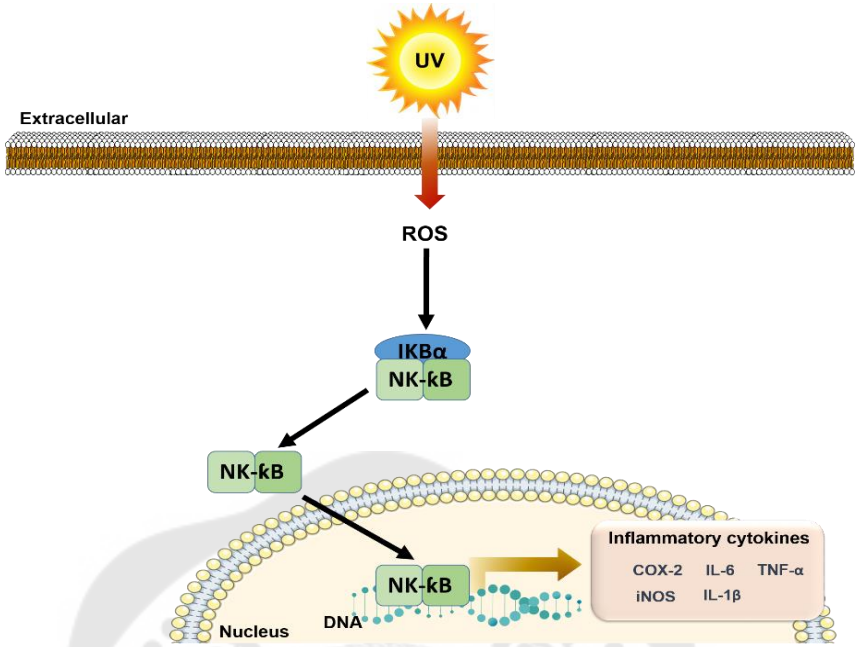

Figure 7 The inflammatory response of cell after UV exposure. Cells respond to UV irradiation by activating NF-ƙB translocate into the nucleus follow by transcript the inflammatory genes, which leads to cellular inflammation.

Source: Park J, et al. (2021). Heat treatment improves UV photoprotective effects of licorice in human dermal fibroblasts. Processes. p. 10.

2.3.2.2 Long-term UV effects on human skin

2.3.2.2.1 UV-induced skin photoaging

Around 80% of facial aging is due to the UV exposure. The characteristic of skin aging includes wrinkling, sagging, and skin laxity. Exposure to UV radiation, especially UVA is the primary factor of skin aging. Photoaging is caused by damage to the structural components of connective tissue, referred to the dermal extracellular matrix (ECM) of the dermis. The main function of ECM is to maintain the elasticity and hydration of the skin. Collagen type I and III in skin supported the tensile strength of the dermal tissue. UV exposure induces intracellular ROS mediating collagen degradation via the activation matrixdegenerating metalloproteases (MMPs) which play key role to degrade ECM. In addition, UV can activated various intracellular signaling including

MAPK and NF-ĸB signaling pathway which regulates the transcription of MMPs. Moreover, activation of AP-1 downregulates TGFβRII and decrease Smad signaling pathway resulting in the reduced *COL3A1* and *COL1A1* genes expression which encoded collagen type III and I. While glycosaminoglycans support strength, flexibility and maintain connective tissue hydration. Glycosaminoglycans is a long chain of polysaccharide component with hexuronic acid. UV destroys these structures through producing ROS via breaking the disaccharide backbone of GAG [42].

2.3.2.2.2 UV-induced skin carcinogenesis

Carcinogenesis is multiple step of gene mutation. The accumulation of mutant genes, especially genes that encode cell proliferation, cell differentiation, and cell death proteins, increase high risk on carcinogenesis. The uncontrolled proliferation and cell growth lead to carcinogenesis [4, 62]. UV radiation has been reported to cause several genes mutation in skin cells such as *p53, p19*, and *ras* genes. The evidence reported that non-melanoma skin cancer exerted p53 gene mutation found to be 50-90% frequency are mainly mutations of C to T and CC to TT transitions at dipyrimidine sites. In addition, UV radiation induced mutation of *patched* (*Ptc*), $p16^{INK4a}$, and $p19^{ARF}$ ($p14^{ARF}$) genes. In the basal cell carcinoma (BCCs) 41% frequency of *Ptc* gene mutation at chromosome 9q22-31 was found. While 75% gene mutations at $p16^{INK4a}$ and $p19^{ARF}$ was found in squamous cell carcinoma. Furthermore, UV radiation also induces skin carcinogenesis via Initiation of *ras* gene mutations [4].

2.4 Cell Cycle

Cell cycle composes of two main processes included DNA replication and segregation of replicated chromosomes into two daughter cells regulating DNA replication, cell division, and cell growth [63, 64]. The mitotic phase consists of five phases include prophase, metaphase, anaphase, and telophase. In this phase, cells divide nuclear and cytoplasm to make two new cells. Another is the interphase where cells synthesize biomolecules and replicate the DNA before entering the mitotic phase [63]. The interphase consists of G1, S and G2 phases. G1 phase, the cell is preparing biomolecules for DNA synthesis. Then, cells are transmitted to S phase for DNA

replication. G2 phase, the cell prepares biomolecules and replicated DNA for entering the mitotic phase. While non-proliferating cells exit from the G1 phase of the cell cycle to a quiescent state or a resting state referred to as G0 (Fig. 8) [64, 66].

To prevent accumulating genetic abnormalities in the cell cycle, each stage of the cell cycle is controlled with multiple regulatory proteins such as CDKs and cyclins. Briefly, CDKs bind to the specific cyclins, then cyclin-CDK complexes activate transforming in each stage. In case of DNA damage during cell cycle progression, CKIs arrest the cell cycle and trigger to repair the damage before resuming to cell division. The unrepairable damage is eliminated through apoptosis cell death [65].

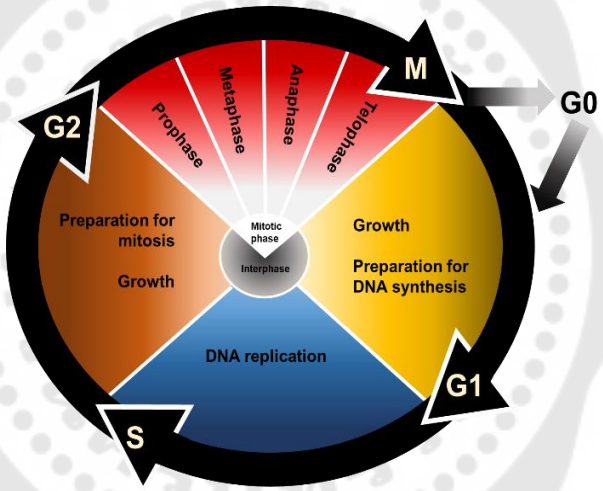

Figure 8 Cell cycle distribution. Cell division consists of the mitotic phase (M) and interphase. M-phase is divided into 5 phases; prophase, metaphase, anaphase, and telophase. While the interphase is divided into 3 phases; G1, S, and G2. G0 is the resting state.

Source: Wang Y, McIntyre C, and Mittar D. Cell cycle and DNA content analysis using the BD Cycletest assay on the BD FACSVerse™ system. Available from: https://www.bdbiosciences.com/content/dam/bdb/marketing-documents/BD_Instruments_FACSVerse_CellCycle_DNA_Analysis_AppNote.pdf.

2.4.1 Cyclin-dependent kinase (CDK) regulation

The cyclin-CDK complex regulates the progression of the cell cycle. The CDKs is a family of serine/threonine protein kinases consists of CDK1, CDK2, CDK4, and CDK6. To initiate cell progression, CDK activate the catalytic subunit of specific cyclin proteins in the cell cycle [64, 67]. CDK activation is required by two steps; 1) the binding between cyclin and CDK. 2) CDK activating kinase, called CAK, phosphorylate CDK on the Thr160 acts as positive regulation [68]. While, the negative regulation is controlled by Wee1-type protein kinases and myelin Transcription Factor 1 (Myt1), which phosphorylate inhibitory site of CDK at the Thr14 and Thr15 residues. The inhibitory effect is exerted until dephosphorylation by Cdc25 to activate CDK activity. Cdc25 is phosphatases serving as key regulators of the cell cycle consisting of three related proteins; Cdc25A, Cdc25B, and Cdc25C. Cdc25A regulates both early and late cell cycle transitions by activating the CDK2 activity whereas Cdc25B and Cdc25C have more limited roles in promoting progression from G2 phase to mitosis (Fig. 9) [48, 49, 51, 66].

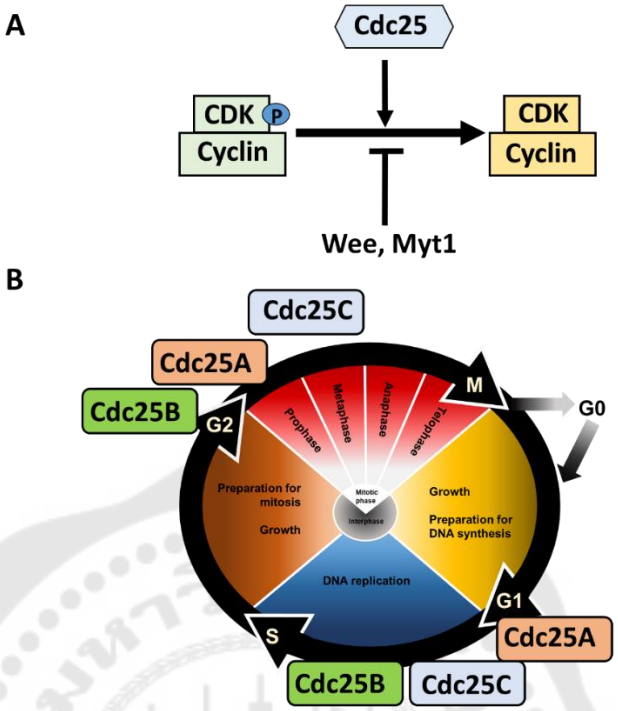

Figure 9 The Cdc25 phosphatases control cell cycle progression. A) CDK/cyclin activity is activated through Cdc25-dependent dephosphorylation. In contrast, the inactivation can be occurred by phosphorylation by the Wee1 and Myt1 kinases. B) The transition of cell cycle processes after activate CDK/cyclin complexes by three Cdc25 phosphatases.

Source: Boutros R, Dozier C, and Ducommun B. (2006). The when and wheres of CDC25 phosphatases. Current Opinion in Cell Biology. p. 186.

During the cell cycle, the specific cyclin proteins are required and increased in each phase [65]. The various types of cyclins are required at specific phases in the cell cycle. For example, D-CDK complexes are necessary to the entry in the G1 phase in the initiation of the cell cycle [69]. Cyclin D is not expressed periodically but is synthesized if growth factor stimulation persists. The Cyclin D-CDK complex phosphorylate the retinoblastoma leads to activating E2F which serve as a transcription factor triggers transcription of S phase promoting factors (SPF) genes such as cyclin A and cyclin E.

Then cyclin E bind to CDK2 to control the transition from G1 to S phase. In S phase, cyclin D and cyclin E is degraded by proteasome 26s. Then cyclin A binds to CDK2 and stimulates DNA replication. In late G2 phase and early mitotic phase, cyclin A complexes with CDK1 (Cdc2) to promote transition to mitotic phase. Mitosis is further regulated by cyclin B in complex with CDK1 (Table 3) [64, 69]. Cyclin B-CDK1 phosphorylate at the Thr14 and Thr15 of CDK1 resulting in activating Cyclin B-CDK1 activity leads to spindle fiber formation. At the end of cell division, cyclin B is degraded by proteasome 26s [51].

Table 3 Cyclin-CDK complexes and their activities

CDK	Cyclin	Cell cycle phase activity
CDK4	Cyclin D1, D2, D3	G1 phase
CDK6	Cyclin D1, D2, D3	G1 phase
CDK2	Cyclin E	G1/S phase transition
CDK2	Cyclin A	S phase
CDK1 (Cdc2)	Cyclin A	G2/M phase transition
CDK1 (Cdc2)	Cyclin B	Mitotic phase
CDK7	Cyclin H	CAK, all cell cycle phase

2.4.2 Cyclin-dependent kinases inhibitors

The CDK activity can be inhibited by CKIs via binding to CDK only and CDK-cyclin complex (Table 4). CKIs is divided into two families include INK4 and Cip/Kip family. The INK4 family proteins consist of p15 (INK4b), p16 (INK4a), p18 (INK4c), and p19 (INK4d), which specifically suppress CDK4 and CDK6 in G1 phase through binding to CDK proteins before the CDK-cyclin formation. This event is resulting in destabilizing the binding between cyclin and CDK. The Cip/Kip family protein consists of p21 (Waf1/Cip1), p27 (Cip2), and p57 (Kip2), which inactivate cyclin-CDK complexes, contributing to cell cycle arrest as shown in table 4 [64]. CKIs activities are occurring due

to the mistakes during the cell cycle process to trigger cell cycle arrest. However, if the mistake cannot be repaired, CKIs stimulate apoptosis cell death.

Table 4 The function of cyclin-dependent kinases inhibitors

CKI family	Function	Family members	
IKK4 family	Inactivation of G1 CDK	p15	(INK4b)
	(CDK4, CDK6)	p16	(INK4a)
		p18	(INK4c)
		p19	(INK4d)
Cip/Kip family	Inactivation of cyclin-CDK	p21	(Waf1, Cip1)
	complexes	p27	(Cip2)
		p57	(Kip2)

Normally, cells are resting in G0 phase without DNA replication until cells receiving transduction signals such as growth factors to promote cell proliferation. Cells exit from the G0 phase and enter the G1 phase. At this stage, the diploid cells have two complete sets of chromosomes (2N). After cells transit into the S phase, DNA replication is started. DNA synthesis is continuing until the DNA content increase into four complete sets of chromosomes (4N) in the G2 phase where cells prepare the macromolecules associated with mitotic phase such as maturation promoting factor (MPF); Cyclin B and CDK1. Followed by dividing cells into diploid daughter cells containing two complete sets of chromosomes (2N) [51, 66]. In contrast, if cells damage and cannot repair or senescence, program cell death or apoptosis is required. Then, DNA is cleaved into smaller fragments as oligonucleosomal-sized fragments and removed by phagocytosis [70]. Consequently, apoptotic cells contain lower DNA content than the living cells, which appear in sub-G1 peak in flow cytometer (Fig. 10) [71].

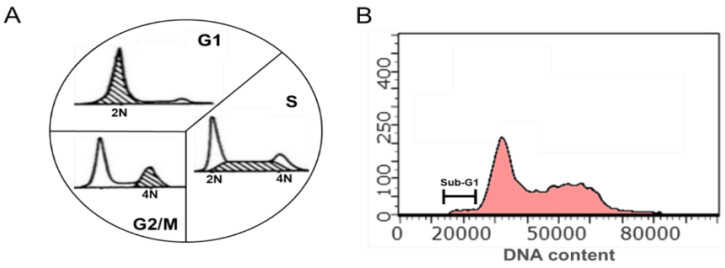

Figure 10 The histogram shows DNA content in the interphase. A) DNA content in G1/G0 phase, cells contain 2N amount of DNA. S-phase, the original cell is duplicate DNA, which increase amount of DNA from 2N to 4N. Once the cell has finished synthesizing, its DNA contains 4N of DNA in G2/M phase. B) In contrast, DNA fragments in apoptotic cells contain an amount of DNA less than 2N, called as Sub-G1 phase.

Source: Phoenix flow systems. Available from: http://www.phnxflow.com/MultiCycle.stand.alone.html

2.5 Apoptosis

Apoptosis is necessary in the essential physiological processes such as remodeling during fetal development and senescence. Furthermore, apoptosis serves as a homeostatic mechanism maintaining cell population through eliminated of aged, damaged, and mutant cells in the unicellular and multicellular organism [(72)]. In contrast, apoptosis is also involved in many diseases such as acute neurological injuries, cardiovascular diseases, and cancer [(73)]. Apoptosis is stimulated by both of exogenous and endogenous signals such as cytokines, UV radiation, stress, and chemicals [(74)]. This process can be characterized through morphological and biochemical changes such as cell shrinkage, chromatin condensation, exposing phosphatidylserine (PS) on the outer membrane, and apoptotic bodies [(73)]. The apoptotic bodies can be found in late apoptosis, are the budding of plasma membrane consist of cytoplasm packing with with/without a nuclear fragment which are eliminated through phagocytosis by neighboring phagocytic cells or macrophages without inflammatory reactions [(72)].

2.5.1 Morphology of Apoptosis

During apoptosis, cells present morphological changes, which can be observed under the microscopes. Chromatin condensation, cell shrinkage, and cytoplasmic condensation are the characteristic of cells in the early apoptosis. After that, cellular organelles are tightly packed into cytoplasm together with membrane blebbing with/without a nuclear fragment and form apoptotic bodies, referring to late apoptosis. The apoptotic bodies are subsequently engulfed and digested by phagocytic cells without stimulating inflammation [72]. In contract, necrosis is a pathological mode of cell death resulting in the inflammatory reaction. The different characteristics of morphological changes between necrosis and apoptosis is that necrosis induces cytoplasm and organelles swelling lead to cell lysis. The releasing cellular contents and cytokines in necrosis cells resulting in the inflammation reactions on the neighboring cells (Fig. 11) [75, 76].

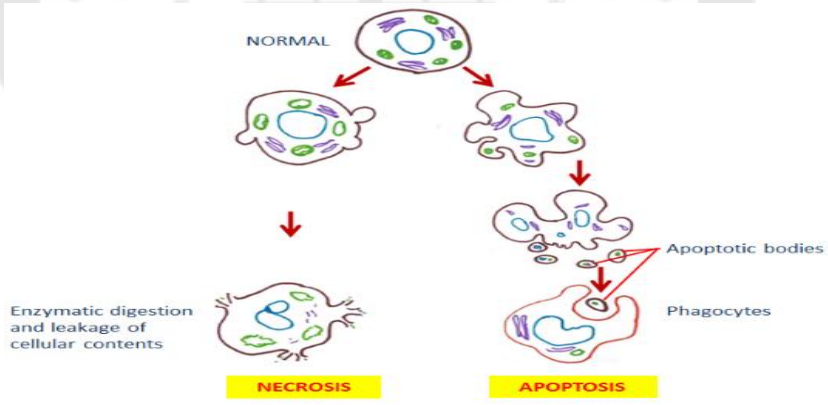

Figure 11 The characteristic of apoptosis versus necrosis. Left) present characteristic of necrotic cells; cell swelling, loss membrane integrity and releases cell contents. Right) Shows characteristic of apoptotic cells; nuclear being condense, cell shrinkage and blebbing, and breaks into apoptotic bodies. Finally, apoptotic bodies are eliminated by phagocytosis.

Source: Priante G, Gianesello L, Ceol M, Prete DD, and Franca Anglani F. (2019). Cell death in the Kidney. International Journal of Molecular Sciences. p. 2.

2.5.2 Biochemical change of apoptosis

Apoptotic cells demonstrate multiple biochemical modifications such as protein cleavage and phagocytic recognition. Caspase enzymes are one of the apoptosis markers. In a latent stage, the enzymes are present in an inactive proenzyme (procaspase) form. When apoptosis occur, the protease caspase cascade amplifis the apoptotic signaling through activators and effectors caspases pathway and resulting in rapid cell death [72].

2.5.3 Mediators of apoptosis

2.5.3.1 Caspases

Cysteinyl aspartate proteinases (Caspases) family proteins consist of 14 members [77]. Major caspases have been characterized into initiators (caspase2,-8,-9, and -10), effectors or executioners (caspase3,-6, and -7), and inflammatory caspases (caspase1,-4, and -5). First, caspase enzymes are synthesized as inactive zymogens consisting of p20 large subunit as a prodomain and p10 small subunit. Caspases, activated through proteolytic cleavage to remove prodomain, are divided into two groups: initiators caspases including caspase2,-8,-9, and -10 and effectors caspases or apoptosis executioner including caspase3, -6, and -7. The protein-protein interaction motifs in the prodomain of Initiator caspases consist of the death effector domain (DED), or caspase recruitment domain (CARD). These domains are associated with interacting with the upstream adapter molecules. Effector caspases , consisting of short prodomain, stimulate the cleavage of multiple cellular substrates such as PARP, PKCδ, ICAD, ROCK1, MST1, and transcription and translation initiation factors (Fig. 12) [55, 78-80].

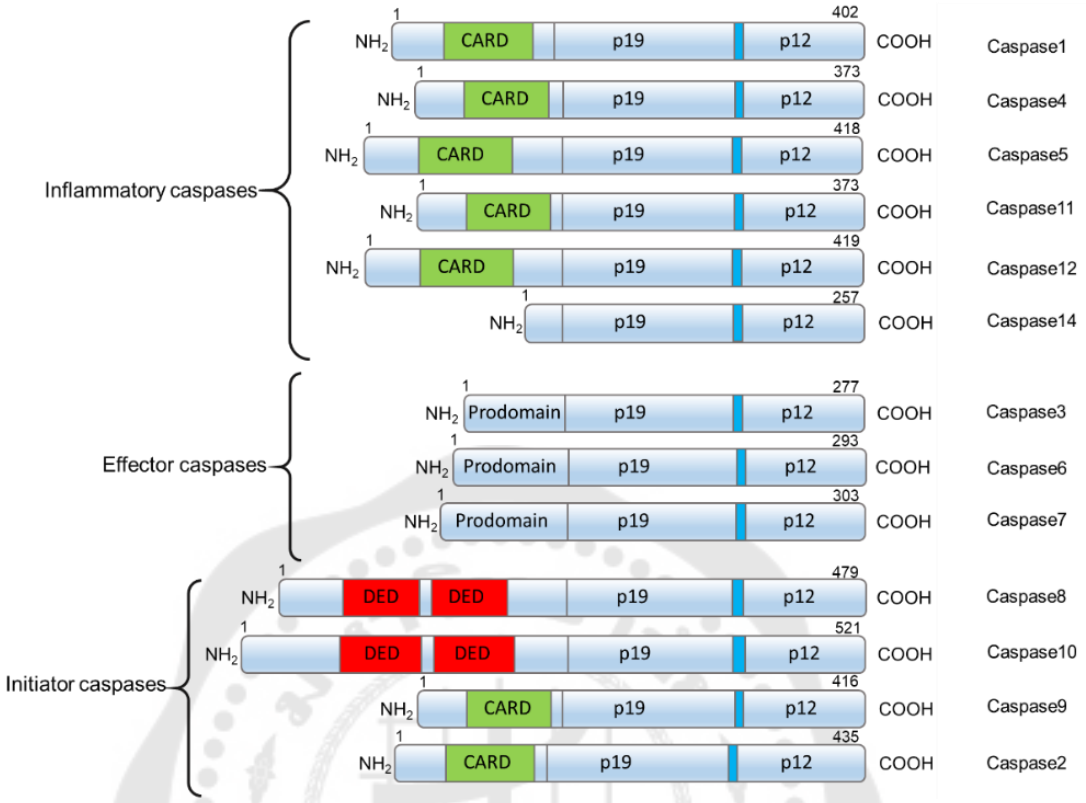

Figure 12 Structure and domain organization of mammalian caspases including; CARD, DED), the large (p20), and the small (p10) catalytic subunits are indicated

Source: Ribe EM, Serrano-Saiz E, Akpan N, and Troy CM. (2008). Mechanisms of neuronal death in disease: defining the models and the players. Biochemical Journal. p.166.

2.5.3.2 Bcl-2 family proteins

B-cell lymphoma 2 (Bcl-2) family proteins consist of 20 members which control apoptosis through promotion or suppression. The Bcl-2 family members have Bcl-2 homology domain as a conserved region include BH1, BH2, BH3, and BH4 domain. The Bcl-2 family is classified into three subfamilies according to the homology and functions of each protein. Group1 is prosurvival or Bcl-2 subfamily serve as anti-cell death such as Bcl-2, Bcl-xL, and Mcl-1. Proteins in this group consist of BH4 conserved domain which suppress cell death induction. In contrast, group 2 is proapoptosis or Bax

subfamily consists of homology BH1, BH2, and BH3 except BH4 domain. Proteins in this group function as apoptosis induction such as Bax and Bak. Group 3 is proapoptosis or BH3 subfamily consists of BH3 domain only such as Bid and Bik (Fig. 13) [81, 82].

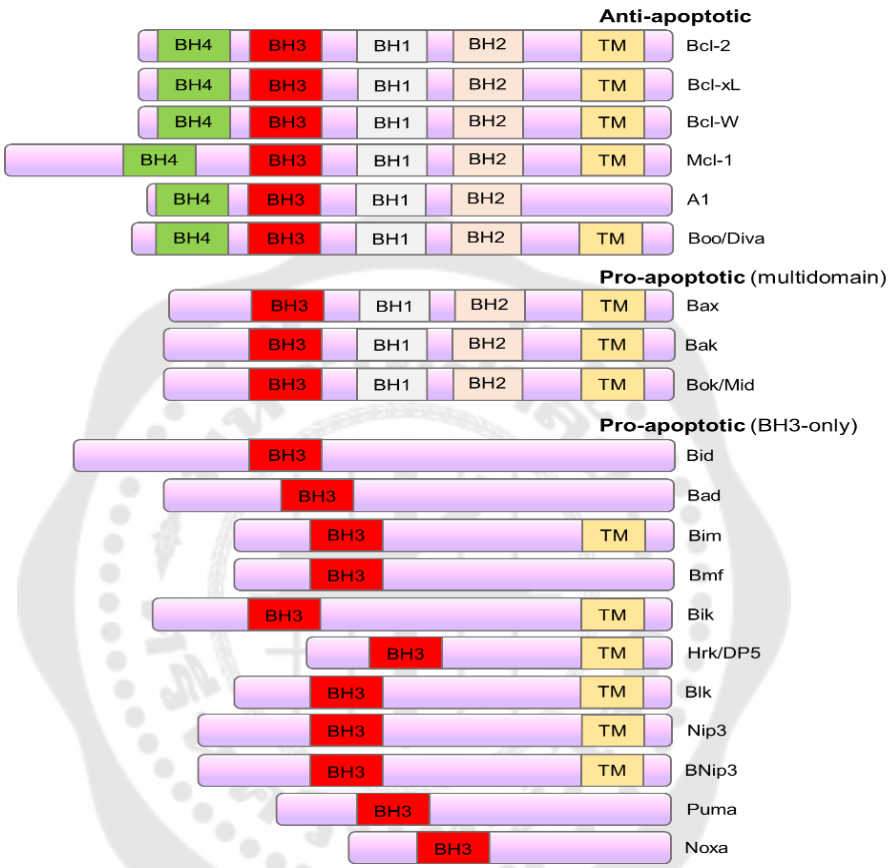

Figure 13 Members and domain structure of Bcl-2 family proteins. According to their activities. The general architecture of the proteins is shown; Bcl-2 homology domains (BH); Transmembrane domain (TM)

Source: Kuwana T and Newmeyer DD. (2003). Bcl-2-family proteins and the role of mitochondria in apoptosis. Current Opinion in Cell Biology. p.693.

The BH domains of Bcl-2 family proteins is essential for their activity. The BH4 domain serve as antiapoptosis molecules or death inhibition function. BH1 and BH2 plays an important role in death repression. Whereas BH3 consists of death promoters

which are essential for apoptosis induction [83]. The intrinsic apoptosis is mainly regulated by Bcl-2 family proteins. Once the imbalance between pro-and anti-apoptotic proteins is occurring by proapoptotic proteins (Bax and Bak) are increased and antiapoptotic proteins (Bcl-2 and Bcl-xL) are decreased led to the loss of the permeabilization mitochondrial membrane. Mitochondrial dysfunction leads to the releasing apoptosis induction molecules such as cytochrome c and activation of caspase cascade, respectively resulting in intrinsic apoptosis [84].

2.5.3.3 Poly (ADP-ribose) polymerase (PARP)

PARP is a family of proteins play an important role in cellular processes including chromatin modulation, recombination, and DNA repair. PARP proteins consist of 18 members localized in the nucleus. Many evidence support that PARP play a key role in DNA repairing. The genotoxic agents, oxidative stress, and radiation can induce DNA damage leading to the accumulation of DNA lesions and significantly increase in PARP activities in cells [85, 86]. PARP mainly repair single- and double-strand breaks (SSBs and DSBs) [87]. PARP1 and PARP2 are the best isoforms demonstrate DNA repair process. Several studies related DNA repair to PARP expression, referring to PARP1 isoform [87, 88]. In the DNA repair, PARP bind to DNA breaks with strong affinity. The nicotinamide adenine dinucleotide (NAD^+) is cleaved by PARP generating nicotinamide and ADP-ribose. Higher levels of ADP-ribose enhance long and branched chains of PAR formation. PAR covalently attached to receptor proteins and DNA repair proteins lead to the initiation of DNA repair mechanism (Fig. 14) [86].

In contrast, PARP is also widely known as the death substrate of various proteins such as calpains, cathepsins, granzymes, and especially effectors caspases (Fig. 13). PARP contains a protease cleavage site for caspase3 (DEVD) can be recognized and cleaved by caspases at this site. During apoptosis, PARP is cleaved by caspase7 and caspase3 into inactive form (cleaved-PARP). The cleaved-PARP separating into 2 fragments include 89 kDa and 24 kDa. This event contributes to suppress PARP activity because the 89 kDa fragment containing the catalytic domain. The loss catalytic domain of PARP leads to a reduction of DNA binding capacity and the

89 kDa fragment is translocated from the nucleus into the cytosol. While 24 kDa fragment consists of DNA-specific binding domain (DBD) which remained binding with DNA lesions. Thus, this event leads to irreversibly inhibits PARP activities and inhibits DNA repairing. Finally, cells are undergoing apoptosis [87, 88]. Thus, the expression of cleaved-PARP protein is popular to investigate apoptosis induction.

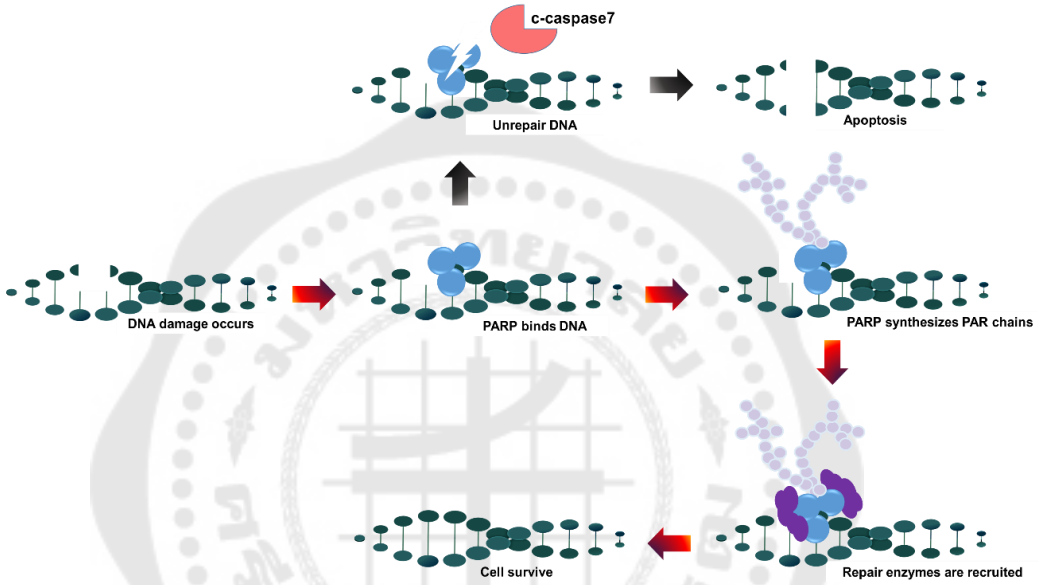

Figure 14 Mechanism of PARP on DNA repair. PARP recruit the protein involved in DNA repair, leads to DNA repairing and cell survival. However, cells undergoing apoptosis, PARP is inhibited via cleavage by caspase3/7.

Source: PARP screening and profiling services. Available from: https://scienceofparkinsons.com/2018/11/03/parp/.

2.5.4 The apoptosis signaling

Apoptosis pathway consists of two major pathways include extrinsic and intrinsic pathway. The extrinsic pathway is associated with death receptor, also known as a death receptor apoptotic pathway. This pathway can be activated through extracellular signaling, while the intrinsic pathway can be activated through the change of mitochondria [51].

2.5.4.1 The Extrinsic pathway

The extrinsic pathway is activated by the transmembrane death receptors (DRs) in TNFR Family proteins such as FasL/FasR, Apo3L/DR3, and Apo2L/DR5 [89]. The TNFR consist of cysteine-rich in the extracellular domain and death domain (DD) containing 80 amino acids in the cytoplasmic domain [90]. The death domain of DRs is important to induce apoptosis by transduction signal through the binding with adaptor proteins such as FADD, TNF receptor-associated death domain proteins (TRADD), and death domain-associated protein (DAXX). These adaptor proteins consist of DED homologous DED motif to procaspase8. The complex forming of Fas and FADD together with procaspase8 are called the death-inducing signaling complex (DISC). The DISC complex activates self-cleavage of procaspase8. The active caspase8 subsequently activates effector caspases (caspase3,-6, and -7) resulting in apoptosis induction (Fig. 15) [72, 91].

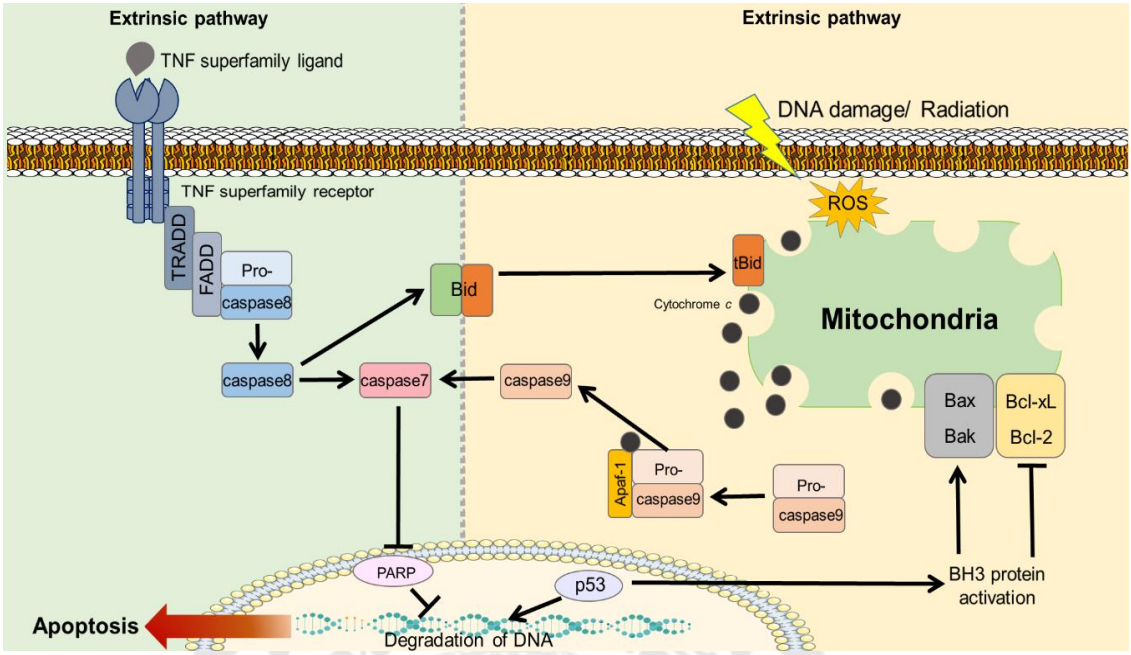

Figure 15 Overview of the extrinsic and intrinsic apoptosis pathways. Left) The extrinsic pathway is initiated by the binding of cell membrane receptor in TNF family, leads to the activation of downstream signaling proteins; FADD, TTRADD, and caspase8. Right) the intrinsic pathway, is initiated by radiation, DNA damage, and cellular stress causes BH3 activation, cytochrome c release, and caspase9 activation. Both pathways activate the effector caspase3/7 and promote apoptosis. In addition, cross-talk between extrinsic and intrinsic is activated by caspase8 leads to the translocation of tBid to mitochondrial membrane and activating intrinsic pathway.

Source: Yuan CH, Filippova M, and Duerksen-Hughes P. (2012). Modulation of apoptotic pathways by human papillomaviruses (HPV): mechanisms and implications for therapy. Viruses. p.3834.

2.5.4.2 The intrinsic pathway

The intrinsic pathway is activated by various molecules such as the absence of certain growth factors, UV radiation, toxins, hypoxia, DNA damage, and oxidative stress. This pathway affects directly primary cellular components and mitochondrial-initiated events. This activation leads to an imbalance of Bcl-2 family proteins by suppressing anti-apoptotic protein and increasing the pro-apoptotic proteins [92]. Proapoptotic proteins are oligomerized at the mitochondrial membrane. This event leads to depolarization of mitochondrial membrane potential resulting in the efflux of cytochrome c and AIF from the intermembrane space of mitochondria into the cytosol. After that, cytochrome c is associated with Apaf-1 together with procaspase9 in heptamer, called apoptosome. The apoptosome activates autocleavage of procaspase9 into an active form, cleaved-caspase9 which subsequently activating effectors caspases (caspase3,-6, and -7) resulting in apoptosis. (Fig. 15) [72].

Furthermore, the cross-talk between the extrinsic pathway and the intrinsic pathway can be activated through Bid activities. Bid protein is activated by caspase8 (extrinsic pathway) which cleavage Bid into 2 fragments include p17 (17 kDa) and p15 (15 kDa). The p15 is truncated Bid (tBid), translocate and insert into the mitochondrial outer membrane to produce mitochondrial pore and enhance the recruitment of cytosolic Bax into the mitochondrial membrane (intrinsic pathway) leading to cytochrome c release and caspase3/7 activation resulting in the apoptosis (Fig. 15) [72, 93].

2.6 Mitogen-activated protein kinase (MAPK) signaling pathway

MAPK is a protein Serine/threonine (Ser/Thr) kinases response to the extracellular signals such as mitogens, growth factors, stress, osmotic shock, UV radiation, and cytokines [51]. This signaling pathway leads to activate or inhibit some cellular mechanisms through regulating protein activities and genes expression, involving, survival, apoptosis, inflammation, development, and differentiation of cells [94]. MAPKs signaling pathway compose three enzymes cascade that is activated via series phosphorylation of MAPKK kinase (MAPKKK), MAPK kinase (MAPKK), and MAPK,

respectively [50]. The active MAPKKKs phosphorylated MAPKKs and MAPKs at the Thr and Tyr residue, respectively, to activation their activities. The classical MAPKs is consist of ERK1/2, JNK1/2/3, p38 isoforms, and ERK5. The ERK1/2, JNKs, and p38 are the most extensively studied groups in the mammalian cells (Fig. 16) [94, 95].

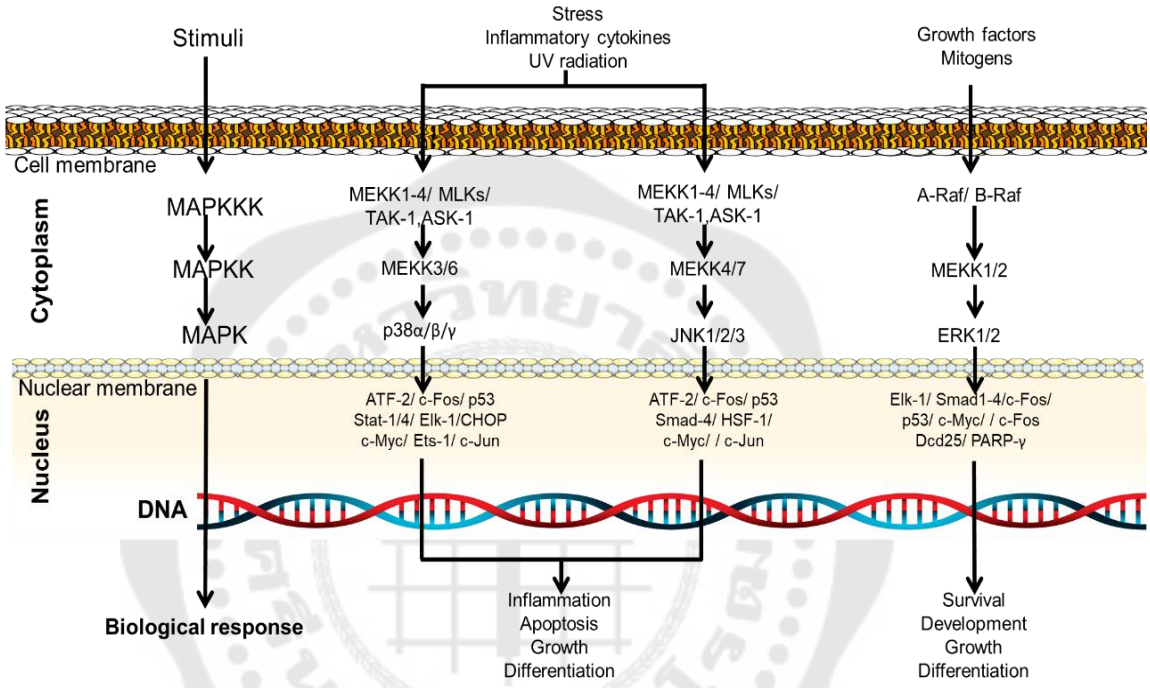

Figure 16 Schematic of the MAPK cascades and their nuclear targets. The MAPK core consists of three kinases (MAPKKK, MAPKK, and MAPK), which form a signal transduction cascade by phosphorylation. The MAPK cascade is stimulated by several stimuli including UV radiation, cytokines, growth factor, and mitogens. Each MAPKs regulating gene expression leads to various biological response of cells.

Source: Plotnikov A, et al. (2011). The MAPK cascades: Signaling components, nuclear roles and mechanisms of nuclear translocation. Biochimica et Biophysica Acta. p. 1621.

2.6.1 The extracellular signal-regulated kinases 1/2 (ERK1/2) signaling pathway

The ERK signaling pathway is a cascade of protein kinases, which play an important role in promoting growth, differentiation, and mitosis. This pathway can be stimulated by growth factors such as EGF, PDGF, and FGF. These signals are transmitted through cell surface receptor include tyrosine kinase receptor (TKR) and heterotrimeric G-protein coupled receptor (GPCRs). Then, the signal transduction is delivered via the phosphorylation of Ras/Raf proteins which serve as MAPKKK. The active MAPKKK activate MAP/ERK kinase1 and -2 (MEK1/2) and ERK1/2 through the phosphorylation at Ser residue of MAP/ERK, and Thr202 and Tyr204 residues of ERK1/2, respectively. ERK1 is 44 kDa and ERK2 is 42 kDa, thus ERK1/2 referring as p44/p42 MAPK. The activate ERK1/2 plays a key role to activate transcription factors such as Fos, Myc, ATF-2, Ets2, and STAT1/3 (Fig. 16) [51]. For example, the ERK1/2 signaling pathway regulates cell proliferation through Ras/Raf/MEK/ERK1/2 cascade to activate c-Myc, which controls the expression of genes in the cell cycle such as Cdc25 (Cdc25A, B, C). Moreover, ERK1/2 stabilizes c-Fos protein to promote AP-1 complexes and increases cyclin D1 expression in cell cycle progression, respectively [94]. In addition, the high level of c-Myc prevents the association of p27 with Cyclin E-CDK2 complexes. This event results in p27kip1 protein facilitating ubiquitination and degradation. In contrast, the reduction of ERK1/2 activity increases p27 and p15 expression to delay the G1/S transition of the cell cycle [50].

2.6.2 c-Jun amino (N)-terminal kinases 1/2 (JNK) signaling pathway

JNK is a stress-activated protein kinase (SAPK). JNK is activated mainly through stress signals such as UV radiation, ionizing radiation, oxidative stress, cytokines, and heat shock. The JNK family proteins consist of three JNK isoforms include JNK1, JNK2, and JNK3. JNK1/2 is widely distributed in tissue, whereas JNK3 is primary localized in the neuron, testis, and cardiac tissue. JNKs is activated by several MAPKKKs such as MEKK1-4, MLKs, Tpl-2, DLK, TAO1/2, TAK1, and ASK1/2. Then, MAPKKKs phosphorylate MAPKK, MKK4/7, and MAPKs; JNKs as a cascade. The active JNKs induce the activities of transcription factor such as p53, ATF-2, NF-ATc1,

Elk-1, HSF-1, STAT3, and c-Myc. JNK1/2 is plays important roles in the control of cellular responses through phosphorylation of AP-1 transcription factor subunit, c-Fos and c-Jun at Ser63 and Ser73 residues to promotes AP-1 activities and transcribe genes such as cyclinD1, Fas-L, MMP9, and COX-2 [94, 96, 97]. Chen, et al (2016) suggest that the JNK induces AP-1 activities through phosphorylation c-Jun and c-Fos proteins resulting in increases iNOS and COX-2 expression in the inflammatory response in LPS-induced RAW264.7 cells [97]. Furthermore, many reports suggest that UV induce apoptosis through activities of JNK to promote cytochrome C release [98]. Briefly, the prolonged JNK activation leads to the cleavage of Bid into tBid and 21 kDa fragment (jBid), which is a novel proteolytic fragment of Bid. The tBid and jBid translocate to mitochondria and promotes Bax activities and the Smac releasing lead to the inhibition of IAP-1 (Fig. 16) [98]. In addition, JNK regulates apoptosis via p53 mediated DNA damage responses. The active p53 acts as the transcription factor to transcribe proapoptotic genes such as Bax. Moreover, p53 increases the modulator of apoptosis (PUMA). Previous study reported that the UV responding of cells, the JNK signaling pathway is activated through enhancing c-Jun activities to promoting p53-mediated apoptosis [99].

2.6.3 p38 MAPK signaling pathway

p38 is a classical MAPK. The p38 MAPK is consists of 4 isoforms include p38α, p38β, p38γ, and p38δ. In mammalian cells, p38 is predominantly activated through environmental stresses such as oxidative stress, UV radiation, hypoxia, ischemia, IL-1, and TNFα. p38 is involving in the various physiological processes include apoptosis differentiation, proliferation, inflammation, and other stress responses. The p38 is activated by activation of MAPKKKs such as MAPKK1-4, MLK2, MLK3, DLK, ASK1, TPL2, and TAK1. Then, the active MAPKKKs phosphorylated MAPKKs including MKK3 and MKK6, and p38, respectively. The active p38 activates the substrates include cPLA2, MNK1/2, MK2/3, Bax, and Tau (cytoplasm), and ATF1/2/6, MEF2, Elk-1, Ets1, p53, and MSK1/2 (nucleus) (Fig. 16) [50, 94]. For example, a previous study reported that p38 plays important roles in UV-induced inflammation and apoptosis in skin cells

through increases COX-2, IL-6, and IL-8 as well as activates the translocation of Bax to mitochondrial membrane in apoptosis induction [100].

2.7 Akt Signaling Pathway

Akt is Ser/Thr protein kinase, also known as protein kinase B (PKB). Akt plays an important role in various processes such as cell proliferation, growth, angiogenesis, and migration. This pathway activated by growth factor, neuronal growth factor (NGF), UV radiation, heat shock, ischemia, hypoxia, and oxidative stress [101]. Akt has three isoforms include Akt1 (Aktα), Akt2 (Aktβ), and Akt3 (Aktγ). The Akt1 isoform found in the most tissue. The signals activate Akt through tyrosine kinase receptor (TKR) activation which lead to the activation of phosphatidylinositol 3-kinase (PI3K). PI3K phosphorylates phosphatidylinositol 4 phosphate and $PI(4,5)P_2$ to generate the second messengers $PI(3,4)P_2$ and $PI(3,4,5)P_3$, which lead to stimulation of cell survival through the PDK1/PKB mediated pathway. In addition, PDK1 activates Akt through the phosphorylation at Thr308 and Ser473. PDK1 is has a pleckstrin homology (PH) domain which binds to the second messengers $PI(3,4)P_2$ and $PI(3,4,5)P_3$ and leading to their membrane translocation. The PDK1 is activated Akt by phosphorylation resulting phosphorylation the numerous downstream substrates. For example, Activated Akt has phosphorylated Bad at Ser136 resulting Bad inhibition via the forming complex with Bcl-2/Bcl-xL proteins leading to block of releasing of cytochrome c from mitochondria, preventing activation of caspases. In addition, caspase9 has been reported to be phosphorylated on Ser196 by Akt resulting in attenuation of its activity and result in prevent apoptotic cell death [101]. Moreover, Akt also phosphorylate of forkhead box transcription factors (FOXO) to inhibit their activity leading to inhibition of FOXO-induce the expression of multiple proapoptotic members (Bcl2-family) and cell cycle inhibitory genes ($p21^{WAF}$ and $p27^{Kip1}$). In addition, Akt also phosphorylates p21WAF and p27Kip1 proteins resulting in cell cycle progression [102, 103]. In addition, Akt also stimulates cell cycle progression by stabilizing cyclin D1 expression which activates cellular proliferation [104]. Furthermore, Akt has the ability to phosphorylate GSK3 and PFK2 enzymes which activate metabolic processes necessary for growth such as glycogen biosynthesis. Akt can also activate NK-κB

through regulation of IκB (IKK) leading to the transcription of the prosurvival gene such as including Bcl-xL, caspase inhibitors, and c-Myb (Fig. 17) [101, 102, 105]. Thus, PDK1 and Akt are importent enzymes in the cell survival pathway, transduce cell growth and survival messages between cell compartments [102].

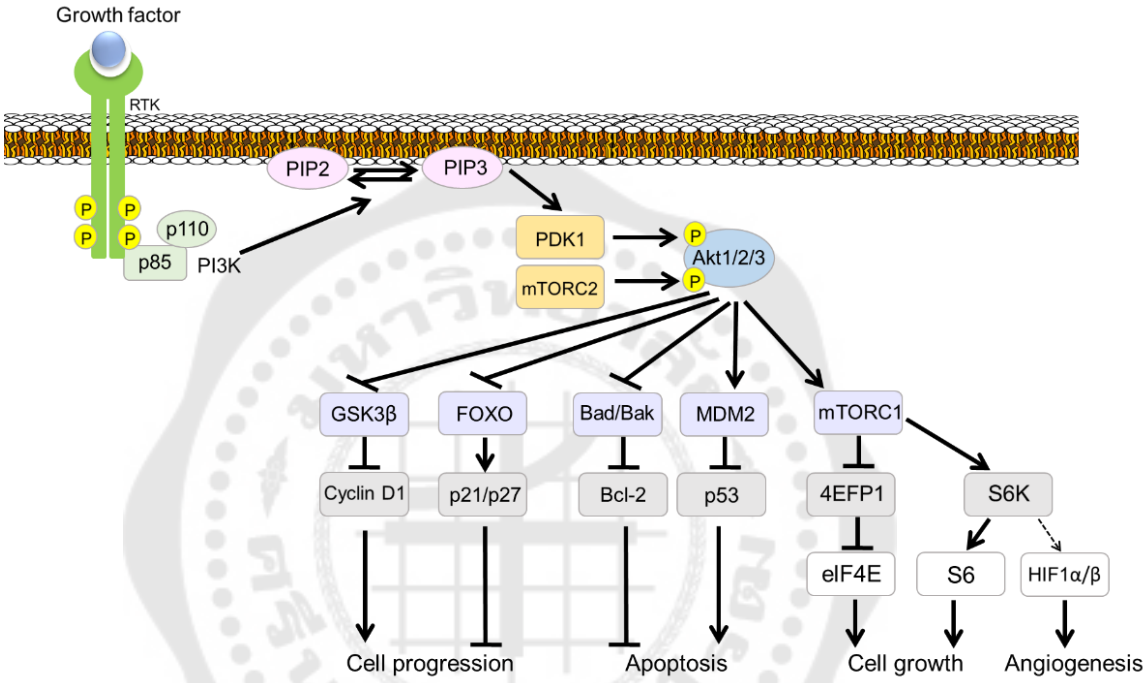

Figure 17 The overview of Akt signaling pathway. Receptor tyrosine kinase (RTK) induces PI3K activaties leads to synthesis of the second messengers PIP3, PIP2, PDK1 and mTORC2. p-Akt activates/inhibits several proteins involved in cell progression, apoptosis, cell growth, and angiogenesis.

Source: Klungsaeng S and Senggunprai L. (2020). Protein serine-threonine kinases as drug target in cancer treatment. Srinagarind Medical Journal. p. 492.

2.8 Purple corn silk (*Zea mays* L.)

Purple corn is a large grain plant in the Poaceae family. Purple corn is a pigmented variety of *Zea mays* L., originally cultivated in Latin America and was introduced in China. Nowadays, purple corn is a widely cultivated cereal around the

world. Many studies suggest that purple corn is an important source of anthocyanins, phenolic compounds, and carotenoid [106-109]. The anthocyanins and phenolic compounds are known that high-antioxidant activity. Ramos-Escudero F, et al (2012) found that the purple corn has antioxidant activity. The results showed that the purple corn extract reduced lipid peroxidation and increased CAT, GPx, and SOD activities in hydrogen peroxide-induced oxidative stress in mouse organs (mouse kidney, liver, and brain) [109]. In 2003, Zhang Z, et al. demonstrated that purple corn extract showed potential against fluoride-induced oxidative damage in livers and kidneys in rats. Moreover, the purple corn extract significantly inhibited pathological changes in cells included nuclear shrinkage, mitochondrial swelling, and vacuole formation. In addition, their results demonstrated that purple corn extract-treated rats significantly enhanced antioxidant enzymes (SOD and GPx) compared with the fluoride-treated alone. Meanwhile, purple corn extract also reduced the decreasing of Bcl-2 protein expression and the increasing of Bax protein expression in cells induced by fluoride [108]. While, Fukamachi K, et al (2008) exhibited that the purple corn extract and its major component, cyanidin 3-O-β-d-glucoside (C3G), significantly inhibited DMBA-induced mammary carcinogenesis. In addition, purple corn extract and C3G inhibited cell survival rate and increased apoptosis in mammary tumor cells derived from human c-Ha-ras proto-oncogene transgenic (Hras128) rats through induced of caspase3 activity and reduced Ras protein levels in tumor cells [110].

Corn silk is an agricultural waste. It is a part of stigma/style or female flower of corn silk, commonly known as “corn/maize silk or stigma maydis”. It has been used in traditional Chinese medicine for treatment of various diseases such as edema, prostate disorder, and urinary infections [9]. Moreover, in China, Japan, Korea, the USA, and France also modified the corn silk to cosmetics ingredients in cosmetics formulation, tea, and corn powder [14]. The previous studies reported that corn silk contains proteins, vitamins, carbohydrates, flavonoids, and is rich in phenolic compounds such as anthocyanins, p-coumaric acid, vanillic acid, protocatechuic acid, and quercetin [9, 10].

Ebrahimzadeh MA, et al (2008) demonstrated that corn silk extract has antioxidant properties when compared with the standard compounds, butylated hydroxytoluene; BHT and quercetin analysis by using DPPH assay, were found IC_{50} value at 0.59, 0.053, and 0.025 mg/mL, respectively [10]. Furthermore, Olaniyan MF, et al (2016) suggested that corn silk extract increased the GPx and CAT in corticosterone-induced oxidative stress in rabbits [111]. While, in 2013, Nessa F, at el. reported that the corn silk extract against pathogenic bacteria such as *Bacillus cereus*, , *Staphylococcus aureus*, *Pseudomonas aeruginosa*, *Enterobacter aerogenes*, *Salmonella typhi*, *Escherichia coli*, and one yeast *Candida albicans* [112]. Furthermore, the maysin from the corn silk reduced intracellular ROS level, inhibited PARP cleavage, inhibit DNA damage via increased mRNA levels of antioxidant enzymes in a dose-dependent manner [13]. In the same year, Lee J, et al. demonstrated that maysin isolated from the corn silk induced apoptosis in prostate cancer PC-3 cell line through reducing the cell viability, Bcl-2 and procaspase3 levels. Furthermore, a combined treatment between maysin and other known anticancer agents include fluorouracil (5-FU), etoposide, cisplatin, and camptothecin, synergistically enhanced PC-3 cell death [12]. While, Choi SY, et al. demonstrated that corn silk extract decreased melanin production, was found to be 37.2% inhibition without cytotoxicity in cells. This result showed corn silk extract had higher efficiency than arbutin (whitening agent), which exhibited 26.8% inhibition at the same concentration. However, they suggested that the corn silk extract did not suppress tyrosinase activities but greatly decreased the protein expression of tyrosinase enzyme in Melan-A cells. In addition, the application of corn silk extract on faces with hyperpigmentation volunteers significantly reduced skin pigmentation [15].

The purple corn silk is a style present purple color, is rich in fiber, anthocyanins, and flavonoids. When compare phytochemicals and antioxidant activity between corn silk from purple waxy corn, white waxy corn, sweet corn, and baby corn found that purple waxy corn silk showed the highest phenolics, flavonoids, and anthocyanins content, and antioxidant activities [14]. Chaiittianan R, et al. (2017) reported that purple corn silk extract contains anthocyanins, quercetin, and phenolic acids as major

components. Moreover, purple corn silk extract showed potential against obesity in adipocytes cells (Mouse 3T3-L1) via significant inhibited preadipocyte proliferation and decreased total lipid accumulation. At the same time, the purple corn silk extract induced lipolysis and apoptosis through enhanced the releasing of glycerol content and increased nuclei condensing and apoptotic bodies in cells [113]. Recently, Rimdusit, et al. (2019) demonstrated that cob and silk extract from purple waxy corn is abundant with anthocyanins. They found that cob and silk extract increased collagen production in human skin fibroblast cells [114]. However, the purple corn silk is an agricultural waste without value and is not popular for the development of commercial skincare products. Furthermore, the study of hydroglycolic purple corn silk extract on UVB-induced cell damage in human keratinocytes has not yet been reported.

CHAPTER 3
METERIALS AND METHODS

3.1 Conceptual framework

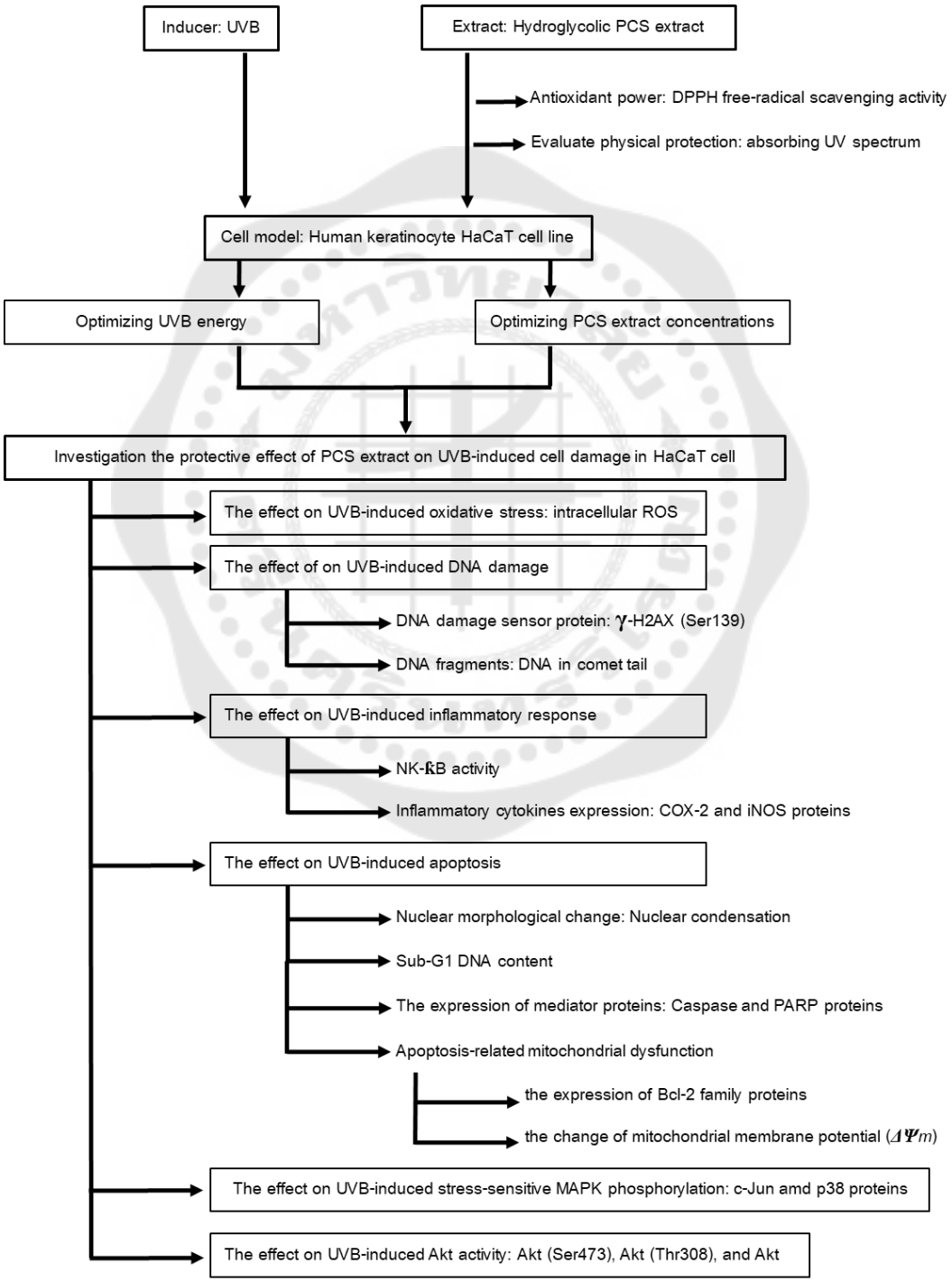

3.2 Material and Chemical reagents

Dulbecco's modified Eagle's medium (DMEM) medium, penicillin-streptomycin, bovine serum albumin, 0.25% trypsin-EDTA, and fetal bovine serum (FBS) were purchased from HiMedia (HiMedia, Mumbai, India), MTT was purchased from USB Corp (USB Corp, USA), dimethyl sulfoxide (DMSO) was purchased from RCI Labscan (RCI labscan CO., Thailand), polyvinylidene difluoride membrane (PVDF), EDTA, β-mercaptoethanol, bromophenol blue, trypan blue, glycine and phenylmethylsulphonyl fluoride (PMSF), DPPH, L-ascorbic acid was purchased from Sigma (Sigma-Aldrich, USA), SYBR® gold fluorescent dye, TEMED, sodium dodecyl sulfate (SDS), 40% acrylamide, immobilon Western chemiluminescent-HRP substrate, guava cell cycle® reagent, and 2',7'-dichlorofluorescin diacetate (DCFH-DA) dye were purchased from Merck Millipore (Merck Millipore Corp., Germany), JC-1 and H33342 dye were purchased from Thermo Fisher Scientific (Invitrogen™, Thermo Fisher Scientific Inc., USA), mouse monoclonal antibodies; γ-H2AX (Ser139) and β-actin were purchased from Merck Millipore were purchased from Merck Millipore (Merck Millipore Corp., Germany), rabbit monoclonal antibodies; NF-ƙB, COX-2, c-PARP/PARP, Cleaved-caspase9/Caspaes9, Cleaved-caspase7/Caspaes7, Bax, Bak, Bcl-2, Bcl-xL, p-p38, p38, p-c-Jun, c-Jun, p-Akt (Ser473), p-Akt (Thr308), and Akt were purchased from Cell signaling (Cell signaling Technology, Danvers, MA), Mouse monoclonal antibodies; Cleaved-caspase8/Caspaes8 was purchased from Cell signaling (Cell signaling Technology, Danvers, MA), anti-mouse and rabbit IgG conjugated with HRP secondary antibody, and anti-mouse IgG conjugated with FITC fluorescent dye were purchased from Cell signaling (Cell signaling Technology, Danvers, MA), anti-rabbit IgG conjugated with Alexa fluoro546 fluorescent dye was purchased from Thermo Fisher Scientific (Invitrogen™, Thermo Fisher Scientific Inc., USA), mini protease inhibitor cocktail was purchased from Roche (Roche Diagnostics GmbH, Germany) protein assay kit was purchased from Bio-Red (Bio-Red Lad, USA), tris-base was purchased from Vivantis (Vivantis, USA), and triton X-100 was purchased from Pharmacia (Pamacia, Sweden).

3.3 Preparation of purple corn silk (PCS) extract

The crude PCS extract is purple stigma of *Zea mays* L., obtained from Prof. Dr. Malyn Ungsurungsie, S & J International Enterprises Public Company Limited, Bangkok, Thailand. The fresh purple stigma was harvested from Khonkaen province in March, 2014 (Voucher sample Number 050914T001). The extraction was following previously published [115]. Briefly, the fresh purple corn silk was dried at 50°C and ground. Then, the crude powder was immersed in propylene glycol (PG): water at 50% PG (10% W/V) for 2 days and was filtered through the cheesecloth and filter paper Whatman No.4, respectively. After that, the PCS extract was evaporated and kept in 4°C before use[116]. The PCS extract was dissolved in dimethyl sulfoxide (DMSO) for experiments. The crude extract were dissolved in 100% DMSO at the stock concentration of 200 mg/ml for experiments.

3.4 Measurement of antioxidant activities

The antioxidant activity of PCS extract was carried out by 2,2-Diphenyl-1-(2,4,6-trinitrophenyl) hydrazyl (DPPH) assay base on the colorimetric method described by Oliveira, et al (2019) [7]. Briefly, 100 μL PCS extract at a concentration of 0, 0.2, 0.4, 0.6, 0.8, and 1 mg/mL were added in 96-wells plate. Then, PCS extract was mixed with 100 μL of 65 μM DPPH solution. L-ascorbic acid at a concentration of 0, 0.005, 0.01, 0.02, 0.04, 0.08, and 0.1 mg/mL was used as standard antioxidant agent. The mixture was placed for 30 min in the dark and the absorbance was measured at 517 nm by using a microplate reader spectrophotometer (Multiskan Sky, Thermo Fisher Scientific Inc., USA). A negative control solution 100 μL of methanol mixed with 100 μL of DPPH were used. The results demonstrated that L-ascorbic acid, a positive control agent showed strong antioxidant activity with the EC_{50} values of 0.009 mg/mL. While the PCS extract showed antioxidant activity in a dose-dependent manner, which presented EC_{50} values at 0.53 mg/mL as shown in figure 18.

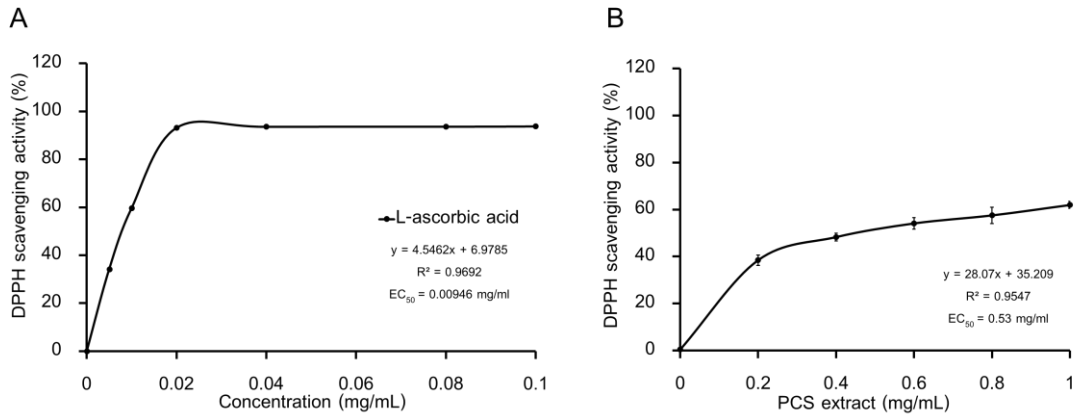

Figure 18 The DPPH scavenging activity of A) L-ascorbic acid and B) PCS extract.

.

3.5 Cell culture

Spontaneously immortalized human keratinocyte (HaCaT) cell line was obtained from American Type Culture Collection (ATCC, Manassas, VA). The cells were maintained as a monolayer in Dulbecco's modified Eagle's medium (DMEM) supplemented with 10% fetal bovine serum (FBS), 100 U/mL penicillin and 100 μg/mL streptomycin at 37°C in a humidified atmosphere of 5% carbon dioxide (CO_2).

3.6 Ultraviolet-B (UVB) irradiation system and UVB-irradiation on HaCaT cells

The UVB light source for the studies is a UV incubator (Vilber UV Bio-Sun, Vilber Lourmat, France). There are consist of two UV sources (4 x 30 W 365 nm and 2 x 30 W 312 nm) and cooled UV irradiation system. Irradiation distance was 25 mm and the irradiation stopped automatically when the energy received matches the programmed energy. Before UVB irradiation, cells were covered with thin layer of phosphate buffer saline (PBS) and irradiated without plastic dish lid. While, the non-UVB group, cells were treated the same conditions without UVB exposure. After UVB irradiation, cells were returned to medium and subsequent experiments.

3.7 Cell viability assay

MTT assay is based on a colorimetric principle to assess the mitochondrial reductase enzymes activity, indicating cell viability. This enzyme is found in viable cells, which can reduce MTT (yellow color) to generating solid formazan crystal in purple color. In contrast, dead cells lack this enzyme resulting in yellow color without formazan crystal production. The solid formazan crystals can be dissolved in DMSO, present as the purple color solution, which absorbs a range wavelength at 570 nm correlate with survival rate of cells.

To determine the cytotoxicity of PCS extract on HaCaT cells, cells were seeded in a 96-wells plate (0.7×10^4 cells/well) and incubated overnight. Then, cells were treated with various concentrations of PCS extract (0-1 mg/mL) in complete medium while the control group was treated with 0.5% DMSO for 24 h. After that, the medium was removed and 0.5 mg/mL MTT solution was added to each well and incubated at 37°C for 2-4 h. Then, the MTT solution was removed and DMSO was added into each well, respectively. The absorbance was measured at 570 nm by using the spectrophotometer (UV/visible, Biotek Epoch). The percentage of cell viability was calculated related to the non-treated group. Finally, the PCS extract at concentrations of 0.3, 0.5, and 1 mg/mL were chosen for the subsequent experiments.

Phototoxicity of UVB radiation on HaCaT cells was determined by using MTT assay. Cells were seeded in 35-mm dish (3×10^5 cells/well) and incubated overnight, then exposed to UVB in a serial of UVB energy (0-50 mJ/cm^2) and incubated in complete medium for 24 h, respectively. While the control group was treated with 0.5% DMSO for 24 h without UVB exposure (Non-UVB group). After treatment, the medium was removed and 0.5 mg/mL of MTT solution was added to each well and incubated at 37°C for 2-4 h. After that, the MTT solution was removed and DMSO was added into each well. The absorbance was measured. The percentage of cell viability was compared with the non-UVB group. Then, the UVB energy was chosen at 25 mJ/cm^2 for the next experiment.

The protective effect of PCS extract on UVB-induced cell death on HaCaT cells was investigated by using MTT assay. The cells were seeded in 35-mm dish (3 x10^5 cells/well) and incubated overnight. Then, cells were pretreated with 0.3, 0.5, and 1 mg/mL of PSC extract or 0.5% DMSO for 1 h before 25 mJ/cm^2 UVB exposure. After that, cells were subsequently incubated in the medium for 24 h. While the control group (non-UVB group) were treated with 0.5% DMSO without UVB exposure for 24 h. After treatment, the medium was removed and 0.5 mg/mL MTT solution was added into each well and incubated at 37°C for 2-4 h, respectively. Then, the MTT solution was removed and replaced with DMSO into each well. The protective effect of PCS extract on UVB-induced cell death was assessed as % of cell viability compared with non-UVB group.

3.8 Intracellular ROS Measurement

Intercellular reactive oxygen species (ROS) is associated with the generation of oxidative stress and inducible lipids, proteins, and DNA damage [29]. Thus, intracellular ROS is considered as a biomarker for detecting oxidative stress which detected by using the cell-permeable dichlorodihydrofluorescein (DCFH-DA) dye. This dye permeabilize into the cells as a non-fluorescent form before deacetylation by cellular esterase enzymes and oxidized to a highly fluorescent compound as DCF by intracellular ROS, respectively. The DCF-fluorescence signals was detected by using a fluorescence spectroscope or flow cytometer at maximum excitation of 495 nm and emission of 529 nm.

The intracellular ROS in HaCaT cells was determined by DCFH-DA assay. Briefly, the cells were seeded in 35-mm dish (3 x10^5 cells/well) and incubated overnight. Cells were pretreated with 0.3, 0.5, and 1 mg/mL of PCS extract or 0.5% DMSO for 1 h and exposed to 25 mJ/cm^2 UVB, respectively. After UVB irradiation, cells were subsequently incubated 20 μM DCFH-DA for 30 min. Acetate group was removed from DCFH-DA by esterase enzyme and DCFH-DA was oxidized by intracellular ROS generated green-fluorescence of DCF, respectively. After staining, cells were washed with PBS twice and the images were acquired by using a fluorescence microscope

(IX71, Olympus, Japan). The relative fluorescence intensity compared with the non-UVB group was quantified by using Image J densitometer.

3.9 Immunofluorescence staining

The immunofluorescence staining is to detect the expression of interested biomolecules. Currently, this method is popular to investigate localization of cellular protein including γ-H2AX, serve as a sensor of DNA damage and NF-ƙB translocation to analysis inflammatory response. This method is based on the affinity between antibodies against target proteins. The antibodies is conjugated with fluorescent dyes. The protein expression is through fluorescence signals observed under a fluorescence microscope.

To determine the γ-H2AX (Ser139) localization and the translocation of NF-ƙB, immunofluorescence staining was carried out. Briefly, cells were seeded in 35-mm dish (3 x10^5 cells/well) and incubated overnight. Then, cells were pretreated with 0.3, 0.5, and 1 mg/mL of PCS extract or 0.5% DMSO for 1 h before 25 mJ/cm^2 UVB exposure. While the non-UVB group was treated with 0.5% DMSO without UVB exposure. After that, cells were incubated in medium for 1 h and 24 h to analysis of NF-ƙB translocation and γ-H2AX (Ser139) localization, respectively. After treatment, cells were fixed with absolute ice-cold methanol for 10 min. Then, cells were washed with PBS for 3 times and blocked non-specific proteins with 3% FBS (in PBS) for 60 min, respectively. Then, cells were incubated with a primary antibody against NF-ƙB (1:250 dilution), and γ-H2AX (Ser139) (1:250 dilution) at 4°C overnight. Then, cells were incubated with secondary antibody conjugated with Alexa fluoro546 (1:500 dilution) for NF-ƙB detection or secondary antibody conjugated with FITC (1:500 dilution) for γ-H2AX (ser139) detection for 60 min. After incubation, the nucleus were stained with hoechst33342 dye for 30 min. Images were acquired by using a fluorescence microscope (IX71, Olympus, Japan).

3.10 Alkaline single-cell gel electrophoresis (SCGE, Comet assay, pH > 13)

The Comet assay or SCGE is a standard method for assessing DNA damage [117]. Briefly, cells were embedded in agarose gel on a Comet slide. The embedded cells were lysed to degrade the cell membrane, cytoplasm, and nuclear membrane by using lysis buffer. Then, the DNA fragments were separated by using electrophoresis. After electrophoresis, the DNA in the Comet slide was stained with fluorescent dye and observed under a fluorescence microscope. The comet tail length depends on the migration of DNA fragments.

The assay was modified from Calò R and Marabini L [118]. Briefly, the Comet slide was modified by pre-coat slide with 1% normal melting-point agarose gel and placed at 4°C for 10 min before use. To determine DNA damage in HaCaT cells, cells were seeded in 35-mm dish (3 $x10^5$ cells/well) and incubated overnight. Cells were pretreated with 0.3, 0.5, and 1 mg/mL of PCS extract or 0.5% DMSO for 1 h and exposed to 25 mJ/cm^2 UVB, respectively. While the non-UVB group was treated with 0.5% DMSO without UVB exposure. Then, cells were incubated in medium for 24 h. After treatment, cells were collected by trypsinization and centrifuged at 2,000 rpm for 5 min, respectively. Cells were prepared by counting to 3 x 10^5 cells in 500 μL fresh medium. The cell suspension was mixed with 0.5% low-melting-point agarose and transferred onto pre-coated slides. The slides were kept at 4°C for 10 min. After that, the slides were immersed in lysis buffer solution (2.5 M NaCl, 100 mM Na-EDTA, 10 mM Tris-base, and 250 mM NaOH, pH 10) at 4°C for 1 h. The cells were immersed in ice-cold alkaline unwinding solution or electrophoresis buffer (300 mM NaOH and 1 mM EDTA, pH 13.0) in a Comet tank and the electrophoresis was performed at 0.3 A for 30 min at 4°C. Then, the slides were washed with neutralizing solution and fixed with absolute ethanol for 5 min. After fixation, the slides were stained with SYBR® gold for 10 min, and rinsed with distill water for 5 min for 3 times, respectively. The migration of DNA fragments was visualized using a fluorescence microscope (IX71, Olympus, Japan). The percentage of

DNA in the comet tail in each sample was quantified by Image J plugin OpenComet (version 1.3.1).

3.11 Nuclear morphological change assay

The nuclear condensation, membrane blebbing, and apoptotic bodies are characteristics of cells undergoing apoptosis. Hoechst33342 staining fluorescent dye is a permeable DNA stain, which binding to A-T rich of double-strand DNA. Cells present characteristics of apoptosis marker are showing the blue-brightness of Hoechst33342 in nuclei which are easily identified under a fluorescence microscope.

The protective effect of PCS extract on UVB-induced chromatin condensation in HaCat cells was determined by Hoechst33342 staining. Briefly. The cells were seeded in 35-mm dish (3 $x10^5$ cells/well) and incubated overnight. Then, cells were pretreated with 0.3, 0.5, and 1 mg/mL of PCS extract or 0.5% DMSO for 1 h. After that, cells were exposed to 25 mJ/cm^2 UVB while the non-UVB group was treated with 0.5% DMSO without UVB exposure. Then, cells were incubated in medium for 24 h. After treatment, the Hoechst33342 dye was added to each well with 5 μg/mL and incubated at 37°C for 30 min. The stained cells were observed under a fluorescence microscope (IX71, Olympus, Japan). The average percentage of nuclear condensed cells compared with the non-UVB group was quantified using OPTIKA PROView software Version 5.0 (OPTIKA, Srl, Italy).

3.12 Cell cycle analysis

Cell cycle is characterized into 2 phase including interphase; G0, G1, S, G2, and mitotic phase. The interphase, cells contain duplicate DNA represented the change of DNA contents during DNA synthesis [(119)]. At the interphase, the chemicals, radiation, and stress can disturbed DNA synthesis leading to the changing of DNA content in each phase. This event can be monitored by probing the DNA with a fluorescent dye and analyzed by using a flow cytometer. The fluorescent dye widely used is propidium iodide, which interacts with DNA and absorbs in ranges wavelength at fluorescence excitation 535 nm and emission 615 nm. The flow cytometer sort the fluorescence

intensity correlated with amounts of DNA in cells and represents DNA content in each phase as a histograms.

The sub-G1 content in HaCaT cells induced by UVB was determined by a flow cytometer. The cells were seeded in 35-mm dish (3 x10^5 cells/well) and incubated overnight. Then, cells were pretreated with 0.3, 0.5, and 1 mg/mL of PCS extract or 0.5% DMSO for 1 h and exposed to 25 mJ/cm^2 UVB, respectively. While the non-UVB group was treated with 0.5% DMSO without UVB exposure and incubated for 24 h. Then, cells were harvested and centrifuged at 2,000 rpm for 3 min. After that, cell pellets were fixed with 70% cold-ethanol before flow-cytometry analysis. Then, cells were washed and stained with Guava cell cycle® reagent for 30 min, respectively. The percentage of sub-G1 content was determined by using a Guava EasyCyte™ flow cytometer and GuavaSoft™ software (Merck Millipore Crop., Merck KGaA).

3.13 Detection of mitochondrial membrane potential

ATP synthesis is an important function of mitochondria to produce cellular energy. Furthermore, the mitochondria contain protein-related apoptosis such as cytochrome c and AIF. During apoptosis, mitochondria lose membrane potential and release cytochrome c to the cytosol. Cytochrome C is associated with Apaf-1 and form as the apoptosome. This event activate caspase9 and -7 activities resulting in apoptosis. Thus, the mitochondrial membrane potential is considered as apoptosis marker [120]. JC-1, a lipophilic cationic fluorescent dye, is used to detect mitochondrial membrane potential. In healthy cells, JC-1 forms complex as a J-aggregates and presents red fluorescence signals. In contrast, in unhealthy cells, JC-1 remains monomeric with a green fluorescence signals.

To investigate the change of mitochondrial membrane potential ($\Delta\Psi m$) on UVB-induced cell damage in HaCaT cells. The cells were seeded in 35-mm dish (3 x10^5 cells/well) and incubated overnight. Then, cells were pretreated with 0.3, 0.5, and 1 mg/mL of PCS extract or 0.5% DMSO for 1 h and exposed to 25 mJ/cm^2 UVB, respectively. While the non-UVB group was treated with 0.5% DMSO without UVB

exposure. Then, cells were incubated in medium for 24 h. After treatment, JC-1 dye was added to each well at final concentration of 5 μg/mL for 10 min. Then, the cells were washed with PBS for 3 times followed by observation under a fluorescence microscope (IX71, Olympus, Japan). The relative red-fluorescence intensity compared with non-UVB group was quantified by Image J densitometer.

3.14 Western blot analysis

Western blotting is a powerful technique for investigating protein expression. Briefly, protein samples were separated by using SDS-polyacrylamide gel electrophoresis (SDS-PAGE) and transferred onto a PVDF membrane, respectively. Then, the proteins on PVDF membranes were probed with the specific primary antibodies and secondary antibodies conjugated with enzymes such as horseradish-peroxidase (HRP), respectively. The protein expression was enhanced the chemiluminescence signals by using chemiluminescence ECL regent and detected under gel documentary consists of CCD camera.

3.14.1 Sample preparation

Cells were seeded in 35-mm dish (3 x10^5 cells/well) and incubated overnight. Then, cells were pretreated with 0.3, 0.5, and 1 mg/mL of PCS extract or 0.5% DMSO for 1 h before exposed to 25 mJ/cm^2 UVB. While the non-UVB group was treated with 0.5% DMSO without UVB exposure. Then, cells were incubated in medium for 1 or 24 h. After treatment, cells were harvested by scraping and lysed with RIPA lysis buffer (50 mM Tris-HCl, 5 mM EDTA, 250 mM NaCl, 0.5% Triton X-100, pH 7.5) containing 10 mM PMSF and complete with mini protease inhibitor cocktail. After that, the supernatant was centrifuged at 13,000 rpm at 4°C for 30 min. Protein lysates were transferred to a new 1.5 mL tube and the concentration of protein samples was determined by using a Bradford's assay kit.

3.14.2 Protein determination

The concentration of total proteins was determined by Bradford's assay kit. BSA was used as a standard protein diluted with Milli Q water at concentrations of 0.2, 0.4, 0.6, 0.8, and 1 mg/mL, while the protein samples were diluted in a ratio of 1:10.

After protein preparation, 10 μL of the sample proteins and standard BSA was added into a new 1.5 ml tube and mixed with 190 μL of Bradford's solution before measuring the absorbance at 595 nm by using spectrophotometer (Thermo Fisher Scientific Inc., MA, USA), respectively. Then, protein samples were mixed with 5X sample dye (60 mM Tris-HCl, 25% glycerol, 2% SDS, 14.4 mM β-mercaptoethanol, and 0.1% bromophenol blue) and boiled at 100°C for 5 min. The protein samples were kept at -20°C before being used.

3.14.3 SDS-PAGE and Immunoblotting

SDS-PAGE is a technique for separating proteins in an acrylamide gels under electrophoresis condition leads to the migration of proteins from anode to cathode. In general, the acrylamide gels consists of two-part of include a stacking gel for packing proteins in a base line before start electrophoresis. And, a separating gel is a part of proteins separating were begin, based on molecular weight of proteins.

3.14.3.1 Separating gel

The percentage of polyacrylamide gel in this layer depends on the molecular weight of interested proteins. The proteins with low molecular weight suit to separate in a high percentage of polyacrylamide gel, while a high molecular weight suit to separate in the low percentage of the polyacrylamide gel. The separating gel was prepared to follow the reference table 5.

Table 5 Separating gel preparation (0.375 M Tris-HCl, pH8.8)

Stock solution	10%	12%
dH_2O	2.42 ml	2.17 ml
1.5 M Tris-HCl, pH8.8	1.25 ml	1.25 ml
10% SDS	50 μl	50 μl
40% acrylamide	1.25 ml	1.5 ml
10% ammonium persulfate	25 μl	25 μl
TEMED	2.5 μl	2.5 μl
Total volume	**5 ml**	**5 ml**

3.14.3.2 Stacking gel

After preparation the separating layer, the stacking gel is loaded between two glass plates in a gel caster. In this layer, proteins lysates is packed and migrated at the same position. The preparation of stacking gel is followed a reference table 6. After loading the stacking gel, the combs is suddenly inserted. After gel completely polymerized, the comb was removed. The proteins lysate is loaded to the gel and start electrophoresis, respectively.

Table 6 Stacking gel preparation (4% polyacrylamide gel, 0.125 M Tris-HCl, pH6.8)

Stock solution	4%
dH_2O	1.52 ml
1.0 M Tris-HCl, pH8.8	0.25 ml
10% SDS	20 μl
40% acrylamide	0.196 ml
10% ammonium persulfate	10 μl
TEMED	2 μl
Total volume	**5 ml**

20 μg protein of each samples were loaded into the stacking gel followed by electrophoresis at 100 V for 1.30 h in running buffer (0.025 M Tris-HCl, 0.192 M glycine, and 0.1% SDS). Then, the electrophoresis gels were transferred onto PVDF membrane by using Trans-Blot Cell® (Bio-Red Lad, Hercules, CA, USA) at 100 V for 2 h in transfer buffer (0.025 M Tris-HCl, 0.192 M glycine, and 20% methanol). After that, the membranes were washed with TBST buffer (10 mM Tris-HCl, 150 mM NaCl, and 0.1% tween, pH7.5) and blocked non-specific bands with 5% skim milk in TBST for 1 h, respectively. After blocking, the membranes were washed with TBST for 10 min for 3 times before probed with a specific primary antibody against COX-2, iNOS, NF-ƙB, γ-H2AX (Ser139), c-PARP/ PARP, Cleaved-caspase8/ Caspaes8, Cleaved-caspase9/ Caspaes9, Cleaved-caspase7/ Caspaes7, Bax, Bak, Bcl-2, Bcl-xL, p-p38, p38, p-c-Jun,

c-Jun, Akt (Ser473), Akt (Thr308), Akt, and β-actin at dilution of 1:1000 at 4°C overnight. After incubation times, the membranes were washed with TBST for 10 min for 3 times and probed with secondary antibody conjugated with HRP (1:10,000 dilution) for 1 h. The immunoreactive protein bands were detected by adding enhanced chemiluminescent ECL reagent and exposed to a CCD camera in a gel documentary (UVITEC, Alliance Q9 Advanced, Cambridge, UK). The protein band intensity compared with non-UVB group was quantified using Image J densitometer.

3.15 Statistical analysis

All of the data were presented as mean±standard deviation (SD) in three independent experiments ($n=3$). The fluorescence and band intensity was quantified by using an Image J densitometer. The percentage of DNA tail in Comet assay was examined by Image J plugin OpenComet (version 1.3.1). Data statistical analysis was performed by SPSS version 20.0 (SPSS, Inc.). Statistical significance comparisons were calculated by one-way analysis of variance (ANOVA) followed by Tukey's *post hoc* test. The difference was considered statistically significant at $p<0.05$, $p<0.01$, and $p<0.001$.

CHAPTER 4
RESULTS

4.1 UV-absorbing properties of PCS extract

The solar UV radiation exposure to the Earth's surface ranges between the wavelengths of 290-400 nm, divided into UVB (280-320 nm) and UVA (320-400 nm). Generally, the epidermal skin layer acts as a first line of defense against solar UV through absorbing and reducing photons in UV radiation. Thus, UV-absorbing is one of the main properties of sunscreen agents or skincare products to minimize the effects of UV on skin cells. The absorbance data showed that 1 mg/mL of PCS extract (in 100% DMSO) absorbs ranges wavelengths both UVB and UVA spectrum. While, 100% of DMSO which performed as a control group showed slightly absorb in range of UVB spectrum (Fig. 19). This data indicated that PCS extract could prevent UVB energy from entering skin cells. Thus, we suggested that PCS extract might be a new candidate as a physical UV protection agent. Subsequently, we investigated the biochemical UV protection properties of PCS extract in keratinocyte HaCaT cells.

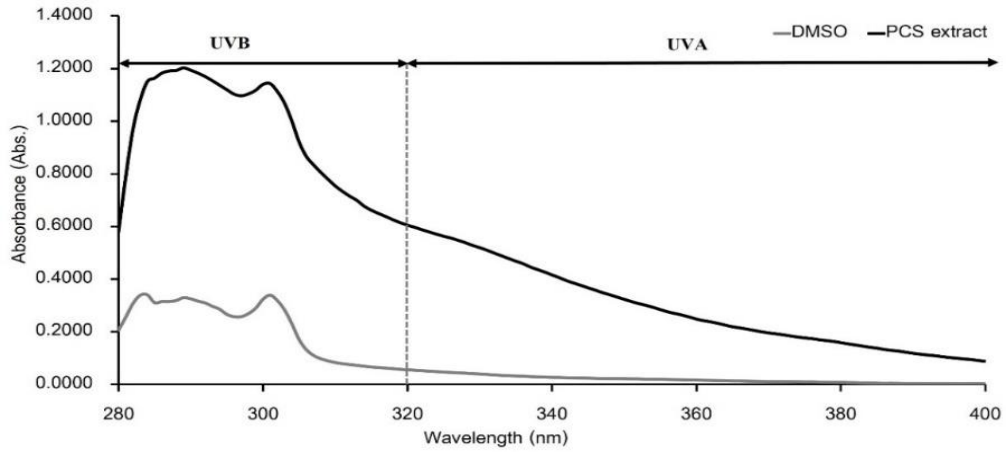

Figure 19 UV-absorbing of PCS extract in UV-spectrum. The Gray-line shows UV-absorbing of DMSO, it was used as a control group. The Black-line shows UV-absorbing of PCS extract at 1 mg/mL (in DMSO). The UV-absorbing was measured every 1 nm covering a range of wavelengths between 280-400 nm by using a spectrophotometer.

4.2 Cytotoxicity of PCS extract and UVB-irradiation in HaCaT cells

Before investigating the UV protection properties of PCS extract in keratinocyte HaCaT cells, the cytotoxicity of PCS extract and UVB radiation in HaCaT cells was assessed by using MTT assay. The results showed that after cells treatment with PCS extract at the maximal concentration at 1 mg/mL for 24 h obtained 94.0±0.41% cell viability when compared with the non-treated cells, indicating PCS extract is safe for application in keratinocyte HaCaT cells (Fig. 20A). Then, we optimized UVB energy irradiated in HaCaT cells for the next experiments. The phototoxicity of UVB radiation in HaCaT cells was assessed by MTT assay. The results showed that serial UVB energy decreased survival rate of cells in an energy-dependent manner as shown in figure 20B. Based on these results, we performed using 25 mJ/cm^2 of UVB radiation with 63.15±2.494% cell viability and the PCS extract was used at 0.3, 0.5, and 1 mg/ml for subsequent experiments.

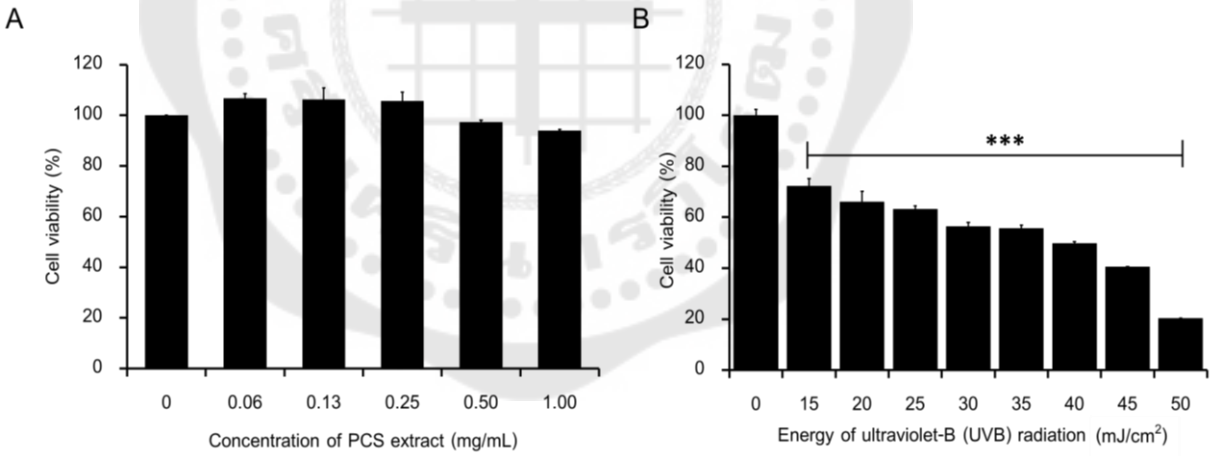

Figure 20 The cytotoxicity of PCS extract and UVB-radiation in HaCaT cells. HaCaT cells were treated with various concentrations of PCS extract (0-1 mg/mL) or a serial of UVB energy (0-50 mJ/cm^2), then cells were incubated for 24 h and the percentage of viable cells was examined by MTT assay, respectively. A) Shows cell viability of HaCaT cells after treated with PCS extract. B) Shows cell viability of HaCaT cells after treated with UVB radiation. Data are mean values±SD (*n=3*). *** $p< 0.001$ *vs*. non-UVB group.

4.3 Effect of PCS extract on UVB-induced cytotoxicity in HaCaT cells

After we optimized the concentrations of PCS extract and UVB radiation, we monitored morphological changes of cells by a phase-contrast microscope. The results revealed cell shrinkage and membrane blebbing after cells exposed to UVB compared with the non-UVB group. Whereas pretreated-HaCaT cells at various concentration of 0.3, 0.5, and 1 mg/mL prevented the morphological change in cells induced by UVB as shown in figure 21A. Additionally, the results showed that cells pre-treated with PCS extract for 1 h before UVB exposure showed significantly inhibited cell death induction, which presented cell survival rate as 72.66±2.59%, 75.42±0.68%, and 79.10±1.87% cell viability, respectively. While the UVB-control group was found to be 58.19±1.31% cell viability (Fig. 21B). These results imply that PCS extract prevents HaCaT cell death from UVB radiation.

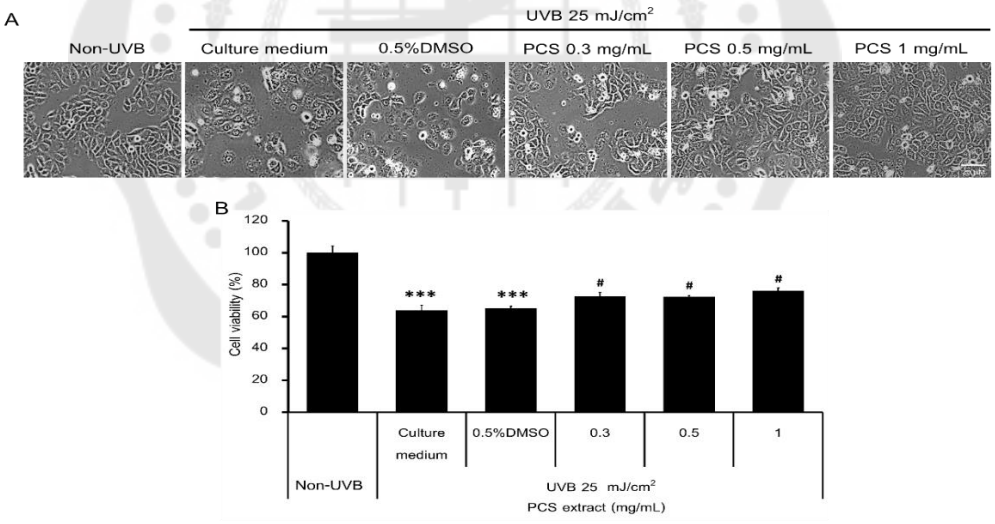

Figure 21 Shows the preventive effect of PCS extract against UVB-induced cell death. HaCaT cells were treated PCS extract for 1h, then cells were exposed to 25 mJ/cm^2 UVB. After irradiation, cells were placed in the medium for 24 h and the percentage of cell viability was determined by MTT assay, respectively. A) Shows an image of HaCaT cells observed by using a phase-contrast microscope. B) Histogram shows cell viability of HaCaT cells. Data are mean values±SD (*n*=3). *** $p< 0.001$ *vs*. non-UVB group and # $p< 0.05$ *vs*. UVB-control group.

4.4 Effect of PCS extract on UVB-induced intracellular ROS in HaCaT cells

Several reports demonstrated that UV radiation increases intracellular ROS levels in skin cells. The overproduction of intracellular ROS leads to oxidative damages. Thus, we investigated the effect of PCS extract on UVB-induced intracellular ROS in HaCaT cells by using fluorescent DCFH-DA dye. The results demonstrated that UVB radiation strongly increased intracellular ROS levels, were found the relative DCF-fluorescence intensity to be 5.92±0.41 fold of the non-UVB group. However, the PCS extract at 0.3, 0.5, and 1 mg/mL significantly attenuated intracellular ROS levels compared to the UVB-control group. The relative DCF-fluorescence intensity was found to be 3.41±0.32, 3.27±0.65, and 2.17±0.35 fold of the non-UVB group, respectively (Fig. 22). These results suggest that the PCS extract inhibit UVB-induced oxidative stress in keratinocyte HaCaT cells through directly decreased intracellular ROS production.

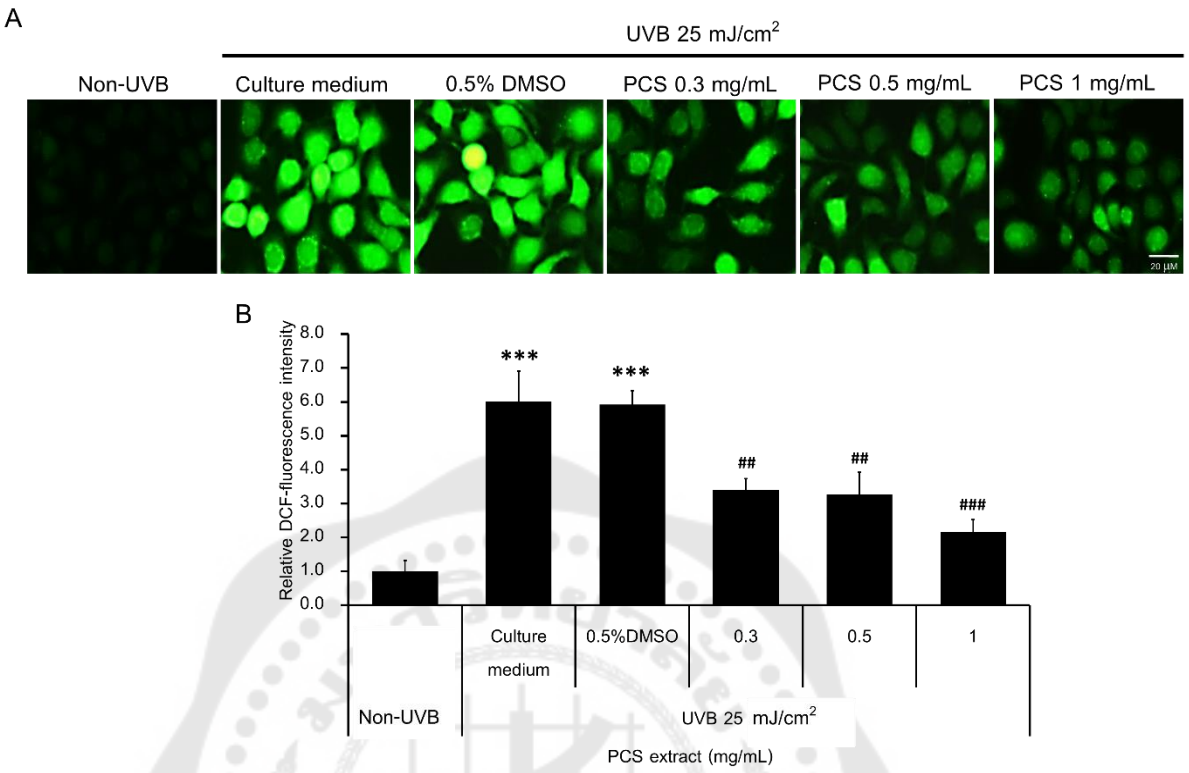

Figure 22 Shows the radical scavenging effect of PCS extract on UV-induced intracellular ROS production. After UVB irradiated, cells were stained with 20 µM of DCFH-DA fluorescent dye for 30 min and the DCF-fluorescence signal was visualized by a fluorescence microscope. A) Shows DCF-fluorescence signal (green-color) in HaCaT cells observed by using a fluorescence microscope. B) Histogram represents the average relative DCF-fluorescence intensity values, which was quantified by Image J densitometer. Data are mean values±SD (*n=3*). *** $p< 0.001$ *vs.* non-UVB group and ## $p< 0.01$; ### $p< 0.001$ *vs*. UVB-control group.

4.5 Effect of PCS extract on UVB-induced DNA damage in HaCaT cells

Then, we evaluated the effect of PCS extract on UVB-induced DNA damage by using immunofluorescence staining and Western blot analysis to examine γ-H2AX (Ser139) levels, and Comet assay. γ-H2AX (Ser139) serves as a DNA damage sensor. The presence of γ-H2AX activates DNA repair, cell cycle arrest, and apoptosis. Thus, we studied the effect on UVB-induced DNA damage by analyzing phospho-H2AX (Ser139) localization and protein expression using immunofluorescence staining and Western blotting, respectively. The results demonstrated that γ-H2AX (Ser139) significantly increased in nuclei in UVB-irradiated cells compared with the non-UVB group, presenting green-fluorescence (FITC). While PCS extract significantly decreased γ-H2AX (Ser139) nuclei accumulation compared with the UVB-control group as shown in figure 23A. In addition, Western blot analysis also showed that UVB induced γ-H2AX (Ser139) protein levels which can be suppressed by PCS extract (Fig. 23B). The Comet assay was conducted to confirm that the decreasing of γ-H2AX (Ser139) in cells was not caused by lacking DNA repair mechanisms. Comet assay is based on the migrating DNA fragments of a single cell under electrophoresis conditions. The Comet tail distance referred to the movement of DNA fraction. The results showed that UVB significantly increased DNA in tail (%) to 15.18±6.04% compared with the non-UVB group (3.19±2.05%). In contrast, 0.3 and 0.5 mg/mL of PCS extract slightly decreased DNA tail (11.18±3.96 and 9.07±4.61%%), while 1 mg/mL of PCS extract significantly inhibited DNA damage, was found the percentage of DNA in tail to 4.35±1.75% (Fig. 23C and D). These results indicate that PCS extract decrease UVB-induced DNA damage in keratinocyte HaCaT cells. However, the effect on DNA repair mechanism in HaCaT cells induced by UVB needs further studies.

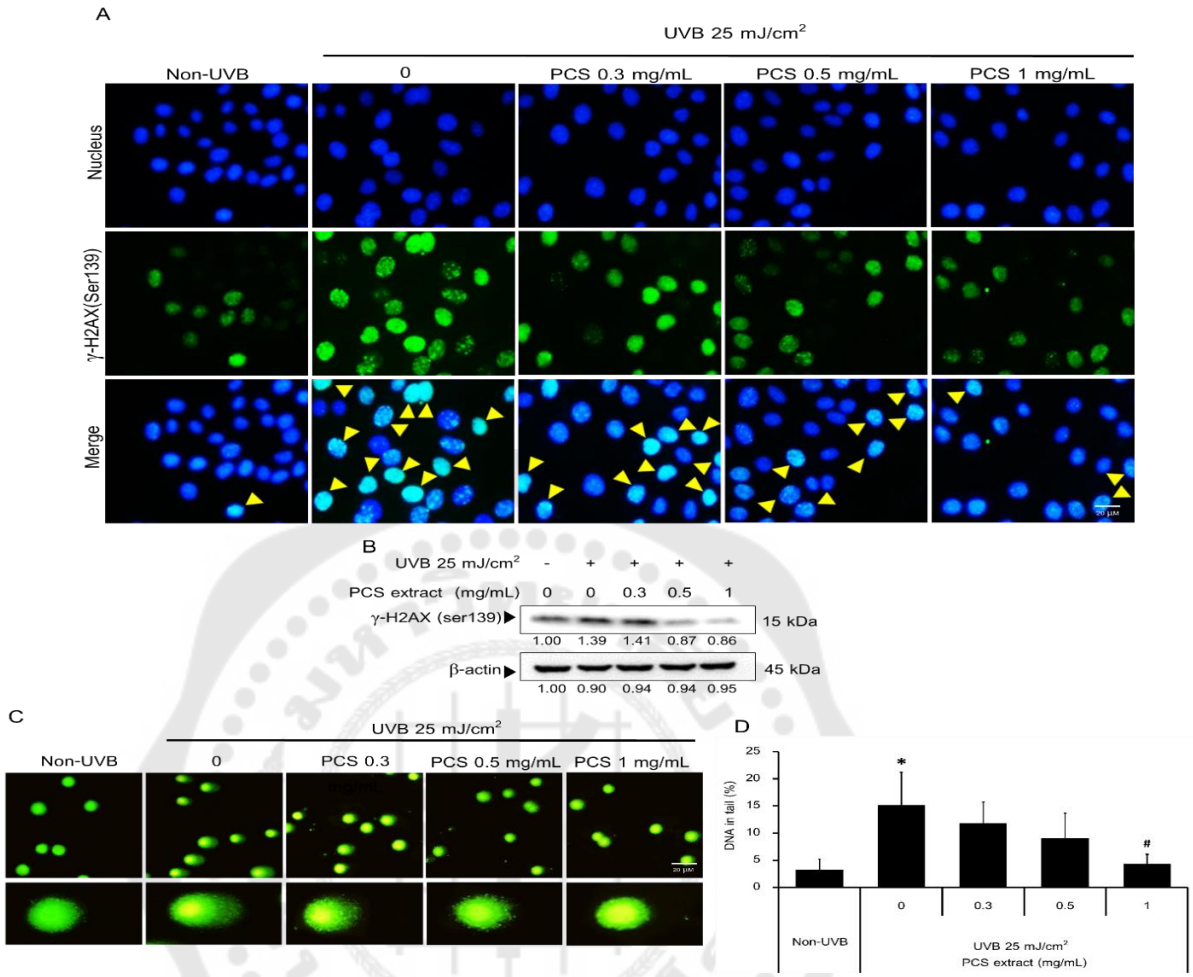

Figure 23 Shows effect of PCS extract attenuate UVB-induced DNA damage. HaCaT cells were treated with PCS extract at 0.3, 0.5, and 1 mg/mL for 1 h before exposed to 25 mJ/cm^2 UVB followed by incubated in medium for 24 h. A) Representative immunofluorescence analysis; FITC-fluorescence (green-color) signal is indicating γ-H2AX (Ser139), and Hoechst3342-fluorescence (blue-color) signal is indicating nuclei. The yellow arrows shows the localization of γ-H2AX in the nucleus. B) The proteins expression of γ-H2AX. β-actin was used as the internal control. C) Representative Comet analysis, after rewinding DNA, the comet slide was stained with SYBY-gold and observed by using a fluorescence microscope. D) The average of percentage DNA in the comet tail of 50 comets in each sample were quantified by Image J plugin OpenComet (version 1.3.1). Data are mean values±SD. * $p< 0.05$ *vs*. non-UVB group and # $p< 0.05$ *vs*. UVB-control group.

4.6 Effect of PCS extract on UVB-induced NF-ƙB translocation in HaCaT cells

From the data analysis, we demonstrated that PCS extract attenuated overproduction of intracellular ROS in HaCaT cells induced by UVB radiation. As it is well known, ROS-mediated NF- ƙB activation triggers inflammatory response. Thus, we investigated the effect of PCS extract on the kinetics of NF-ƙB translocation and protein expression in HaCaT cells induced by UVB. The results exhibited that UVB activated NF-ƙB translocation and increased NF-ƙB protein levels. In contrast, PCS extract reduced NF-ƙB translocation and protein expression in HaCaT cells induced by UVB as shown in figure 24.

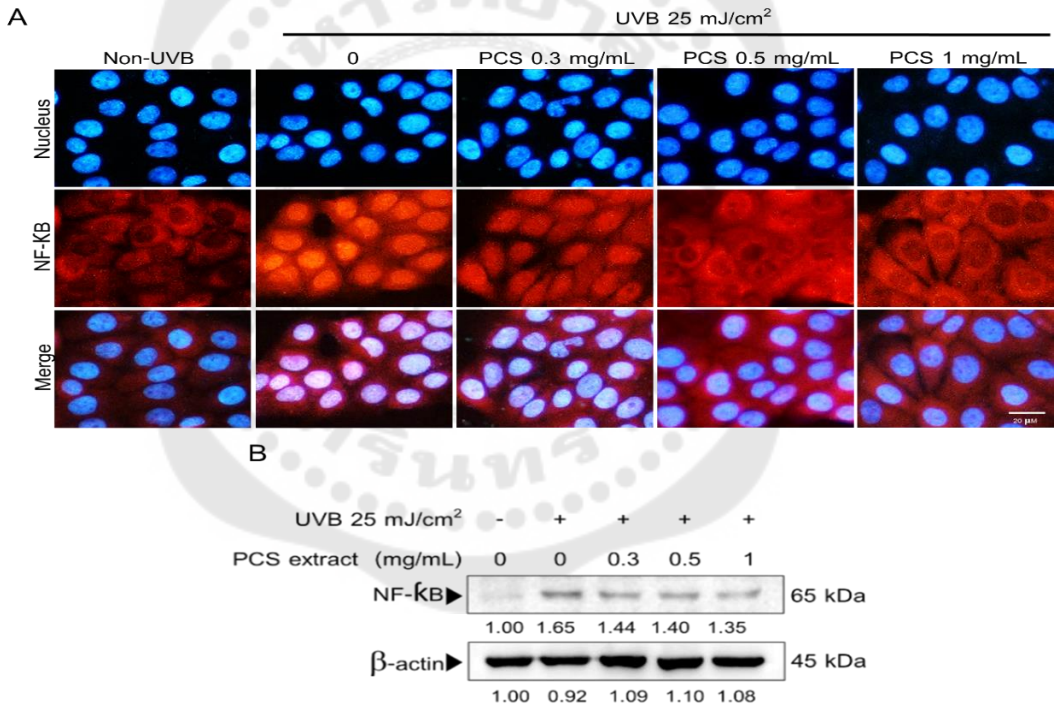

Figure 24 Shows effect of PCS extract against UVB-stimulated NF-ƙB activities. After UVB irradiated, cells were incubated for 1 h. Then, cells were investigated by using immunofluorescence analysis and Western blotting. A) Images represent translocation activity of NF-ƙB; Alexa froro546-fluorescence (red-color) signal is indicating NF-ƙB, and Hoechst3342-fluorescence (blue-color) signal is indicating nuclei. B) Representative Western blot analysis of NF-ƙB protein levels. β-actin was used as an internal control.

4.7 Effect of PCS extract on UVB-induced inflammatory cytokines production in HaCaT cells

Until now, we found that PCS extract inhibited UVB-enhanced NF-ƙB activities which possibly attenuate inflammatory response in HaCaT cells. Thus, we determined key inflammatory cytokines including iNOS and COX-2 protein expression. The result showed that UVB significantly increased the expression of iNOS and COX-2 compared with the non-UVB group. In contrast, concentrations of 0.3, 0.5, and 1 mg/mL of PCS extract decreased iNOS and COX-2 levels with a significant difference when compared to the UVB-control group as shown in figure 25.

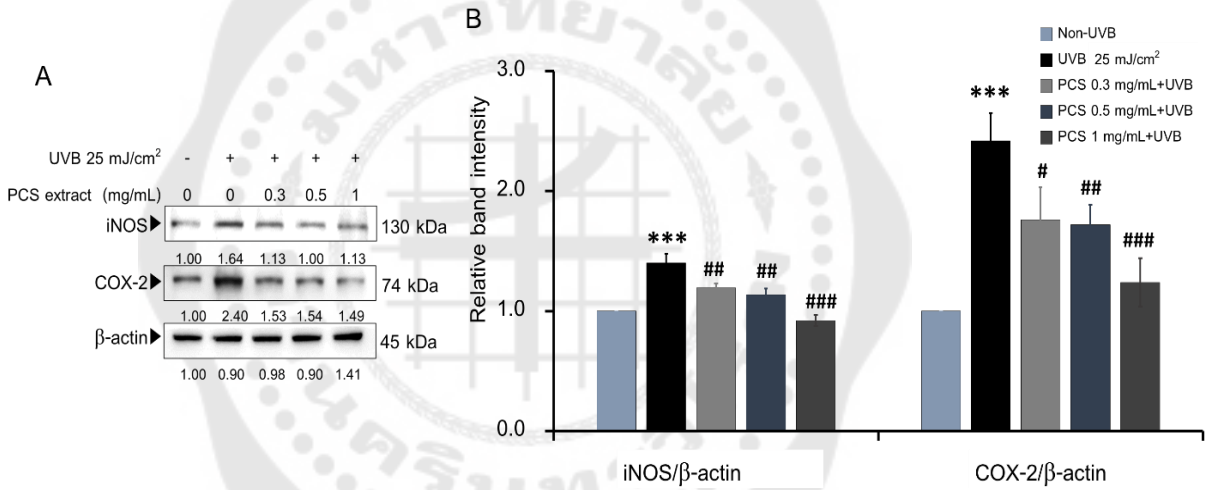

Figure 25 Shows the effect of PCS extract on decreasing inflammatory cytokine proteins expression in HaCaT cells induced by UVB. After 24 h of treatment, cells were collected and protein expression was perfumed by Western blot analysis. A) Shows the proteins level of iNOS and COX-2, β-actin was used as an internal control. B) Shows the average relative band intensity, was quantified by Image J densitometer. Data are mean values±SD (*n=3*). *** $p< 0.001$ *vs*. non-UVB group and # $p< 0.05$; ## $p< 0.01$; ### $p< 0.001$ *vs*. UVB-control group.

4.8 Effect of PCS extract on UVB-induced nuclear condensation in HaCaT cells

To determine the apoptosis induction of UVB and the preventive effect of PCS extract in UVB-induced apoptosis, Hoechst33342 nuclear staining assay was carried out. Cells with blue-bright fluorescence referred to nuclear condensed cells, membrane blebbing, and apoptotic bodies. The result showed that UVB increased nuclear condensation and apoptotic bodies as shown in yellow arrow in figure 26A. Whereas, PCS extract was significantly inhibited UVB-induced nuclear condensation compared with the UVB-control group (Fig. 26B). These results imply that the PCS extract probably attenuated UVB-induced apoptosis.

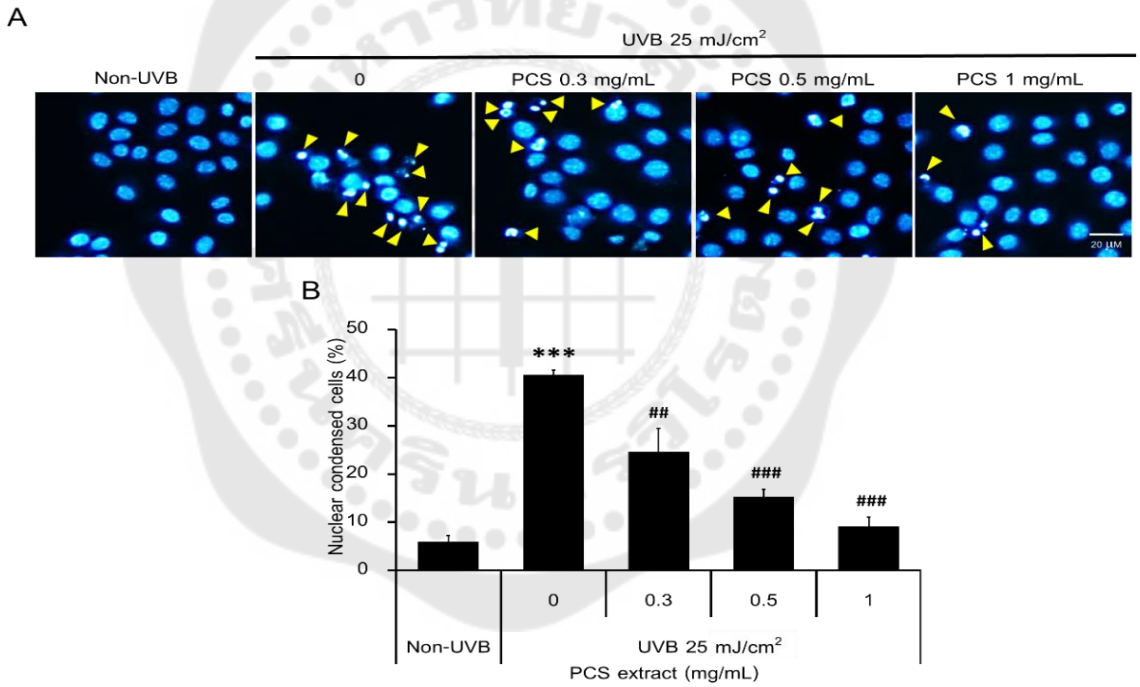

Figure 26 Shows PCS extract prevents UV-induced nuclear condensation in HaCaT cells. After 24 h of treatment, cells were stained with Hoechst33342 dye and visualized by a fluorescence microscope. A) Images represent nuclear condense cells and apoptotic bodies (yellow arrows). B) Shows the average of fluorescence intensity values was quantified by OPTIKA PROView software Version 5.0 (OPTIKA, Srl, Italy). Data are mean values±SD (*n=3*). *** $p< 0.001$ *vs*. non-UVB group and ## $p< 0.01$; ### $p< 0.001$ *vs*. UVB-control group.

4.9 Effect of PCS extract on UVB-induced sub-G1 population in HaCaT cells

During apoptosis, the cellular DNA has been degraded and represents as a sub-G1 peak analyzed by flow cytometer. The results showed that UVB increased the percentage of sub-G1 population to 2.45±0.71% changed compared with non-UVB group was obtained 0.54±0.10% of sub-G1. However, PCS extract at 0.3, 0.5, and 1 mg/mL decreased sub-G1 population were found to 0.87±0.37%, 0.75±0.33%, and 0.74±0.35%, respectively compared with the UVB-control group as shown in figure 27. This result indicates that PCS extract protects UVB-induced apoptosis in HaCaT cells.

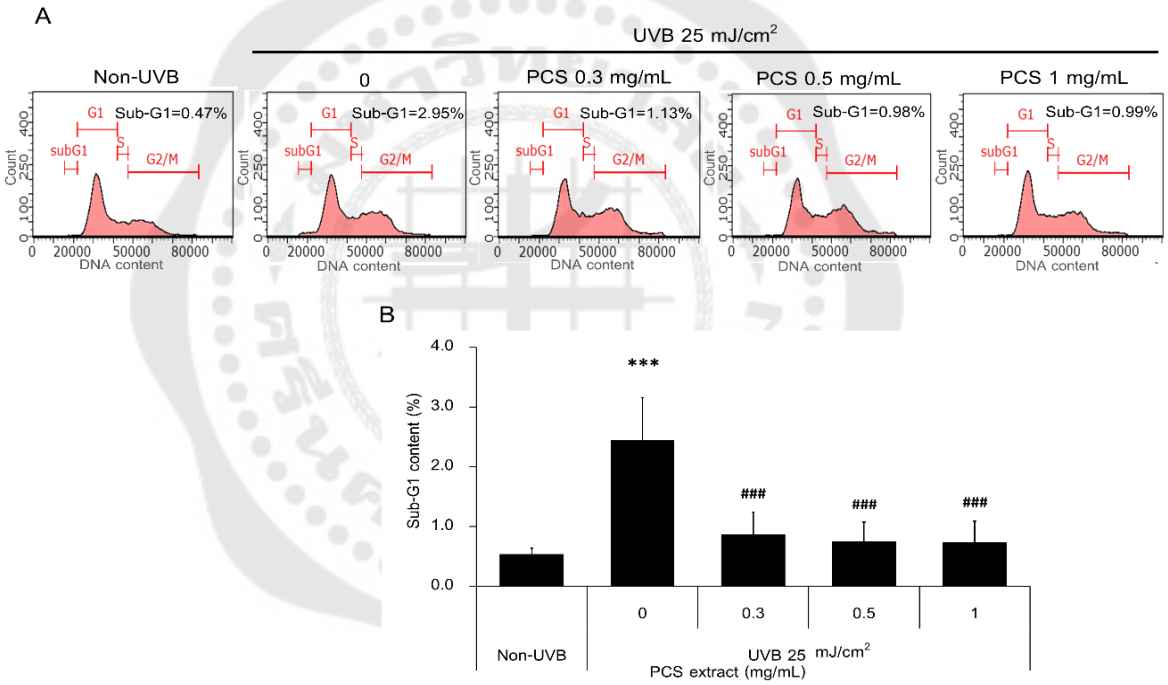

Figure 27 Shows the inhibitory effect of PCS extract on UV-induced apoptosis through the decreasing of sub-G1 population. After 24 h of treatment, cells were stained with Guava cell cycle reagent. The cell cycle analysis was assessed by flow cytometry. The sub-G1 content is present as cells undergoing apoptosis. A) Shows DNA content in each phase. B) Histogram presents sub-G1 DNA content. Data are mean values±SD (*n=3*). *** $p< 0.001$ *vs*. non-UVB group and ### $p< 0.001$ *vs*. UVB-control group.

4.10 Effect of PCS extract on UVB-mediated apoptosis in HaCaT cells

The apoptotic cells were examined by Hoechst 33342 staining and flow cytometry revealed that PCS extract protected nuclear condensation and decreased sub-G1 content in HaCaT cells induced by UVB. PCS extract may prevent UVB-mediated apoptosis. To confirm the hypothesis, the activation of caspase8, -9, and -7 which play an important role in apoptosis mediators were conducted by Western blot analysis. The result showed that UVB significantly increased cleaved form of caspase8, -9, and -7, and cleaved-PARP. In contrast, cleavage of caspase8, -9, and -7, and PARP proteins was decreased when cells were pre-treated with PCS extract at 0.3, 0.5, and 1 mg/mL compared to the UVB-control group (Fig. 28). The results exhibit that PCS extract protects UVB-mediated apoptosis in HaCaT cells.

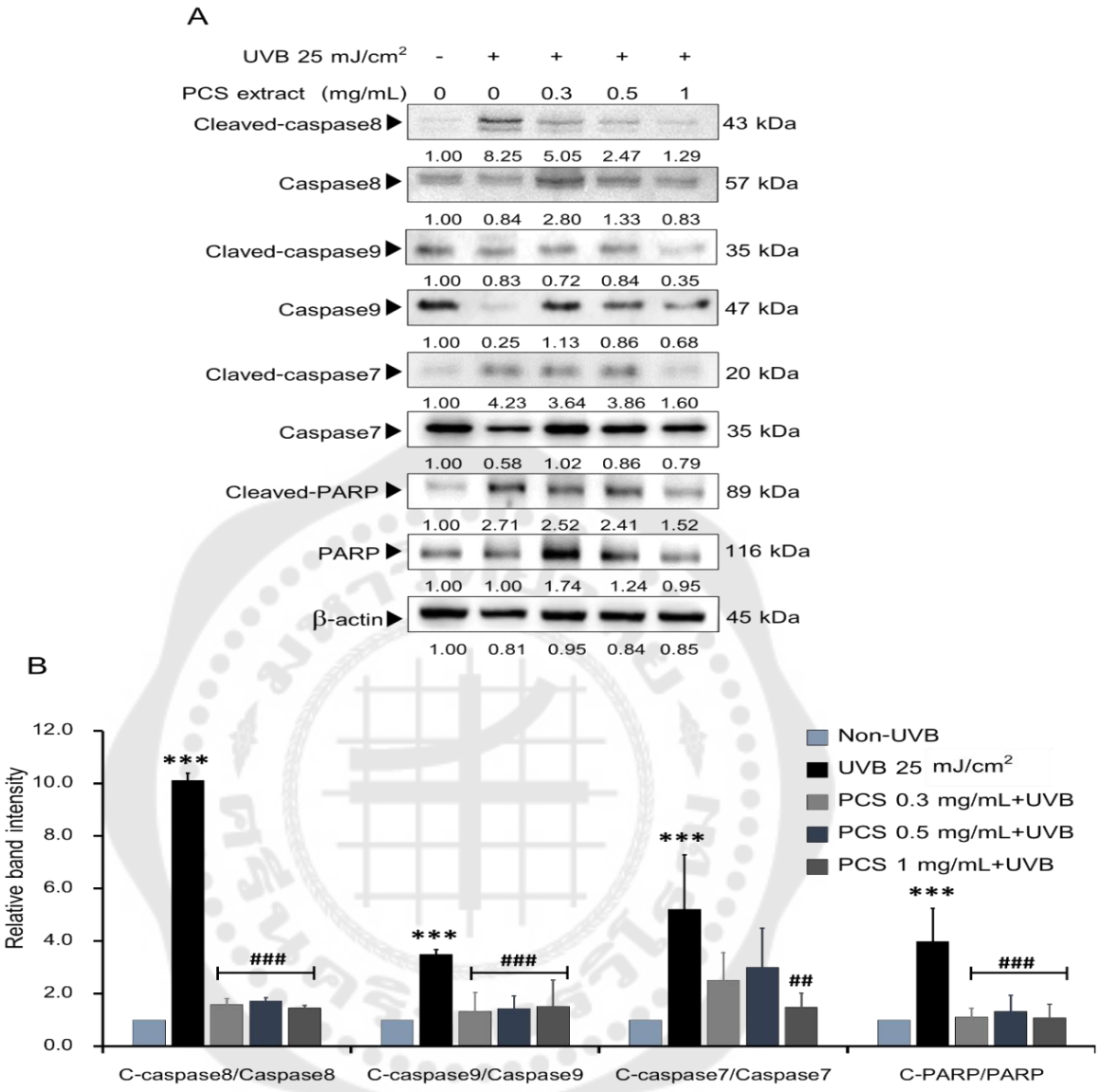

Figure 28 Shows the effect of PCS extract against UVB-induced apoptosis-related proteins. After 24 h of treatment, cells were collected and protein expression was performed by Western blot analysis. A) Shows the protein expression of cleaved-caspase8/Caspase8, cleaved-caspase9/caspase9, cleaved-caspase7/caspase7, and cleaved-PARP/PARP. β-actin was used as the internal control. B) Shows the average relative band intensity was quantified by Image J densitometer. Data are mean values±SD (*n=3*). *** $p< 0.001$ *vs*. non-UVB group and ## $p< 0.01$; ### $p< 0.001$ *vs*. UVB-control group.

4.11 Effect of PCS extract on UVB-induced mitochondrial dysfunction in HaCaT cells

To understand the anti-apoptosis activity of PCS extract on UVB-induced HaCaT cells, the expression of apoptosis-related Bcl-2 family proteins were determined. The results demonstrated UVB decreased Bcl-xL and Bcl-2 expression, and significantly increased Bax and Bak expression in HaCaT cells. Meanwhile, PCS extract at 0.3, 0.5, and 1 mg/mL showed the up-regulated Bcl-2 and Bcl-xL protein levels. In addition, the results exhibited that the PCS extract down-regulated Bax and Bak, especially PCS extract at 1 mg/mL, which showed significantly inhibited both pro-apoptotic proteins (Fig. 29A and B). As well known, the intracellular ROS and the imbalance of Bcl-2 family proteins are involved in mitochondrial dysfunction-mediated apoptosis. Thus, we investigated the mitochondrial membrane potential using a JC-1 cation fluorescent probe. The results demonstrated that the UVB showed red-fluorescence intensity was significantly lower than the non-UVB group, indicating UVB disrupted mitochondrial membrane potential. On the other hand, the PCS extract showed red-fluorescence intensity significantly higher than the UVB-control group (Fig. 29C and D). These data confirm that the PCS extract protects UVB-induced apoptosis via attenuated cleaved-caspases and pro-apoptotic proteins expression.

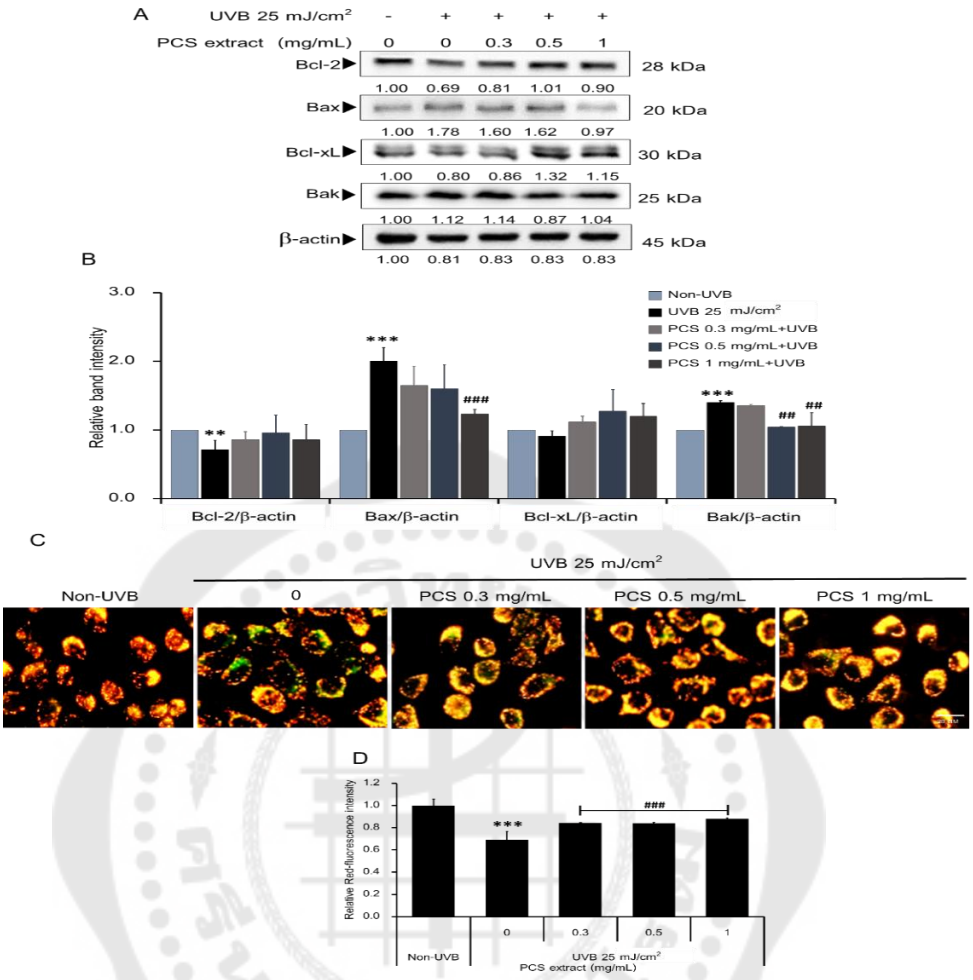

Figure 29 Shows the effect of PCS extract against UVB-induced apoptosis via stabilized mitochondrial membrane potential. After 24 h of treatment, cells were collected and proteins expression was performed by Western blot analysis. While, detection of $\Delta\Psi m$, cells were stained with JC-1 dye followed by observed under a fluorescence microscope. A) Shows proteins expression of Bcl-2 family proteins including Bcl-2, Bax, Bcl-xL, and Bak. β-actin was used as an internal control. B) Shows the average relative band intensity, was quantified by Image J densitometer. C) Shows the $\Delta\Psi m$; green-fluorescence preferred to unhealthy mitochondria with loss $\Delta\Psi m$, red-fluorescence preferred to healthy mitochondria. D) The histogram presents the average relative red-fluorescence intensity, was quantified by Image J densitometer. Data are mean values±SD (*n=3*). ** $p< 0.01$; *** $p< 0.001$ *vs*. non-UVB group and ## $p< 0.01$; ### $p< 0.001$ *vs*. UVB-control group.

4.12 Effect of PCS extract on UVB-induced stress-sensitive MAPK proteins phosphorylation in HaCaT cells

The MAPK signaling pathway plays an important role to control cell proliferation, differentiation, inflammation, and apoptosis in mammalian cells, which can be activated by extracellular and intracellular signals such as intracellular ROS or UV radiation. Therefore, the effect of PCS extract on MAPKs protein expression in HaCaT cells induced by UVB was investigated. The results showed that UVB induced MAPKs phosphorylation by significantly increased in p-c-Jun and p-38 levels. Whereas, PCS extract significantly suppressed c-Jun phosphorylation in a dose-dependent manner. In addition, we found that PCS extract slightly decreased p38 activity without statistically significant difference at $p<0.05$ as shown in figure 30. These results indicate that PCS inhibited UVB-induced MAPKs phosphorylation, majorly suppressed p-c-Jun protein expression.

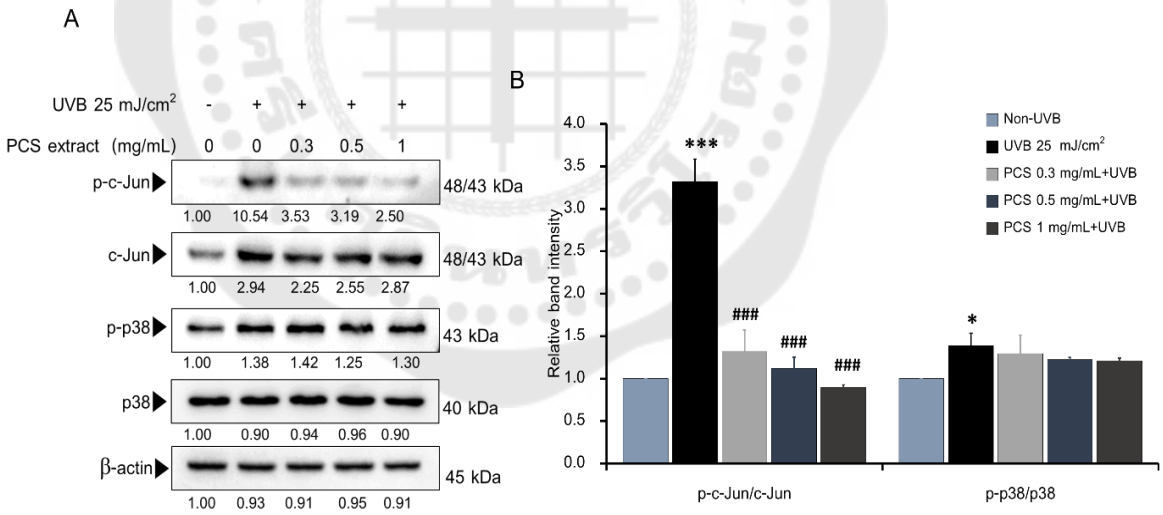

Figure 30 Shows the effect of PCS extract on UVB-induced MAPKs phosphorylation. After 24 h of treatment, cells were collected and protein expression was performed by Western blot analysis. A) Shows the expression of p-c-Jun, c-Jun, p-p38, and p38. β-actin was used as an internal control. B) Shows the average relative band intensity was quantified by Image J densitometer. Data are mean values±SD (*n=3*). * $p< 0.05$; *** $p< 0.001$ *vs*. non-UVB group and ### $p< 0.001$ *vs*. UVB-control group.

4.13 Effect of PCS extract on UVB-induced Akt phosphorylation in HaCaT cells

The Akt signaling pathway plays an important role in various processes such as cell proliferation, growth, angiogenesis, migration, and inhibit cell death. This pathway also activated by extracellular and intracellular signals such as intracellular ROS or UV radiation. Therefore, the effect of PCS extract on Akt expression in HaCaT cells induced by UVB was investigated. The results showed that 25 mJ/cm^2 UVB increased p-Akt compared to the non-UVB group, which slightly reduced by PCS extract without statistically significant (p<0.05) as shown in figure 31.

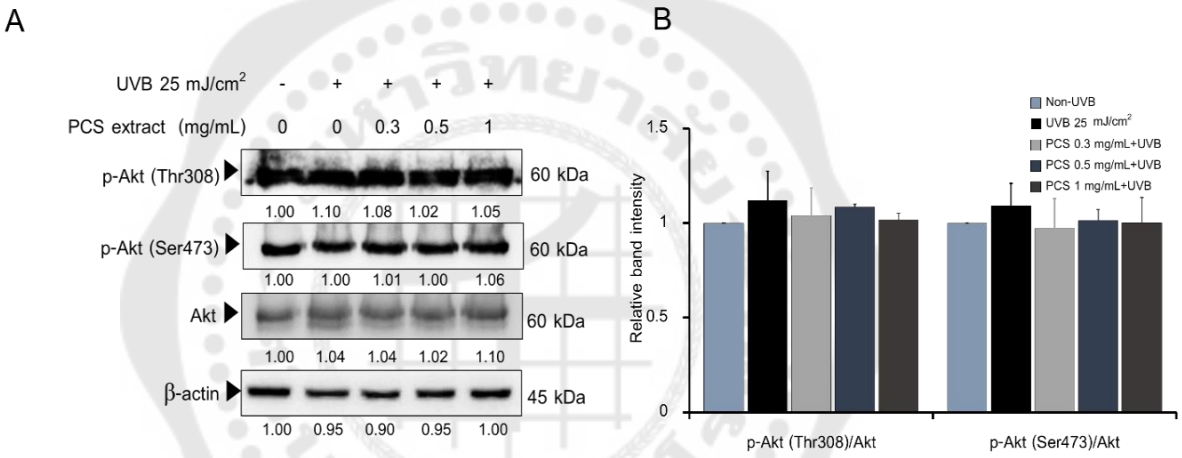

Figure 31 Shows the effect of PCS extract on UVB-induced Akt phosphorylation. After 24 h of treatment, cells were collected and protein expression was performed by Western blot analysis. A) Shows the expression of p-Akt (Thr308), p-Akt (Ser473), Akt. β-actin was used as an internal control. B) Shows the average relative band intensity was quantified by Image J densitometer. Data are mean values±SD(*n=3*).

CHAPTER 5
SUMMARY DISCUSSION AND SUGGESTION

5.1 Discussion

It is well known that hydroglycolic extraction is a useful method in cosmetic applications [116]. The reports demonstrated that the hydroglcolic plant extracts showed high phenolic content and bioactivities on skin cells such as antioxidant and anti-tyrosinase activities [115, 121]. Besides, pigments in plants/fruits range between red to deep blue color showed high efficiency against UV radiation such as strawberry, blueberry, raspberry, red grape, and black soy [122-127]. These extracts are suited for skincare formulation development [115, 121]. Currently, evidence has shown that purple corn and purple corn silk are rich in many phytonutrients mainly anthocyanins, and possessed antioxidant activities [14, 17, 113, 128]. However, the phytocomponents of hydroglycolic PCS extracts have not yet been reported. In this study, we found that PCS extract exhibited high ability on UVB absorbing and antioxidant activity as shown in figure 22. Therefore, we hypothesized that the PCS extract might suit to be developed as a UV preventive agent in cosmetic ingredients. Thus, we evaluated the effect of PCS extract in UVB-induced cell damage in human keratinocyte HaCaT cells. Previous studies showed that UVB radiation disrupts the balance between proliferation and cell death in keratinocyte cells through increasing skin cells death [2, 39, 129]. Our results supported that UVB induced morphological changes and significantly decreased cell viability in HaCaT cells. While the PCS extract can inhibit these events. Thus, it is possible that PCS extract protects skin cell death from UVB.

Intracellular ROS are byproducts of cell metabolism. The UVB induces overproduction of intracellular ROS led to an imbalance intracellular redox status, which mediates cellular inflammation, injury, and apoptosis [42, 130-132]. Our results demonstrated that PCS extract reduced intracellular ROS in HaCaT cells induced by UVB correlated with the effect of cyanidin-3-galactoside (C3G) and cyanidin 3-lathyroside on inhibited UVB-induced oxidative stress via decreased hydrogen peroxide and enhanced

antioxidant enzyme activities [127, 133, 134]. Thus, we suggest that PCS extract against UVB-induced oxidative stress through decreased intracellular ROS.

DNA is certainly one of the key targets for UV-induced cell damage. γ-H2AX (Ser139) is popular for consistent and quantitative markers of DNA damage [135]. Previous studies demonstrated that UVB induces γ-H2AX (Ser139) nuclear accumulation leading to apoptosis induction [131, 136-139]. These evidence correlate with our results. Interestingly, our finding revealed that PCS extract decreased γ-H2AX (Ser139), both of nuclear accumulation and protein expression. This finding in accordance with C3G showed inhibitory effects on UVB-induced DNA damage via decreased γ-H2AX (Ser139) and DNA photoproducts in skin cells [140]. In fact, the absence of γ-H2AX (Ser139) may be leading to the accumulation of DNA breaks without repair enhancement, which is the cause of gene mutation and skin carcinogenesis. Hence, to confirm that the decreasing of γ-H2AX (Ser139) in cells was not caused by lacking DNA repair mechanisms, the comet assay was conducted. Comet assay is a technique for measuring DNA breaks in individual cells for the examination of the genotoxicity [141]. In this study showed that PCS extract reduced the length of comet tail in UVB-treated cells. Thus, we confirm that PCS extract decreased DNA lesions without enhancing skin carcinogenesis risk. Our finding is correlated with Perde-Schrepler, et al (2013) revealed that anthocyanins-rich in grape seed extract inhibited UVB-induced skin cancer through reduced DNA photoproducts and lesion score of DNA comet tail [122]. As in the previous study, suggested that proanthocyanins enhanced DNA repair on UVB-induced skin tumor development in Female C3H/HeN mice [142]. However, the explanations for the mechanisms of the effects of hydroglycolic PCS extract against UVB-induced DNA damage and photocarcinogenesis need to be further studied and confirmed.

In keratinocyte cells, NF-κB activities increase the sensitivity of UVB-induced inflammatory response through increase the expression of inflammatory cytokines such as COX-2 and iNOS [143-147]. We found that PCS extract attenuated UVB-induced NF-κB activation and significantly decreased iNOS and COX-2. As in previous studies, suggested the UVA and UVB induced skin inflammation through NF-κB activation

leading to increased COX-2, PGE_2, TNFα, IL-6, and IL-1β, which were attenuated by anthocyanins-rich extract such as raspberry, black soybean, and strawberry extract [123, 124, 148]. Thereby, we suggest PCS extract could reduce skin inflammation in skin cells induced by UVB.

UVB causing apoptosis induction in keratinocyte cells [72], thus we investigated effect of PCS extract on UVB-induced apoptosis in HaCaT cells. Our result revealed that at 20 mJ/cm^2 of UVB increased nuclear condensation and Sub-G1 population in cell cycle distribution, which can be reduced by PCS extract. Furthermore, we found that UVB increased cleaved-caspase8, -9, and -7 and subsequently increased cleaved-PARP protein levels in HaCaT cells, which were inhibited by PCS extract. Our results are correlated with anthocyanins from black soybean coat extract, which showed an inhibitory effect on UVB-induced apoptotic cell death via decreased Sub-G1 and caspase3 activity in HaCaT cells [127]. Besides, previous studies demonstrated that the imbalanced pro- and anti-apoptotic proteins together with overproduction of intracellular ROS caused mitochondrial swelling and induced the opening of large pores and depolarized mitochondrial membrane potential, impaired ATP production, and efflux of apoptogenic proteins, subsequently apoptosis induction [2, 8]. These data correlated with our study that UVB radiation is the cause of the imbalance between pro-and anti-apoptotic proteins and decreased mitochondrial membrane potential. Additionally, we found that PCS extract mainly attenuated Bax and Bak expression in UVB-treated HaCaT cells.

Due to several studies, it has been suggested that the strong activation of stress-sensitive JNK and p38 MAPK is remarkable in dominantly responding to stress signals and UV. Thus, in these studies, we did not investigate the effect of UVB on ERK1/2 signaling pathway [8, 149, 150]. The active JNK consequently improves transcription factor activities such as c-Jun, ATF2, and Elk [150, 151]. Papavassiliou, et al (2020) suggested that c-Jun activity mostly activates through JNK pathway. Following activation, JNK phosphorylates c-Jun at Ser63 and Ser73, and Thr91 and Thr93, which are positive regulatory domain. This event leads to the homodimerization of c-Jun or

heterodimerization with c-Fos [152]. While, the p38 is activated via phosphorylation of Thr180 and Tyr182 [151]. These events regulated protein expression mediated inflammatory response and apoptosis, including MMPs, COX-2, iNOS, Smad3, Bcl-2 family, p53, and cell cycle-regulated proteins [8, 150, 151, 153, 154]. Likewise, Akt pathway plays an important role in various processes, activated by UV and oxidative stress [96]. The Akt activation via the phosphorylation at Thr308 and Ser473, thereby the forming complex with Bcl-2/Bcl-xL proteins inhibiting apoptosis. In addition, Akt pathway also control inflammatory response through NF-ĸB and AP-1 activation [155, 156]. Choi, et al (2015) demonstrated that UVB increased Akt and NF-ĸB activities in mice skin [156]. Previous study demonstrated that the red raspberry extract and C3G compound inhibited skin damage in UVB-treated HaCaT cells through attenuated p-p38 and p-c-Jun [63, 123, 125]. Whereas in 2014, Huh, et al. showed that *Pinus densiflora* leaf extract and its active compounds, Ttans-communic acid suppressed p-c-Jun, c-fos, and Akt pathway, but no effect on p38 MAPKs in UVB-induced photoaging in skin cells [155]. While our results demonstrated that PCS extract mainly inhibited c-Jun phosphorylation in HaCaT cells induced by UVB. Hence, we suggest that the hydroglycolic PCS extract could attenuate skin inflammation and apoptosis by reduced intracellular ROS, prevented DNA damage as well as mainly suppressing the activities of NF-ĸB, caspases, pro-apoptotic, and c-Jun.

5.2 Conclusion

In summary, we found that PCS extract present antioxidant activity and exhibited high ability on UVB absorbing. Meanwhile, PCS extract reduced intracellular ROS and DNA breaks in UVB-treated HaCaT cells. Moreover, PCS extract reduced NF-ĸB activity and decreased COX-2 and iNOS levels. Interestingly, PCS extract also inhibited apoptosis by significantly attenuating Bax and Bak expression, and suppressed caspase8, -9, and -7 activities, subsequently inhibited PARP degradation in UVB-treated HaCaT cells. In addition, the results showed that PCS extract decreased UVB-induced skin inflammation and apoptosis through suppressing c-Jun

phosphorylation (Fig. 32). Therefore, to increase the value of agricultural waste, we suggest that hydroglycolic PCS extract is a new candidate suited for development as an UVB preventive agent in skincare products.

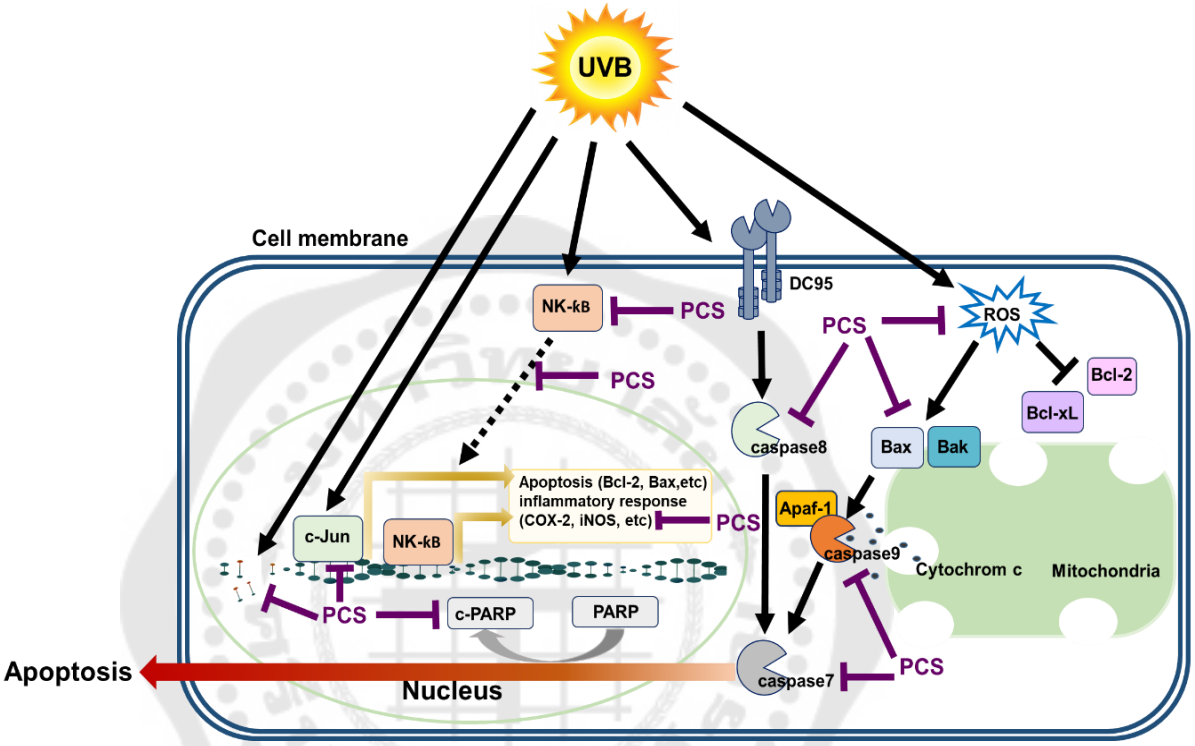

Figure 32 Represents the summary effect of PCS extract on UVB-induced cell damage in keratinocyte HaCaT cells

REFERENCES

1. Skin cancers. WHO [cited 2018 Sep 12]. Available from: http://www.who.int/uv/faq/skincancer/en/index1.html.
2. Assefa Z, Laethem AV, Garmyn M, Agostinis P. Ultraviolet radiation-induced apoptosis in keratinocytes: on the role of cytosolic factors. Biochim Biophys Acta. 2005;1755(2):90-106.
3. Daya-Grosjean L, Sarasin A. The role of UV induced lesions in skin carcinogenesis: an overview of oncogene and tumor suppressor gene modifications in xeroderma pigmentosum skin tumors. Mutat Res. 2005;571(1-2):43-56.
4. Matsumura Y, Ananthaswamy HN. Toxic effects of ultraviolet radiation on the skin. Toxicol Appl Pharmacol. 2004;195(3):298-308.
5. Park G, Kim HG, Hong SP, Kim SY, Oh MS. Walnuts (seeds of *Juglandis sinensis* L.) protect human epidermal keratinocytes against UVB-induced mitochondria-mediated apoptosis through upregulation of ROS elimination pathways. Skin Pharmacol Physiol. 2014;27(3):132-40.
6. Hseu YC, Chou CW, Senthil Kumar KJ, Fu KT, Wang HM, Hsu LS, et al. Ellagic acid protects human keratinocyte (HaCaT) cells against UVA-induced oxidative stress and apoptosis through the upregulation of the HO-1 and Nrf-2 antioxidant genes. Food Chem Toxicol. 2012;50(5):1245-55.
7. Oliveira MM, Ratti BA, Dare RG, Silva SO, Truiti M, Ueda-Nakamura T, et al. Dihydrocaffeic acid prevents UVB-induced oxidative stress leading to the inhibition of apoptosis and MMP-1 Expression via p38 signaling pathway. Oxid Med Cell Longev. 2019;2419096.
8. Shin SW, Jung E, Kim S, Kim JH, Kim EG, Lee J, et al. Antagonizing effects and mechanisms of afzelin against UVB-induced cell damage. PLoS One. 2013; 8(4):e61971.
9. Shin SW, Jung E, Kim S, Kim JH, Kim EG, Lee J, et al. Antagonizing effects and mechanisms of afzelin against UVB-induced cell damage. PLoS One.

2013;8(4):e61971.

10. Ebrahimzadeh MA, Pourmord F, Hafezi S. Antioxidant activities of Iranian corn silk. Turk J Biol. 2008;32:43-9.
11. Zilic S, Jankovic M, Basic Z, Vancetovic J, Maksimovic V. Antioxidant activity, phenolic profile, chlorophyll and mineral matter content of corn silk (*Zea mays* L): Comparison with medicinal herbs. J Cereal Sci. 2016;69:363-70.
12. Lee J, Lee S, Kim SL, Choi JW, Seo JY, Choi DJ, et al. Corn silk maysin induces apoptotic cell death in PC-3 prostate cancer cells via mitochondria-dependent pathway. Life Sci. 2014;119(1-2):47-55.
13. Choi DJ, Kim SL, Choi JW, Park YI. Neuroprotective effects of corn silk maysin via inhibition of H2O2-induced apoptotic cell death in SK-N-MC cells. Life Sci. 2014;109(1):57-64.
14. Sarepoua E, Tangwongchai R, Suriharn B, Lertrat K. Relationships between phytochemicals and antioxidant activity in corn silk. Int Food Res J. 2013;20(5):2073-9.
15. Choi SY, Lee Y, Kim SS, Ju HM, Baek JH, Park CS, et al. Inhibitory effect of corn silk on skin pigmentation. Molecules. 2014;19(3):2808-18.
16. Wang C, Zhang T, Liu J, Lu S, Zhang C, Wang E, et al. Subchronic toxicity study of corn silk with rats. J Ethnopharmacol. 2011;137(1):36-43.
17. Liu J, Wang C, Wang Z, Zhang C, Lu S, Liu J. The antioxidant and free-radical scavenging activities of extract and fractions from corn silk (*Zea mays* L.) and related flavone glycosides. Food Chem. 2011;126(1):261-9.
18. Nicol NH. Anatomy and physiology of the skin. Dermatol Nurs. 2005;17(1):62.
19. So PL, Bozzone DM. The biology of cancer: skin cancer. 2008.
20. Elizabeth H. Structure and function of the skin. [cited 2018 Nov 15]. Available from: http://www.msdmanuals.com/home/skin-disorders/biology-of-the-skin/structure andfunction-of-the-skin.
21. Ramadon D, McCrudden MTC, Courtenay AJ, Donnelly RF. Enhancement strategies for transdermal drug delivery systems: current trends and applications. Drug Deliv

Transl Res. 2021;1-34.

22. OpenStax. Anatomy and physiology. The integumentary system. [cited 2021 Sep 15]. Available from: https://opentextbc.ca/anatomyandphysiology/chapter/functions-of-the-integumentary-system/.
23. Ultraviolet radiation. [cited 2017 Nov 15]. Available from: https://www.ccohs.ca/oshanswers/phys_agents/ultravioletradiation.html.
24. Thunchapoen W. Skin cancer cell death induction by UV-irradiation and plant extract. [Dissertation, M.SC Molecular biology] Bangkok: Srinakharinwirot Univ;2013.
25. Correa Mde P. Solar ultraviolet radiation: properties, characteristics and amounts observed in Brazil and South America. An Bras Dermatol. 2015;90(3):297-313.
26. UV-C-lamps: could something hat kills bacteria and viruses also harm you?. [cited 2017 Nov 16]. Available from: https://ec.europa.eu/health/sites/health/files/scientific_committees/scheer/docs/citizens_uvc_en.pdf.
27. Nichols JA, Katiyar SK. Skin photoprotection by natural polyphenols: anti-inflammatory, antioxidant and DNA repair mechanisms. Arch Dermatol Res. 2010;302(2):71-83.
28. Amaro-Ortiz A, Yan B, D'Orazio JA. Ultraviolet radiation, aging and the skin: prevention of damage by topical cAMP manipulation. Molecules. 2014;19(5):6202-19.
29. Schieber M, Chandel NS. ROS function in redox signaling and oxidative stress. Curr Biol. 2014;24(10):R453-62.
30. Lucas R, McMichae T, Smith W, Armstrong B. Solar ultraviolet radiation global burden of disease from solar ultraviolet radiation. Environ Burden Dis Ser. 2006;13.
31. Mead MN. Benefits of sunlight: a bright spot for human health. Environ Health Perspect. 2008;116(4):A160-7.
32. Lucas RM, Ponsonby AL. Ultraviolet radiation and health: friend and foe. Med J Aust. 2002;177(11-12):594-8.
33. Engelsen O. The relationship between ultraviolet radiation exposure and vitamin D status. Nutrients. 2010;2(5):482-95.

34. Chen TC, Chimeh F, Lu Z, Mathieu J, Person KS, Zhang A, et al. Factors that influence the cutaneous synthesis and dietary sources of vitamin D. Arch Biochem Biophys. 2007;460(2):213-7.
35. Kimlin MG, Olds WJ, Moore MR. Location and vitamin D synthesis: is the hypothesis validated by geophysical data?. J Photochem Photobiol B. 2007;86(3):234-9.
36. Halliday GM, Norval M, Byrne SN, Huang XX, Wolf P. The effects of sunlight on the skin. Drug Discov Today Dis Mech. 2008;5(2):e201-9.
37. Wong T, Hsu L, Liao W. Phototherapy in psoriasis: a review of mechanisms of action. J Cutan Med Surg. 2013;17(1):6-12.
38. Foundation NP. Light therapy. National Psoriasis Foundation. [cited 2017 Nov 15]. Available from:from https://www.psoriasis.org/phototherapy/.
39. Ichihashi M, Ueda M, Budiyanto A, Bito T, Oka M, Fukunaga M, et al. UV-induced skin damage. Toxicol. 2003;189(1-2):21-39.
40. Schuch AP, Moreno NC, Schuch NJ, Menck CFM, Garcia CCM. Sunlight damage to cellular DNA: Focus on oxidatively generated lesions. Free Radic Biol Med. 2017;107:110-24.
41. Ravanat JL, Douki T, Cadet J. Direct and indirect effects of UV radiation on DNA and its components. J Photochem Photobiol B. 2001;63(1-3):88-102.
42. Kammeyer A, Luiten RM. Oxidation events and skin aging. Ageing Res Rev. 2015;21:16-29.
43. Kuo LJ, Yang L. Gamma-H2AX - a novel biomarker for DNA double-strand breaks. In Vivo. 2008;22(3):305-9.
44. Midori MS, Nakanishi M. Response to DNA damage: why do we need to focus on protein phosphatases?. Front. Oncol. 2013 [cited 2017 Dec 4]. Available from: https://www.frontiersin.org/articles/10.3389/fonc.2013.00008/full.
45. Freeman AK, Monteiro ANA. Phosphatases in the cellular response to DNA damage. Cell Commun Signal. 2010;8:27.
46. Novak B, Sible JC, Tyson JJ. Checkpoints in the cell cycle. Encyclopedia of life sciences. 2002:1-8.

47. Abraham RT. Cell cycle checkpoint signaling through the ATM and ATR kinases. Genes Dev. 2001;15(17):2177-96.
48. Donzelli M, Draetta G. Regulating mammalian checkpoints through Cdc25 inactivation. EMBO Rep. 2003;4(7):671-7.
49. Boutros R, Dozier C, Ducommun B. The when and wheres of CDC25 phosphatases. Curr Opin Cell Biol. 2006;18(2):185-91.
50. Zhang W, Liu HT. MAPK signal pathways in the regulation of cell proliferation in mammalian cells. Cell Res. 2002;12(1):9-18.
51. Limpaiboon T. Molecular oncology. 2011.
52. Lee CH, Wu SB, Hong CH, Yu HS, Wei YH. Molecular mechanisms of UV-induced apoptosis and its effects on skin residential cells: the implication in UV-based phototherapy. Int J Mol Sci. 2013;14(3):6414-35.
53. Lee C, Park GH, Ahn EM, Kim BA, Park CI, Jang JH. Protective effect of *Codium fragile* against UVB-induced pro-inflammatory and oxidative damages in HaCaT cells and BALB/c mice. Fitoterapia. 2013;86:54-63.
54. Aragane Y, Kulms D, Metze D, Wilkes G, Poppelmann B, Luger TA, et al. Ultraviolet light induces apoptosis via direct activation of CD95 (Fas/APO-1) independently of its ligand CD95L. J Cell Biol. 1998;140(1):171-82.
55. Park JY, Ji YJ, Seo KH, Lee JY, Kim G, Kang MH,et al. Heat treatment improves UV photoprotective effects of licorice in human dermal fibroblasts. Processes. 2021;9(6):e1040.
56. Jennifer A. Rogers JWF. Regulation of NF-kB activation and nuclear translocation by exogenous nitric oxide (NO) donors in TNF-a activated vascular endothelial cells. Nitric Oxide. 2007;16:379-91.
57. Noursadeghi M, Tsang J, Haustein T, Miller RF, Chain BM, Katz DR. Quantitative imaging assay for NF-kB nuclear translocation in primary human macrophages. J Immunol Methods. 2008;329:194-200.
58. Hur S, Lee YS, Yoo H, Yang JH, Kim TY. Homoisoflavanone inhibits UVB-induced skin inflammation through reduced cyclooxygenase-2 expression and NF-kappaB nuclear

localization. J Dermatol Sci. 2010;59(3):163-9.

59. Anggakusuma, Yanti, Hwang J. Effects of macelignan isolated from *Myristica fragrans* Houtt. on UVB-induced matrix metalloproteinase-9 and cyclooxygenase-2 in HaCaT cells. J Dermatol Sci. 2010;57(2):114-22.
60. Kim Y, Lee SK, Bae S, Kim H, Park Y, Chu NK, et al. The anti-inflammatory effect of alloferon on UVB-induced skin inflammation through the down-regulation of pro-inflammatory cytokines. Immunol Lett. 2013;149(1-2):110-8.
61. Lohinai Z, Szabo C. Role of nitric oxide in physiology and patophysiology of periodontal tissues. Med Sci Monit 1998;4:1089-95.
62. Hanahan D, Weinberg RA. Hallmarks of cancer: the next generation. Cell. 2011;144(5):646-74.
63. Cell Cycle Checkpoints. [cited 2021 Sep 3]. Available from: https://courses.lumenlearning.com/biology1/chapter/the-cell-cycle/.
64. Vermeulen K, Van Bockstaele DR, Berneman ZN. The cell cycle: a review of regulation, deregulation and therapeutic targets in cancer. Cell Prolif. 2003;36(3):131-49.
65. Pucci B, Kasten M, Giordano A. Cell cycle and apoptosis. Neoplasia. 2000;2(4):291-99.
66. Wang Y, McIntyre C, Mittar D. Cell cycle and DNA content analysis using the BD cycletest assay on the BD FACSVerse™ system. BD Biosciences. 2011 [cited 2021 Sep3]. Available from: https://www.bdbiosciences.com/documents/BD_Instruments_FACSVerse_CellCycle_DNA_Analysis_AppNote.pdf.
67. Cell Cycle and Cancer. [cited 2021 Sep 3]. Available from: http://www.cubocube.com/dashboard.php?a=1642&b=1691&c=1.
68. Lolli G, Johnson LN. CAK-cyclin-dependent activating kinase: a key kinase in cell cycle control and a target for drugs?. Cell Cycle. 2005;4(4):572-7.
69. Cell Cycle Checkpoints. [cited 2021 Sep 3]. Available from: https://courses.lumenlearning.com/wmopen-biology1/chapter/cell-cycle-checkpoints/.

70. Crowley LC, Chojnowski G, Waterhouse NJ. Measuring the DNA content of cells in apoptosis and at different cell-cycle stages by propidium iodide staining and flow cytometry. Cold Spring Harb Protoc. 2016;2016(10).
71. Phoenix flow systems. [cited 2021 Sep 3]. Available from: http://www.phnxflow.com/MultiCycle.stand.alone.html.
72. Elmore S. Apoptosis: a review of programmed cell death. Toxicol Pathol. 2007;35(4):495-516.
73. Blazquez MA, Bermejo A, Zafra-Polo MC, Corte D. Styryl-Lactones from Goniothalamus Species-A Review. Phytochem. Anal. 1999;10;161-70.
74. Rastogi RR, Sinha RP. Apoptosis: Molecular mechanisms and pathogenicity. EXCLI J. 2009;8:155-81.
75. Igney FH, Krammer PH. Death and anti-death: tumour resistance to apoptosis. Nat Rev Cancer. 2002;2(4):277-88.
76. Priante G, Gianesello L, Ceol M, Prete DD, Anglani F. Cell Death in the Kidney. Int J Mol Sci. 2019;20(14):3598.
77. Susin SA, Lorenzo HK, Zamzami N, Marzo I, Snow BE, Brothers GM, et al. Molecular characterization of mitochondrial apoptosis-inducing factor. Nature. 1999;397(6718):441-6.
78. Li J, Yuan J. Caspases in apoptosis and beyond. Oncogene. 2008;27(48):6194-206.
79. Villa P, Kaufmann SH, Earnshaw WC. Caspases and caspase inhibitors. Trends Biochem Sci. 1997;22(10):388-93.
80. Ribe EM, Serrano-Saiz E, Akpan N, Troy CM. Mechanisms of neuronal death in disease: defining the models and the players. Biochem J. 2008;415(2):165-82.
81. Tsujimoto Y. Role of Bcl-2 family proteins in apoptosis: apoptosomes or mitochondria?. Genes Cells. 1998;3(11):697-707.
82. Kuwana T, Newmeyer DD. Bcl-2-family proteins and the role of mitochondria in apoptosis. Curr Opin Cell Biol. 2003;15(6):691-9.
83. Cheng EH, Kirsch DG, Clem RJ, Ravi R, Kastan MB, Bedi A, et al. Conversion of Bcl-2 to a Bax-like death effector by caspases. Science. 1997;278(5345):1966-8.

84. Nys K, Agostinis P. Bcl-2 family members: essential players in skin cancer. Cancer Lett. 2012;320(1):1-13.
85. Morales JC, Li L, Fattah FJ, Dong Y, Bey EA, Patel M, et al. Review of poly (ADPribose) polymerase (PARP) mechanisms of action and rationale for targeting in cancer and ther diseases. Crit Rev Eukaryot Gene Expr. 2014;24(1):15-28.
86. Javle M, Curtin NJ. The role of PARP in DNA repair and its therapeutic exploitation. Br J Cancer. 2011;105(8):1114-22.
87. Chaitanya GV, Steven AJ, Babu PP. PARP-1 cleavage fragments: signatures of cell-death proteases in neurodegeneration. Cell Commun Signal. 2010;8:31.
88. Virag L, Szabo C. The therapeutic potential of poly(ADP-ribose) polymerase inhibitors. Pharmacol Rev. 2002;54(3):375-429.
89. Chicheportiche Y, Bourdon PR, Xu H, Hsu YM, Scott H, Hession C, et al. TWEAK, a new secreted ligand in the tumor necrosis factor family that weakly induces apoptosis. J Biol Chem. 1997;272(51):32401-10.
90. Ashkenazi A, Dixit VM. Death receptors: signaling and modulation. Science. 1998;281(5381):1305-8.
91. Yuan CH, Filippova M, Duerksen-Hughes P. Modulation of apoptotic pathways by human papillomaviruses (HPV): mechanisms and implications for therapy. Viruses. 2012;4(12):3831-50.
92. Cellular Apoptosis Pathway. [cited 2017 Dec 10]. Available from: http://www.sabiosciences.com/pathway.php?sn=Cellular_Apoptosis_Pathway.
93. Wang Y, Tjandra N. Structural insights of tBid, the caspase-8-activated Bid, and its BH3 domain. J Biol Chem. 2013;288(50):35840-51.
94. Cargnello M, Roux PP. Activation and function of the MAPKs and their substrates, the MAPK-activated protein kinases. Microbiol Mol Biol Rev. 2011;75(1):50-83.
95. Plotnikov A, Zehorai E, Procaccia S, Seger R. The MAPK cascades: signaling components, nuclear roles and mechanisms of nuclear translocation. Biochimica et Biophysica Acta. 2011;1813:1619-33.
96. Crowe DL, Tsang KJ, Shemirani B. Jun N-terminal kinase 1 mediates transcriptional

induction of matrix metalloproteinase 9 expression. Neoplasia. 2001;3(1):27-32.

97. Chen CC, Lin MW, Liang CJ, Wang SH. The anti-inflammatory effects and mechanisms of eupafolin in lipopolysaccharide-induced inflammatory responses in RAW264.7 macrophages. PLoS One. 2016;11(7):e0158662.
98. Liu J, Lin A. Role of JNK activation in apoptosis: a double-edged sword. Cell Res. 2005; 5(1):36-42.
99. Dhanasekaran DN, Reddy EP. JNK signaling in apoptosis. Oncogene. 2008;27(48): 6245-51.
100. Laethem AV, Kelst SV, Lippens S, Declercq W, Vandenabeele P, Janssens S, et al. Activation of p38 MAPK is required for Bax translocation to mitochondria, cytochrome c release and apoptosis induced by UVB irradiation in human keratinocytes. FASEB J. 2004;18(15):1946-8.
101. Song G, Ouyang G, Bao S. The activation of Akt/PKB signaling pathway and cell survival. J Cell Mol Med. 2005;9(1):59-71.
102. Harris TK. PDK1 and PKB/Akt: ideal targets for development of new strategies to structure-based drug design. IUBMB Life. 2003;55(3):117-26.
103. Zhang X, Tang N, Hadden TJ, Rishi AK. Akt, Foxo and regulation of apoptosis. Biochim Biophys Acta. 2011;1813(11):1978-86.
104. Hassan B, Akcakanat A, Holder AM, Meric-Bernstam F. Targeting the PI3-kinase/Akt/mTOR signaling pathway. Surg Oncol Clin N Am. 2013;22(4):1-25.
105. Klungsaeng S, Senggunprai L. Protein serine-threonine kinases as drug target in cancer treatment. Srinagarind Med J. 2020;35(4):488-95.
106. Intuyod K, Priprem A, Limphirat W, Charoensuk L, Pinlaor P, Pairojkul C, et al. Anti-inflammatory and anti-periductal fibrosis effects of an anthocyanin complex in opisthorchis viverrini-infected hamsters. Food Chem Toxicol. 2014;74:206-15.
107. Yang Z, Zhai W. Identification and antioxidant activity of anthocyanins extracted from the seed and cob of purple corn (*Zea mays* L.). Innov Food Sci Emerg Technol. 2010;11:169-76.
108. Zhang Z, Zhou B, Wang H, Wang F, Song Y, Liu S, et al. Maize purple plant pigment

protects against fluoride-induced oxidative damage of liver and kidney in rats. Int J Environ Res Public Health. 2014;11(1):1020-33.

109. Ramos-Escudero F, Munoz AM, Alvarado-Ortiz C, Alvarado A, Yanez JA. Purple corn (*Zea mays* L.) phenolic compounds profile and its assessment as an agent against oxidative stress in isolated mouse organs. J Med Food. 2012;15(2):206-15.
110. Fukamachi K, Imada T, Ohshima Y, Xu J, Tsuda H. Purple corn color suppresses Ras protein level and inhibits 7,12-dimethylbenz[a]anthracene-induced mammary carcinogenesis in the rat. Cancer Sci. 2008;99(9):1841-6.
111. Olaniyan MF, Babatunde EM. Corn silk extracts as scavenging antioxidant in oxidative stress induced rabbits using corticosterone. Am. J. Biomed. Sci. 2016;8(1):38-45.
112. Nessa F, Ismailb Z, Mohamed N. Antimicrobial activities of extracts and flavonoid glycosides of corn Silk (*Zea mays* L). Int J Biotechnol Wellness Ind. 2012;1(2):115-21.
113. Chaiittianan R, Sutthanut K, Rattanathongkom A. Purple corn silk: A potential anti-obesity agent with inhibition on adipogenesis and induction on lipolysis and apoptosis in adipocytes. J Ethnopharmacol. 2017;6(201):9-16.
114. Rimdusit T, Thapphasaraphong S, Puthongking P, Priprem A. Effects of anthocyanins and melatonin from purple waxy corn by-products on collagen production by cultured human fibroblasts. Nat Prod Commun. 2019:1-6.
115. Nithitanakool S, Teeranachaideekul V, Ponpanich L, Nopporn N, Junhunkit T, Wanasawas P, et al. In vitro and in vivo skin whitening and anti-aging potentials of hydroglycolic extract from inflorescence of *Etlingera elatior*. JAASP. 2014;3:314-25.
116. Poorahong W, Innalak S, Ungsurungsie M, Watanapokasin R. Protective effect of purple corn silk extract against ultraviolet-B-induced cell damage in human keratinocyte cells. J Adv Pharm Technol Res. 2021;12(2):140-6.
117. Collins AR. The comet assay for DNA damage and repair: principles, applications, and limitations. Mol Biotechnol. 2004;26(3):249-61.
118. Calo R, Marabini L. Protective effect of *Vaccinium myrtillus* extract against UVAand UVB-induced damage in a human keratinocyte cell line (HaCaT cells). J Photochem Photobiol B. 2014;132:27-35.

119. Berridge MJ. Cell cycle and proliferation. Cell Signal Biol. 2012;9:1-42.
120. Green DR, Reed JC. Mitochondria and apoptosis. Science. 1998;281(5381):1309-12.
121. Gawel-Beben K, Strzepek-Gomolka M, Czop M, Sakipova Z, Glowniak K, Kukula-Koch W. Achillea millefolium L. and Achillea biebersteinii Afan. hydroglycolic extracts-bioactive ingredients for cosmetic use. Molecules. 2020;25(15):3368.
122. Perde-Schrepler M, Chereches G, Brie I, Tatomir C, Postescu ID, Soran L, et al. Grape seed extract as photochemopreventive agent against UVB-induced skin cancer. J Photochem Photobiol B. 2013;118:16-21.
123. Wang PW, Cheng YC, Hung YC, Lee CH, Fang JY, Li WT, et al. Red raspberry extract protects the skin against UVB-induced damage with antioxidative and anti-inflammatory properties. Oxid Med Cell Longev. 2019;2019:9529676.
124. Gasparrini M, Forbes-Hernandez TY, Afrin S, Reboredo-Rodriguez P, Cianciosi D, Mezzetti B, et al. Strawberry-based cosmetic formulations protect human dermal fibroblasts against UVA-induced damage. Nutrients. 2017;9(6):605.
125. Gao W, Wang YS, Hwang E, Lin P, Bae J, Seo SA, et al. *Rubus idaeus* L. (red raspberry) blocks UVB-induced MMP production and promotes type I procollagen synthesis via inhibition of MAPK/AP-1, NF-kappabeta and stimulation of TGF-beta/Smad, Nrf2 in normal human dermal fibroblasts. J Photochem Photobiol B. 2018;185:241-53.
126. Lee SG, Brownmiller CR, Lee SO, Kang HW. Anti-Inflammatory and antioxidant effects of anthocyanins of *Trifolium pratense* (red clover) in lipopolysaccharide-stimulated RAW-267.4 macrophages. Nutrients. 2020;12(4):1089.
127. Tsoyi K, Park HB, Kim YM, Chung JI, Shin SC, Shim HJ, et al. Protective effect of anthocyanins from black soybean seed coats on UVB-induced apoptotic cell death in vitro and in vivo. J Agric Food Chem. 2008;56(22):10600-5.
128. Pedreschi R, Cisneros-Zevallos L. Antimutagenic and antioxidant properties of phenolic fractions from Andean purple corn (*Zea mays* L.). J Agric Food Chem. 2006; 54(13):4557-67.
129. Ahn BN, Kim JA, Kong CS, Seo Y, Kim SK. Protective effect of (2'S)-columbianetin

from *Corydalis heterocarpa* on UVB-induced keratinocyte damage. J Photochem Photobiol B. 2012;109:20-7.

130. Afaq F, Mukhtar H. Effects of solar radiation on cutaneous detoxification pathways. J Photochem Photobiol B. 2001;63(1-3):61-9.
131. Perez-Sanchez A, Barrajon-Catalan E, Herranz-Lopez M, Castillo J, Micol V. Lemon balm extract (*Melissa officinalis*, L.) promotes melanogenesis and prevents UVB-induced oxidative stress and DNA damage in a skin cell model. J Dermatol Sci. 2016;84(2):169-77.
132. Tepel M, Echelmeyer M, Orie NN, Zidek W. Increased intracellular reactive oxygen species in patients with end-stage renal failure: effect of hemodialysis. Kidney Int. 2000;58(2):867-72.
133. Hu Y, Ma Y, Wu S, Chen T, He Y, Sun J, et al. Protective Effect of cyanidin-3-O-glucoside against ultraviolet B radiation-induced cell damage in human HaCaT Keratinocytes. Front Pharmacol. 2016;7:301.
134. Cimino F, Ambra R, Canali R, Saija A, Virgili F. Effect of cyanidin-3-O-glucoside on UVB-induced response in human keratinocytes. J Agric Food Chem. 2006;54(11):4041-7.
135. Sinha RP, Hader DP. UV-induced DNA damage and repair: a review. Photochem Photobiol Sci. 2002;1:225-36.
136. Shin S, Kum H, Ryu D, Kim M, Jung E, Park D. Protective effects of a new phloretin derivative against UVB-induced damage in skin cell model and human volunteers. Int J Mol Sci. 2014;15(10):18919-40.
137. Park NH, Lee CW, Bae JH, Na YJ. Protective effects of amentoflavone on Lamin A-dependent UVB-induced nuclear aberration in normal human fibroblasts. Bioorg Med Chem Lett. 2011;21(21):6482-4.
138. Zhang JA, Yin Z, Ma LW, Yin ZQ, Hu YY, Xu Y, et al. The protective effect of baicalin against UVB irradiation induced photoaging: an in vitro and in vivo study. PLoS One. 2014;9(6):e99703.
139. Kinner A, Wu W, Staudt C, Iliakis G. Gamma-H2AX in recognition and signaling of

DNA double-strand breaks in the context of chromatin. Nucleic Acids Res. 2008;36(17):5678-94.

140. Liu Z, Hu Y, Li X, Mei Z, Wu S, He Y, et al. Nanoencapsulation of cyanidin-3-O-glucoside enhances protection against UVB-induced epidermal damage through regulation of p53-mediated apoptosis in mice. J Agric Food Chem. 2018;66(21):5359-67.
141. Beedanagari S, Vulimiri S, Bhatia S, Mahadevan B. Genotoxicity biomarkers: molecular basis of genetic variability and susceptibility. Biomarkers in Toxicology: Elsevier Inc;2014:p729-42.
142. Vaid M, Sharma SD, Katiyar SK. Proanthocyanidins inhibit photocarcinogenesis through enhancement of DNA repair and xeroderma pigmentosum group A-dependent mechanism. Cancer Prev Res (Phila). 2010;3(12):1621-9.
143. Khan N, Syed DN, Pal HC, Mukhtar H, Afaq F. Pomegranate fruit extract inhibits UVB-induced inflammation and proliferation by modulating NF-kappaB and MAPK signaling pathways in mouse skin. Photochem Photobiol. 2012;88(5):1126-34.
144. Liu X, Shi S, Ye J, Liu L, Sun M, Wang C. Effect of polypeptide from *Chlamys farreri* on UVB-induced ROS/NF-kappaB/COX-2 activation and apoptosis in HaCaT cells. J Photochem Photobiol B. 2009;96(2):109-16.
145. Hinata K, Gervin AM, Zhang YJ, Khavari PA. Divergent gene regulation and growth effects by NF-kappa B in epithelial and mesenchymal cells of human skin. Oncogene. 2003;22(13):1955-64.
146. Han Y, Jiang Q, Gao H, Fan J, Wang Z, Zhong F, et al. The anti-apoptotic effect of polypeptide from *Chlamys farreri* (PCF) in UVB-exposed HaCaT cells involves inhibition of iNOS and TGF-beta1. Cell Biochem Biophys. 2015;71(2):1105-15.
147. Liu T, Zhang L, Joo D, Sun SC. NF-kappaB signaling in inflammation. Signal Transduct Target Ther. 2017;2:17023.
148. Tsoyi K, Park HB, Kim YM, Chung JI, Shin SC, Lee WS, et al. Anthocyanins from black soybean seed coats inhibit UVB-induced inflammatory cylooxygenase-2 gene expression and PGE2 production through regulation of the nuclear factor-kappaB and

phosphatidylinositol 3-kinase/Akt pathway. J Agric Food Chem. 2008;56(19):8969-74.

149. Thalhamer T, McGrath MA, Harnett MM. MAPKs and their relevance to arthritis and inflammation. Rheumatology (Oxford). 2008;47(4):409-14.

150. Assefa Z, Vantieghem A, Declercq W, Vandenabeele P, Vandenheede JR, Merlevede W, et al. The activation of the c-Jun N-terminal kinase and p38 mitogen-activated protein kinase signaling pathways protects HeLa cells from apoptosis following photodynamic therapy with hypericin. J Biol Chem. 1999;274(13):8788-96.

151. Zhang Y, Xu M, Zhang X, Chu F, Zhou T. MAPK/c-Jun signaling pathway contributes to the upregulation of the anti-apoptotic proteins Bcl-2 and Bcl-xL induced by Epstein-Barr virus-encoded *BARF1* in gastric carcinoma cells. Oncol Lett. 2018;15(5):7537-44.

152. Papavassiliou AG, Musti AM. The multifaceted output of c-Jun biological activity: focus at the junction of CD8 T cell activation and exhaustion. Cells. 2020;9(11):2470.

153. Hammouda MB, Ford AE, Liu Y, Zhang JY. The JNK signaling pathway in inflammatory skin disorders and cancer. Cells. 2020;9(4):857.

154. Jiang F, Guan H, Liu D, Wu X, Fan M, Han J. Flavonoids from sea buckthorn inhibit the lipopolysaccharide-induced inflammatory response in RAW264.7 macrophages through the MAPK and NF-kappaB pathways. Food Funct. 2017;8(3):1313-22.

155. Huh WB, Kim JE, Kang YG, Park G, Lim TG, Kwon JY, et al. Brown pine leaf extract and its active component Trans-communic acid inhibit UVB-induced MMP-1 expression by targeting PI3K. PLoS One. 2015;10(6):e0128365.

156. hoi YJ, Moon KM, Chung KW, Jeong JW, Park D, Kim DH, et al. The underlying mechanism of proinflammatory NF-kappaB activation by the mTORC2/Akt/IKKalpha pathway during skin aging. Oncotarget. 2016;7(33):52685-94.

VITA

NAME	Watcharaporn Poorahong
DATE OF BIRTH	20 Nov 1990
PLACE OF BIRTH	Bangkok
INSTITUTIONS ATTENDED	2014-present Doctor of Philosophy in Biomedical-science program, Srinakharinwirot University 2009-2013 Bachelor of Science Biology (B. Sc.), University of Phayao 2006-2008 High school, Princess Chulabhorn's College ChiangRai
HOME ADDRESS	894/1 Sanpanart Rd, Chiang Rai, 57000.
PUBLICATION	1. Poorahong W, Innalak S, Ungsurungsie M, Watanapokasin R. Protective effect of purple corn silk extract against ultraviolet-B-induced cell damage in human keratinocyte cells. J Adv Pharm Technol Res 2021;12:140-6.
AWARD RECEIVED	2015 Certificate of training Basics to Advance in cell culture techniques on June 4-5, 2015, Factory of Science, Kasetsart University 2013 Medal of Academic Excellence, Factory of science, University of Phayao 2012 Certificate of Academic Excellence, Factory of science, University of Phayao 2012 Certificate of academic benefits, Factory of science, University of Phayao